THESIS FOR THE DEGREE OF DOCTOR OF PHILOSOPHY (PHD)

Nuclear hormone receptors and lipid antigen presentation in dendritic cells

by Adrienn Gyöngyösi

Supervisor: Prof. Dr. László Nagy

UNIVERSITY OF DEBRECEN
DOCTORAL SCHOOL OF MOLECULAR CELL AND IMMUNE BIOLOGY

DEBRECEN, 2018

TABLE OF CONTENT

1. LIST OF ABBREVIATIONS

ADH	alcohol dehydrogenase
APC	antigen presenting cell
ATRA	all-*trans* retinoic acid
β2m	β2-microglobulin
BM	bone marrow
BM-DC	bone marrow-derived dendritic cell
Cat	cathepsin
CCL	C-C motif chemokine ligand
CCR	C-C motif chemokine receptor
CD1	cluster of differentiation 1
cDC	conventional DC
CFSE	Carboxyfluorescein succinimidyl ester
ConA	concanavalin A
CRABP	cellular retinoic acid binding protein
CRBP	cellular retinol binding proteins
CXCL	C-X-C motif ligand
CX_3CR1	C-X3-C Motif Chemokine Receptor 1
Cyp26a1	cytochrome p450 26a1
DEAB	4-diethyl amino-benzaldehyde
DC	dendritic cell
DC-SIGN	dendritic cell-specific intercellular adhesion molecule-3-grabbing non-integrin
DI	double immunofluorescence
DSS	dextran sodium sulfate
ER	endoplasmic reticulum (ER
ESAM	endothelial cell-specific adhesion molecule
FABP4	fatty acid binding protein 4
Flt3L	fms-related tyrosine kinase 3 ligand

GALT	gut-associated lymphoid tissue
αGC	α-galactosylceramide
αGGC	galactosyl(1-2) galactosylceramide
GM-CSF	granulocyte-macrophage colony-stimulating factor
IBD	inflammatory bowel disease
iDC	immature dendritic cell
IF	immunofluorescent
IFN	interferon
IHC	immunohistochemistry
IL-4	interleukin-4
iNKT	invariant natural killer T cell
IRF	interferon regulatory factor
LC	langerhans cells
LN	lymph node
LP	lamina propria
LTP	lipid transporter protein
MIIC	MHC class II compartment
M-CFS	macrophage colony-stimulating factor
mDC	mature dendritic cell
MDR	medium-chain dehydrogenase/reductase
MHCI/II	major histocompatibility complex class I and II
MLN	mesenteric lymph node
MLR	mixed leucocyte reaction
mo-DC	monocyte-derived dendritic cell
NK	natural killer cell
NS	non-silencing
NS siRNA	non-silencing control small interfering RNA
OVA	ovalbumin
PBMC	peripheral blood mononuclear cell

PBS	phosphate buffered saline
pDC	plasmacytoid dendritic cell
PP	Peyer's patches
PPARγ	peroxisome proliferator-activated receptor γ
RALDH	retinal dehydrogenase
RAR	retinoic acid receptor
RARE	retinoic acid response element
RBP	retinol-binding protein
RBPR2	RBP4 receptor-2
RDH	retinol dehydrogenase
RSG	rosiglitazone
RT-qPCR	real time quantitative PCR
RXR	retinoid X receptor
SAP	saposins
SDR	short-chain dehydrogenase/reductase
siRNA	small interfering RNA
Sirpa	signal regulatory protein alpha
Sp-DC	splenic dendritic cell
TCR	T cell receptor
TGM2	transglutaminase 2
TF	transcription factor
TLDA	TaqMan low-density array
TNFα	tumor necrosis factor α
Treg	regulatory T cell
WT	wild type

2. INTRODUCTION

2.1. Dendritic cells (DCs)

2.1.1. General feature of DCs

The immune system has evolved to exert acute and systemic inflammatory responses and to protect the host against various infectious and tumor diseases with layered defenses of increasing specificity. Humans and mice have two types of immune defense: innate- and adaptive immunity. Cells of the innate immune system are well equipped to recognize conserved pathogen-associated molecular patterns (PAMP) by pathogen recognition receptors (PRRs) like Toll-like receptors (TLRs) (1), and attack immediate invaders that have penetrated cutaneous or mucosal barriers of the host. The innate phase of immunity is rapidly followed by an antigen–specific adaptive immune response, initiated by antigen presenting cells (APCs) (2). Traditional APCs with the ability to present antigen and activate T cells were macrophages and B cells. In 1973, another kind of APC was discovered in the mouse spleen by Ralph Steinman and Zanvil Cohn (3). Dendritic cells (DC) are unique innate immune cells that function as an indispensable link between the innate- and adaptive immunity, and are important sentinels of the host immune system. In their immature state, DCs constantly sample the environment at the periphery for invaders and host cell-associated self-antigens (2). Upon detection of pathogens, tumor necrosis factor-, and inducible nitric oxide synthase-producing DCs (tip-DCs) protect against bacteria by releasing their featured factors and plasmacytoid DCs (pDCs) contribute to T cell-independent pathogen clearance by secreting type I interferons against viruses (4, 5). DCs capture pathogens via receptor mediated endocytosis, phagocytosis or macropinocytosis and process antigens (6, 7). Some DCs migrate in immature state to draining lymph nodes (LNs), present self-antigens and are involved in the maintenance of the peripheral tolerance (8). Mature DCs (mDCs) induce adaptive immune responses in the host by a highly specific antigen presentation process, mediated by their cell surface major histocompatibility complex class (MHC) I molecules that present self-antigens/viruses or by MHCII molecules, required for exogenous antigen presentation. mDCs migrate to LNs from the periphery, present antigens to responding naïve T cells and activate them (9). They also present glycolipids of infectious invaders or self-lipid antigens through the cluster of differentiation 1 (CD1) molecules (10). It has been also demonstrated, that DCs interact with B cells. This cell-to-cell contact can induce

B cell expansion and antibody production (11). Furthermore, DCs directly or indirectly trigger the natural killer (NK) cells which mediate anti-tumor and anti-viral immunity by augmented INFγ production and cytolytic activity (12).

2.1.2. Classification of DCs

DCs are classified as plasmacytoid DCs (pDCs) or conventional DCs (cDCs) (13). pDCs are present mainly in the bone marrow (BM), blood or lymphoid tissues. Phenotypically pDCs are $CD11c^{+}MHCII^{low}$ cells that selectively express TLR7 and TLR9 molecules (14). pDCs as important innate immune cells produce massive quantities of Type I interferons in response to viral infections (5). These cells can also function as APCs, mediating tolerance by induction of regulatory T cells (Treg) or by activating protective adaptive immunity (15).

cDCs comprise all DCs other than pDCs. In mice four cDC classes are known: $CD8a^{+}$ DCs, $CD11b^{+}$ DCs in lymphoid tissues and $CD11b^{+}/CD103^{-}$, $CD103^{+}$ DCs in non-lymphoid tissues (Table 1). Based on their specific cell surface markers, human cDCs can be divided into BDCA-1^{+} ($CD1c^{+}$) or BDCA-3^{+} ($CD141^{+}$) subsets. According to their phenotypic and functional characteristic, blood $CD141^{+}$ DCs resemble to murine $CD8a^{+}$ DCs, while the $CD1c^{+}$ subset is the functional homologue of murine $CD103^{+}$ DCs. We can further classify these heterogeneous cDC populations into migratory or tissue-resident DC subsets (16).

Although DCs share common phenotypic and functional properties in tissues, DCs represent a diverse cell population, grouped in different subsets based on their development, location, migratory capacity and activation status. Their heterogeneity reflects the functional specialization, acquired by the cells in different tissue locations.

2.1.3. Ontogeny of DCs

DC development and the lineage relationship between different subsets have been subjected of extensive investigation. Based on recent *in vitro* and adoptive transfer experiments, pDCs and cDCs develop from common myeloid progenitors (CMPs) in the BM (17). CMPs originate from multipotent stem cells (MSCs) during hematopoiesis and represent an early committed progenitor of the DC differentiation pathway. During this process, committed progenitors differentiate toward these certain cell types, characterized by loss of their ability to become

other cell types. Further studies have indicated that monocytes and DCs may share a common intermedier progenitor, known as the macrophage and dendritic cell progenitor (MDP) (18). Their development diverges, when MDPs become commitment to produce monocytes or common DC progenitors (CDPs) (19). Thereafter CDPs give rise only conventional pre-dendritic cells (pre-cDCs) or plasmacytoid pre-dendritic cells (pre-pDCs) (20). It has been suggested that pDCs complete their development before leaving the BM, whereas pre-cDCs constantly released from bone, circulate through the blood to localize into non-lymphoid or lymphoid tissues and fill the DC compartment (19, 21).

The development and expansion of DC subtypes are determined by a combination of cytokines and transcription factors (TFs). Fms-related tyrosine kinase 3 ligand (Flt3L) was found to be a key cytokine for the myeloid DCs development (reviewed in (16)). This ligand is produced by stromal-, endothelial- and activated T cells. Flt3, receptor for Flt3L, is expressed on all DC progenitors from MSC to pre-DCs and on tissue cDCs. Consequently, the lack of Flt3 or Flt3L leads to decreased pDC and cDC numbers. Moreover, injection of Flt3L or Flt3L-secreting tumor cells into mice resulted in a vastly increased pDC and cDC expansion and the ligand also contribute to the maintenance of DCs under steady state conditions.

Besides the common progenitor (MDP), the common origin of macrophages and DCs has been further supported by the requirement for the macrophage colony-stimulating factor/Colony stimulating factor 1 receptor (M-CSF/CSF-1R) during their development. M-CSF plays a predominant role in the CDP and monocyte development (16). Monocytes under the influence of this cytokine give rise to $CD103^-$ DCs in the lamina propria (LP) (22). Although human circulating monocytes are excellent source of DCs *in vitro*, their contribution to DC homeostasis is still not fully characterized *in vivo*. $CD14^+$ monocytes can be differentiated to monocyte-derived DCs (mo-DCs) in the presence of IL-4/IL-13 and granulocyte-macrophage colony-stimulating factor (GM-CSF/CSF-2), which is the most frequently utilized human DC differentiation model (23). In mice, researchers have confirmed the monocyte to DC transition from the BM, supplemented with GM-CSF *in vivo*. Previously, this differentiation process was found to be restricted to inflamed or infected environments, therefore these *in vivo* DCs are frequently referred as tip-DCs. These results suggested that the *in vitro* generation process models mainly the tissue inflammatory and not the steady state DC development. Subsequent experiments have identified the development of monocyte-derived intestinal $CD103^-/CD11b^+$-, splenic $CD11b^+$/ endothelial cell-specific adhesion molecule $(ESAM)^{low}$- and muscular FC gamma Receptor 1 (FcγRI) bearing DCs under steady state conditions (22, 24, 25) (Figure 1).

Adoptive transfer experiments supported, that DC subsets in the intestinal LP are originated from different precursors (monocytes or pre-cDCs). Monocytes give rise exclusively to $CD103^-$/C-X3-C Motif Chemokine Receptor 1 $(CX_3CR1)^+$ DCs under the control of M-CSF and Flt3L, while GM-CSF and Flt3L are critical factors for the $CD103^+/CX_3CR1^-$ DC differentiation form Pre-DCs (22, 26, 27).

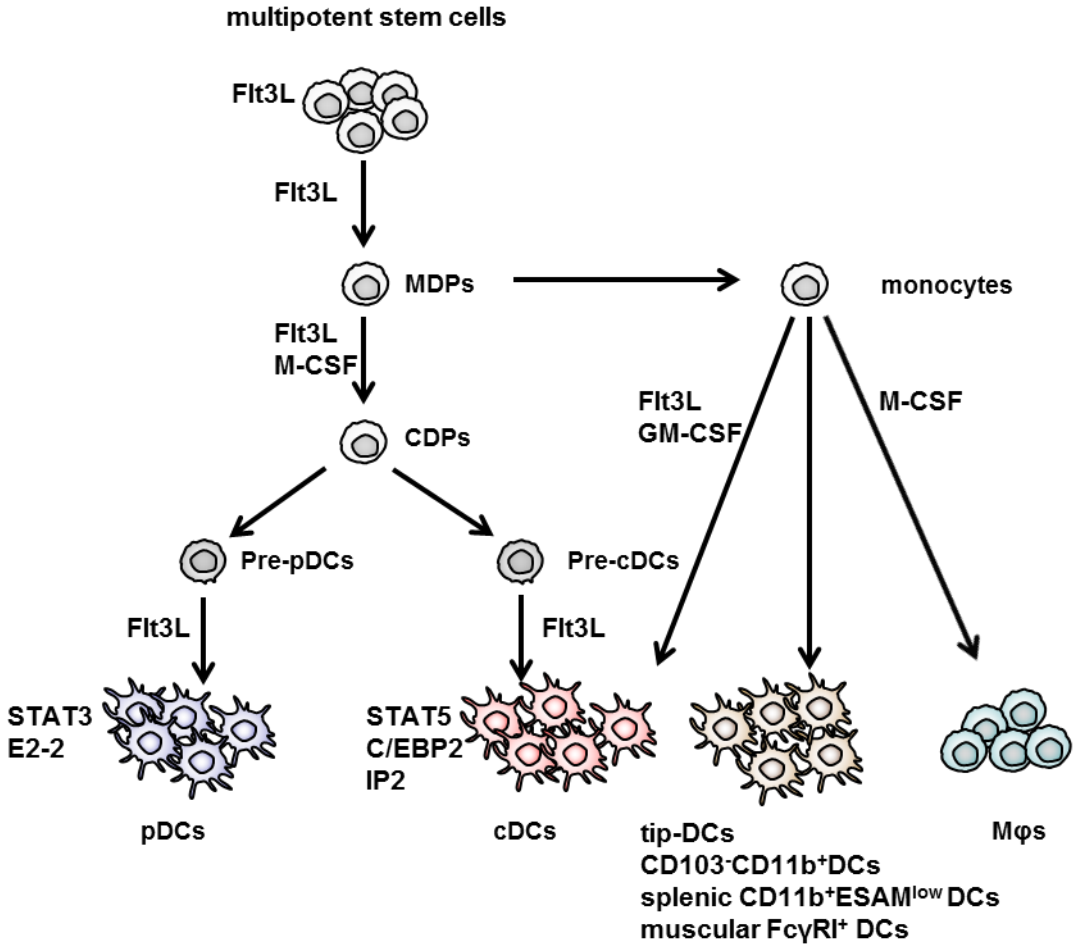

Figure 1: Ontogeny of dendritic cells (DCs): *Hematopoiesis is take place in the bone marrow (BM). DCs are originated from multipotent stem cells and differentiate through committed progenitors (macrophage and dendritic cell progenitor (MDPs), monocytes or common DC progenitors (CDPs), plasmacytoid pre-dendritic cells (Pre-pDC) or conventional pre-dendritic cells (Pre-cDCs) or through monocytes under the control of indicated cytokines and transcription factors (TFs). Macrophages (Mφ). Based on (16, 22, 24, 25, 28).*

Although several TFs have been shown to control DC development during hematopoiesis for example: interferon regulatory factor 8 (IRF8), IRF4, basic leucine zipper transcription factor ATF-like 3 (BATF3), signal transducer and activator of transcription 3 (STAT3), STAT5, CAATT/enhancer binding protein (C/EBP2), DNA-binding protein inhibitor Id2 (IP2)

and E-protein 2-2 (E2-2) (reviewed in (16)); the roles of these TFs in DCs are still to be investigated *in vivo*. As it was mentioned above, Flt3L is required for both pDC and cDC development. The cytokine Flt3L stimulates pDC differentiation via STAT3 and the up-regulation of E2-2 TF, is important for *Tlr7*, *Tlr9* expression. GM-CSF triggers STAT5 in DC progenitors, directs cDC production and inhibits Flt3L–dependent pDC maturation by repressing E2-2. Furthermore, Flt3L also has an important role during cDC lineage differentiation in STAT-independent–manner, in which similarly to GM-CSF, induce the expression of C/EBP2 and up-regulates IP2 to suppress E2-2 in DC progenitors (28).

Genome wide gene transcriptional- and cell surface receptor profiling of small intestinal LP, blood and splenic (Sp-) Sp-DC subpopulations identified a coordinately regulated TF profile that directs subtype specification and development of these cells in various non-lymphoid and lymphoid tissues (29). This analysis also revealed that human intestinal $CD103^-$/signal regulatory protein alpha $(Sirpa)^+$ cDCs have a gene expression profile consistent with mo-DCs. Furthermore, hierarchical clustering analysis demonstrated that human intestinal $CD103^+/Sirpa^-$ DCs were clustered with $CD141^+$ blood DCs and related to mouse LP $CD103^+/CD11b^-/Sirpa^-$ DCs and $CD8a^+$ Sp-DCs. Close relationship was identified of the human $CD103^+/Sirpa^+$ subset in the gut to human $CD1c^+$ blood DCs, mouse intestinal $CD103^+/CD11b^+/Sirpa^+$ and $CD4^+$ Sp-DCs. Distinct TFs drive the development of these mouse and human DC subsets: IRF8, BATF3 and Id2 control mouse $CD103^+/CD11b^-/Sirpa^-$ DCs and $CD8a^+$ Sp-DCs development. Mouse $CD103^+/CD11b^+/Sirpa^+$ and $CD4^+$ Sp-DCs require IRF4 for their differentiation. Bcl-6 controls the subtype specification of both intestinal $CD103^+/CD11b^-/Sirpa^-$ DCs and lymphoid tissue $CD8a^+$ DCs in mice, while IRF4 and positive regulatory domain containing 1 (Prmd1) dictate the development of intestinal $CD103^+/CD11b^+/Sirpa^+$ population and also implicated in human gut $CD103^+/Sirpa^+$ and $CD4^+$ DCs ontogeny. These observations suggest the complexity and integration of cytokine and signaling pathway during DC lineage ontogeny revealing an evolutionarily conserved and divergent transcriptional programming of the myeloid DC development.

Classification of cDCs			
Lymphoid tissue		**Non-lymphoid tissue**	
murine	human	murine/human	
$CD8a^+$ DC ($Sipa^-$)	$CD141^+$ blood DC, $CD8^+$ lymphoid DC	$CD103^+$	
$CD11b^+$DC ($Sipra^+$)	$CD1C^+$ blood DC, $CD11b^+$ lymphoid DC	$CD103^-/CD11b^+$	
Classification of LP DCs (human and murine)			
$CD103^+/CX_3CR1^-$DCs		**$CD103^-/CX_3CR1^{int}$ DCs**	
origin: Pre-DC, cytokines: GM-CSF, Flt3L		origin: monocytes; cytokines: M-CSF, Flt3L	
$CD11b^+/Sirpa1^+$	$CD11b^-/Sirpa1^-$	$CD11b^+/Sirpa1^+$	$CD11b^-/Sirpa1^-$
$Sirpa1^+$	$Sirpa1^-$	$Sirpa1^+$	$Sirpa1^-$

Table 1: *Classification of human and murine conventional DCs (cDCs). Human blood cluster of differentiation 141 (CD141)$^+$ DCs resemble to murine CD8a$^+$ DCs, while the CD1c$^+$ subset is the functional homologue of murine CD103$^+$ DCs. Lamina propria-DCs (LP-DCs) share phenotypic and functional characteristic, having same origin and differentiating cytokines. Both murine (light gray) and human LP-DCs have four different subsets. Genome wide transcriptional- and cell surface receptor profiling identified the close relationship of the upper murine and lower human LP-DCs. CX_3CR1:C-X_3-C Motif Chemokine Receptor 1; GM-CSF:granulocyte-macrophage colony-stimulating factor; Flt3L:fms-related tyrosine kinase 3 ligand; Sirpa:signal regulatory protein alpha. Based on (16, 22, 26, 27, 29).*

2.1.4. Localization of DCs

When pDCs or pre-cDCs arrive to their target tissues, they are exposed to the modulating properties of the local environment.

Based on the cell surface markers of lymphoid tissue DCs, three distinct DC populations reside in the cortex of murine thymus. pDCs, $CD11b^+$ and $CD8a^+$ cDCs enter the thymus in the absence of inflammation (30). These observations indicated that peripheral self-antigens might be delivered and presented to thymic lymphocytes and immigrated DCs have the opportunity to trigger central tolerance through positive or negative selections by inducing natural regulatory T cell (nTreg) development. In the murine spleen, cDCs are grouped by their CD8a expression. $CD8a^-$ DCs localized mainly in the marginal zone and $CD8a^+$ DCs are present in T cell areas. Some $CD11c^+$ cells can also be detected in the red pulp under specific pathogen free condition. Upon inflammation, the majority of DCs migrate to T cell areas in a C-C motif chemokine receptor 7 (CCR7)-dependent manner (31).

DCs are classified by the CD11b marker in murine non-lymphoid tissues. For instance, the $CD11b^+$ DC group in the skin consists of dermal DCs, $CD4^+$, $CD4^-/CD8^-$ DCs and langerhans cells (LCs), whereas $CD103^+$ and $CD8^+$ DCs represent the $CD11b^-$ population. LCs home to the epidermis, anchored to neighboring keratinocytes (KC) by E-cadherin connections under normal circumstances (2). Inflammation induces the migration of LCs and dermal DCs from peripheral areas to LNs, where they activate T cells.

DCs can be found in all lymphoid tissues and are also present through non-lymphoid tissues such as the skin and the intestines. They are localized in organized lymphoid organs, known as Gut-associated lymphoid tissues (GALTs); including Peyer's patches (PP) and mesenteric lymph nodes (MLNs) (32). Moreover, DCs are scattered through the subepithelial LP, localized between the epithelium and the muscularis mucosa. At least four different PP-DC subsets have been characterized to date (33). $CD11b^+$s DC are preferentially found in the subepithelial dome (SED) and capture M cell-transported luminar antigens. $CD8a^+$ DCs are present in the T cell-rich interfollicular region and prime naïve T cells. $CD11b^-/CD8a^-$ double negative cDCs and $B220^+$ pDCs are located in both PP section. The lamina propria-DC (LP-DC) repertoire in the gut epithelium can be divided into subsets by CD11b, CD103, Sirpa and C-X3-C Motif Chemokine Receptor 1 (CX_3CR1) cell surface expression. Following this classification four functionally distinct LP-DC population was determined: 1. $CD103^+/CD11b^+/Sirpa^+/CX_3CR1^-$, 2. $CD103^+/CD11b^-/Sirpa^-/CX3CR1^-$, 3. $CD103^-/CD11b^+/Sirpa^+/CX_3CR1^{int}$ and 4. $CD103^-/CD11b^-/Sirpa^+/CX_3CR1^{low}$ DCs. Intriguingly, LP macrophages express DC-specific markers (MHCII, CD11C) but are distinguished from the $CD103^-/CD11b^-/Sirpa^+/CX_3CR1^{int}$ DC population based on their robust F4/80 and CX_3CR1 positivity (29). Recently, a comprehensive gene expression, cell surface and immune fluorescens study determined the LP-DC subset profile in the human small intestinal and colonic LP. Similar to the murine system, this analysis determined four LP-DC subpopulations: 1. $CD103^+/Sirpa^{+-}$, 2. $CD103^+/Sirpa^-$, 3. $CD103^-/Sirpa^+$ and 4. $CD103^-/Sirpa^-$ DCs. Compared to human intestinal macrophages, $CD103^-/Sirpa^+$ DCs express intermedier level CX_3CR1, while all other DC subpopulation was CX_3CR1^- or CX_3CR1^{low}. All DC subpopulation were detected within the small intestinal villus core that was $CD103^+/Sirpa^+$ DC predominated. Interestingly, the proportion of the $CD103^-/Sirpa^+$ was increased in inflamed small intestinal LP, moreover $CD103^+/Sirpa^-$ and $CD103^-/Sirpa^+$ DCs dominated in the colonic LP (29).

2.1.5. Peptide antigen processing in DCs

The two well-established maturation states for DCs are the “immature” and “mature” forms. Immature DCs (iDCs) are specialized to monitor, take up and process antigens. DCs capture antigens by macropinocytosis, receptor-mediated endocytosis, as well as by phagocytosis (6, 7). Extracellular soluble or particulate antigens are presented by MHCII molecules (9). In the endoplasmic reticulum (ER), MHCII molecules connect to invariant chain (Ii), which directs the molecular complex from the Golgi apparatus to late endosomal/lysosomal MHC class II compartments (MIIC) (34). These lysosome-related intracellular compartments accumulate MHCII molecules and HLA-DM chaperons that promote the catalytic release of Li and antigen-derived peptide loading to the MHCII molecules. Thereafter, the MHCII-peptide complexes transfer to the plasma membrane for recognition by $CD4^+$ naive T cells (9).

DCs present self- and intracellular foreign viral antigens by MHCI molecules and activate cytotoxic $CD8^+$ T cells (9). Intracellular antigens are processed in the cytoplasm by ATP- and ubiquitin–dependent proteosomal mechanism. Antigenic peptides translocate to the ER by TAP1/2 ABC transporters, wherein their binding to MHCI molecules stabilizes the MHCIα chain/β2-microglobulin (β2m) folding. DCs also acquire the ability to present exogenous peptides through cross presentation (exogenous MHCI pathway), such as transplantation antigens, virus- or tumor-derived peptides by MHCI molecules.

2.1.6. Maturation and migration of DCs

Following antigen capture, a series of factors trigger maturation process in iDCs: whole bacteria or bacterial wall-derived LPS, bacterial double stranded deoxyribonucleic acid (DNA), viral products, ligation of cell surface receptors (CD40) and pro-inflammatory cytokines (i.e. IL-1, tumor necrosis factor α (TNFα), GM-CSF) (2). During maturation, DCs undergo a number of phenotypic and functional changes. This continuous process is accompanied by reduced antigen uptake capacity, increased surface expression of co-stimulatory molecules, secretion of cytokines and morphological changes (formation of dendrites).

Initial exposure to inflammatory stimuli and induced antigen uptake followed within hours by a period of maturation, whereby DCs homing tropism is modified. As a consequence of a coordinated chemokine receptor switch (down-regulated cell surface expression of CCR1, CCR5 and CCR6 and up-regulated expression of CXCR4 and CCR7), mDCs lose their

migration affinity toward local cytokine milieu and become sensitive to secondary lymphoid tissue-secreted chemokines such as C-C motif chemokine ligand 19 (CCL19) and CCL21, favoring their migration to the afferent lymph vessels (35). mDCs leave inflamed tissues and enter into the paracortical areas of LNs in CCR7-dependent fashion, following the locally produced CCL21 (36). Langerin^{+} DCs constitutively monitor the dermis and migrate in CCR7-dependent manner to dermal LNs, where they present skin-associated antigens. Epicutaneous sensitization increases CXCR4 expression on migratory skin DCs, whereas the CXCL12 chemokine (CXCR4 ligand), is simultaneously up-regulated in dermal lymphatics. The CXCR4 inhibition impairs LC and dermal DC migration to LNs indicating that both CCR7 and CXCR4 contribute to skin DC migration (37).

Several research studies confirmed that mouse CD103^{+} DCs express CCR7, which controls their migration to MLNs. Characterization of the small intestinal lymphatics for migratory DCs confirmed that both CD103^{+} subsets migrate to LNs. Unexpectedly 14% of migratory cells were CD103^{-}. CD103^{-} DCs can be separated into CD103^{-}/CD11b^{+}/CX_3CR1^{int} and CD103^{-} CD11b^{-}/CX_3CR1^{low} cells. Both subsets are CCR7^{+}; constitutively migrate to peripheral LNs in the uninflamed gut (38). Similar to mouse DCs, CD103^{+}/Sirpa^{+} DC and CD103^{+}/Sirpa^{-} DC are present in MLNs, moreover CD103^{-}/Sirpa^{+} DCs express high level of CCR7, indicating that these DCs access lymphatic vessels and migrate to MLNs (29).

2.1.7. T cell activation

T cells activation by mDCs requires three signals: 1. naïve T cells recognize MHCI/II-peptide complexes that trigger activating signal cascade in responding cells and determinate the antigen specificity of the response. The affinity of TCRs for MHC/ peptide complexes is low to mediate a functional interaction between the two cells (39). 2. For a more stable cellular interaction, immunological synapse formation takes place at the interface between T cells and DCs, stabilized by leukocyte function-associated molecule-1 (LFA-1), intercellular cell adhesion molecule-1 (ICAM-1) and integrin molecules (40). The expression of costimulatory molecules on DC surface is increased during maturation. These molecules trigger the second signal. CD80 and CD86 molecules are recognized by CD28 activator co-receptors on T cells (41). CD40Ls on activated T cells associate CD40 receptors on DCs. This CD40-triggered signal amplifies and sustains the viability and activation of DCs, resulting in a positive feedback loop that triggers even more robust T cell responses (42). 3. The third signal is controlled by DC-secreted cytokines, growth factors and chemokines that direct naïve T cell polarization towards distinct subsets with different effector activity. $CD4^+$ helper T cells (Th) express interleukin 2 (IL-2) and the α subunit of the IL-2 receptor (CD25), enabling a functional receptor on their cell surface. Activated T cells express IL-2 that acts either in autocrine fashion and activates proliferation pathways, or at paracrine manner, activating neighboring clone Th cells to proliferate, leading clonal selection. DCs polarize Th cells either into memory-, effector-, or regulatory T (Treg) cells (43). Th1 cell development requires IL-12 and/or INFγ-stimulated signals through signal transducers and activators of transcription 1 (STAT1), STAT4 and T-bet. IL-4 induces STAT6-mediated signals for Th2 development. The Th17 generation requires IL-6, IL-23 and TGFβ signals and the Retinoid-related orphan receptor gamma (RORγ) receptor, while Treg differentiation is controlled by TGFβ, IL-10 and FOXP3 (Figure 2). DCs also have capability to stimulate $CD8^+$ T cells directly or by the help with Th1 cells, leading to cytotoxic T cell immunity (44, 45).

All signals are required for the full development into effector T cells and the integration of these 3 signals determines their subsequent fate. Alterations in one of these signals may result in apoptosis, anergy of the T cells or they acquire a regulatory phenotype (2).

Th1 cells trigger type 1 immune responses via activation of macrophages, $CD8^+$ T and B cells against tumor cells or intracellular bacteria, while Th2 cells promote type 2 humoral immune responses by activating eosinophils, basophils, mast cells as well as IgE-secreting B cells and IL-4/IL-5-sectreting $CD4^+$ T cells.

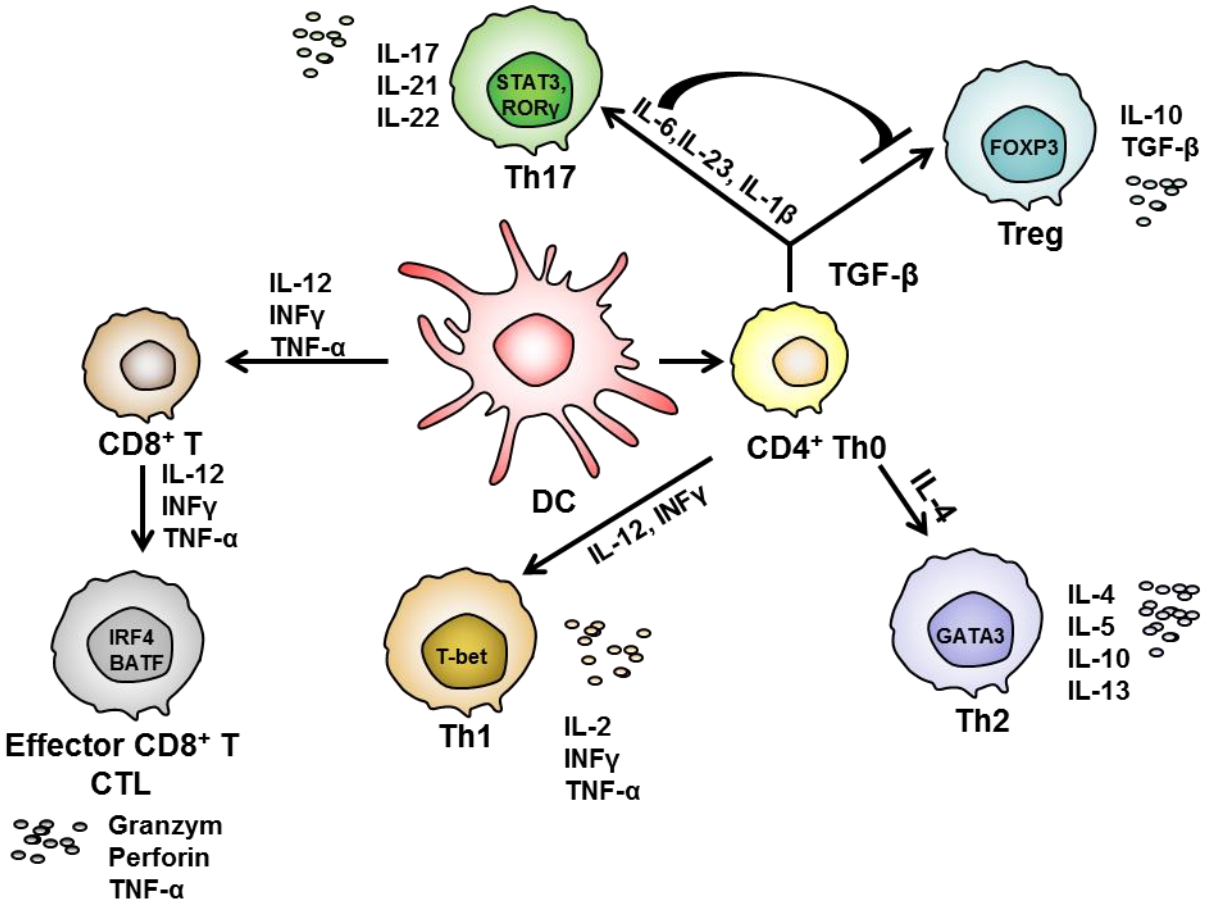

Figure 2: Role of DCs in the differentiation of human T cells. *DCs prime cluster of differentiation 8 ($CD8^+$) T cells and effector $CD8^+$ T cell-mediated immune respone or trigger $CD4^+$ T cell-mediated adaptive immune responses by activating naïve helper T (Th0) cells leading to Th1, Th2, Th17 or regulatory (Treg) differentiation. Based on (43-45).*

DCs stimulate primary T-cell responses and determine whether these responses are immunogenic or tolerogenic.

2.2 Lipid antigen presentation by DCs

2.2.1. Group 1 and Group 2 CD1 molecules

Beside their peptide antigen presentation capacity, DCs acquire the ability to stimulate lipid-mediated T cell responses. The evolutionary conserved lipid antigen-presenting molecules display very limited polymorphism and are specialized for presenting lipids, glycolipids and lipopeptides to reactive T lymphocytes (10). Antigenic lipids are presented by the family of CD1 molecules. Five CD1 proteins are expressed in humans. These isoforms are classified into two groups based on their nucleotide and amino acid sequence homology. Group 1 contains CD1a, CD1b, CD1c and CD1e; and the only Group 2 member is CD1d. Unlike humans, mice express only CD1d, coding by the two homologue genes, namely *Cd1d1* and *2*. *Cd1d2* is a pseudogene; hence *Cd1d1* gives raise to all cell surface CD1d protein in these animals (46). Generally, CD1 genes encode integrated membrane proteins that are structurally similar to MHCI molecules. CD1 isoforms are consisting of a heavy chain with α1, α2, and α3 extracellular domains, associated non-covalently with β2-microglobulin (β2m) (47). Crystallographic analysis of human and mouse CD1 molecules revealed that these antigen presenting molecules have narrow, deep hydrophobic ligand binding pockets, formed by the heavy chain that is optimized to present lipid antigens. The hydrophobic pockets are loaded by the alkyl chains of the lipid antigens and the hydrophilic head group is exposed and protruded at the center of the groove for TCR recognition (Figure 2) (10, 47). Subsequently it has been demonstrated that CD1 molecules can adopt different conformations, facilitating the binding of structurally related lipids, hence allowing the presentation of multiple CD1d-bound lipids and increasing the antigen repertoire to CD1-reactive T cells (48). The characteristic of the antigen binding pocket dictates the substrate specificity of each CD1 molecules. CD1d is specialized for binding long chains lipids, CD1b is able to accommodate lipids with long alkyl chains (C:80) as mycolates, CD1a presents mycobacterial lipopeptides/mycopeptides and glycoproteins and CD1c binds mycobacterial lipids with unsaturated alkyl chains. Moreover, some lipids as phospholipids (PL) and sulfatides can bind multiple CD1 isoforms (10).

2.2.1.1. Group 1 CD1 molecules

Group 1 CD1 molecules are expressed on different human cell types, including thymocytes, monocytes, DCs and B cells. Among DCs, LC express CD1a, c, dermal DCs have CD1b and interdigitating DCs in LNs express all Group 1 CD1 molecules (10). Moreover, Group1 molecules were detected on DCs, infiltrated to inflamed tissues or tumors as well. CD1c is one of the considered markers for a human blood DC subpopulation. Human blood $CD14^+$ monocytes can be differentiated to mo-DCs that express all Group 1 molecules but not CD1d (49). Homogenous human CD1a expression has been considered a quality feature of *in vitro* DC generation, and as long as DCs were cultured in the presence of serum (usually 10% fetal bovine serum (FBS)), the great majority of the DC was indeed $CD1a^+$. When DC research was translated into the clinic, serum-free media were used to generate clinical-grade patient DCs. Under these conditions, human CD1a expression was robustly reduced (50).

DCs regulate anti-microbial immune responses by the presented lipid antigens from mycobacteria to reactive T cells. These cells acquire Th1 effector phenotype by producing high amount of inflammatory cytokines, such as INFγ and TNFα. CD1a, b, and c expression on human DCs was also detected in leprosy lesions. Moreover, T cell reactive to human DC-presented self-lipids in the context of Group 1 CD1 molecules are participated in several autoimmune diseases such as systemic lupus erythematosus (SLE), multiple sclerosis (MS) and autoimmune thyroiditis (10).

2.2.1.2. Assembly and trafficking of CD1 molecules

The assembly of nascent human CD1 molecules occurs in the ER, wherein lipid binding grooves of CD1 molecules associate with calnexin and calreticulin chaperones, regulating the correct folding, and with the thiol oxidoreductase eRp5, required for disulfide bond formation (51). Following correct folding, self-lipids bound to the antigen-binding groove of CD1 molecules. Microsomal triglyceride transfer protein (MTP) plays a role in this self-lipid loading and regulates CD1d-dependent antigen presentation of murine Sp-DCs, BM-DCs and human mo-DCs (52, 53). Lipid-loaded CD1 molecules associate with β2m and the functional lipid-loaded CD1 complexes are transported to the cell surface along the secretory pathway. Thereafter CD1 molecules recycle between the plasma membrane and the endolysosomal compartment. All CD1 molecules follow unique modes of endosomal trafficking, resulting in

distinct cellular localization for sampling relevant antigens (Figure 3) (54). The delivery of human CD1b to acidic, Lysosomal-associated membrane protein 1 (LAMP1^{+}) MIIC endosomal compartments is dependent on its cytoplasmic domain, containing the lysosomal sorting motif. This unique tyrosine-based endocytic motif, a YXXZ sequence (Y, tyrosine; X, any amino acid; Z, a hydrophobic amino acid) was shown to interact with the adaptor protein (AP)-2 complexes of clatrin-coated vesicles and the AP-3, which direct the human CD1b trafficking to lysosomes (10). A similar tyrosine-based motif was found in the cytoplasmic domain of human CD1c, CD1d as well as in mouse CD1d. Mouse CD1d also traffic through early recycling endosomes, thus may be able to survey all potential self- and exogenous lipid antigens in different endosomal compartments. This support that CD1d in the mouse can effectively replace other isotypes present in human cells (54).

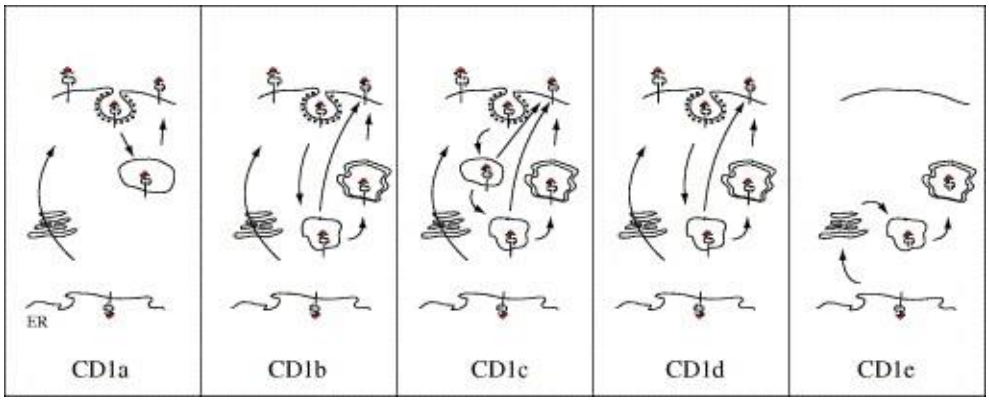

Figure 3: Trafficking of *cluster of differentiation 1 (**CD1) molecules.** CD1a recycle between early endosomes and the cell surface. CD1b is internalized to late endosomes/lysosomes and recycles to the cell surface. CD1c traffics in both early and late endosomes and recycles to cell surface from both compartments. CD1d is internalized into late endosomes/lysosomes from the plasma membrane. A fraction of murine Cd1d also recycles through early endosomes. CD1e does not have cell surface expression. It accumulates in the Golgi of immature DCs (iDC) and, upon DC maturation, traffics to late endosomes/lysosomes. G.Libero, FEBS Letters, Volume 580, 2006, 5580-5587.*

In contrast to other CD1 molecules, human CD1a is expressed without lysosomal sorting motif, thus these molecules do not reach the late endosomes. Human CD1a is internalized from the membrane by clatrine-coated pits and vesicles in mo-DCs. Moreover CD1a and a fraction of CD1c was directed to early endosome in ADP-ribosylation factor 6 (ARF6)-mediated manner and transported back to the membrane following a slow recycling rout (55). A portion of human CD1c similarly to human CD1d is sorted to lysosomes, demonstrating that CD1c is able to recycle in both early and late endosomal complexes. The distinguished trafficking

properties of the different human CD1 proteins suggest that they have evolved to survey all endocytic compartments with specific lipid composition, which results selective presentation of broad spectrum self- and foreign lipid antigens (10, 54) .

2.2.1.3. CD1d molecules

High level of CD1d can be detected on human blood monocytes; this expression is rapidly down-regulated during their differentiation to DCs (49, 56). Despite of the low cell surface expression level, CD1d stimulates the expansion and cytokine secretion of CD1d-restricted, invariant natural killer T cells (iNKTs) when human mo-DCs are loaded with α-galactosylceramide (αGC) (a lipid activator ligand for iNKT cells) (49). *In vivo*, immunohistochemistry (IHC) data has demonstrated the CD1d expression on human dermal DCs, but LC cells do not produce this molecule in the skin (57). CD1d are also present on murine APCs such as Sp-DCs, macrophages, B cells and thymocytes (10). In contrast to human mo-DCs, GM-CSF and IL-4 induce moderately the surface expression of CD1d on murine BM-DCs. Furthermore, Flt3L-stimulated BM-DCs, differentiated in the presence of LPS and INFα, have enhanced surface expression of the protein and under inflammatory condition colonic murine LP-DCs have increased level of CD1d (58, 59). Similar to Group 1 CD1 molecules, human CD1d also associates with β2m before exiting the ER, although functional CD1d can also be detected on the cell surface in β2m-independent manner (60). After assembly, murine CD1d reach the plasma membrane following two different secretory routes. In the intrinsic pathway, CD1d molecules travel directly to cell surface and present self-antigens, while during the extrinsic pathway, a portion of CD1d molecules in association with the Ii, traffic first to the endosomal compartments. This second pathway is critical for CD1d molecules to be loaded by antigenic self- or exogenous-lipids that are presented to autoreactive murine CD1d-restricted NKT cells and is required for the positive selection of NKTs (61).

Similar to human CD1b, the murine cell surface CD1d is reinternalized in AP-2/AP-3-dependent manner. Studies using murine cytoplasmic tail-truncated mutants of murine CD1d, lacking the tyrosine-based sorting motif, revealed that this motif is critical for the lysosomal targeting and mutant CD1d molecules are redistributed from the endosomal compartments to the cell surface (62). iNKT autoreactivity was also dependent on this motif in mice. These tail-deleted mutant CD1d molecules could not reach the MIIC compartment or the lysosomes to sample self-lipid antigens and were not recognized by autoreactive murine NKTs (63).

Moreover AP-3$^{-/-}$ mice had reduced NKT number, suggesting that murine CD1d trafficking to late endosomes was important for NKT positive selection (64). Pharmacological inhibition of the lysosomal acidification also diminished murine iNKT autoreactive responses, suggesting that lysosomal functions were important for the acquisition of autoantigens by CD1d (65).

Contrast to mouse CD1d; the cytoplasmic tail of human CD1d molecule is not associated with AP-3, indicating that this adaptor protein is unnecessary for their cellular distribution and antigen presentation capacity (66). Human iNKTs showed autoreactive responses to chimeric CD1d molecules with cytoplasmic tail of CD1a which trafficked through recycling endosomal system, indicating that human and murine CD1d molecules survey different endosome for autoreactive-lipids (67, 68). Moreover human and murine CD1d molecules showed distinct intracellular trafficking properties (10). The components of the alternative internalization pathway are remained to be characterized. A fraction of human CD1d can be sorted to MIICs by MHCII and Ii molecules, representing an alternative mechanism for lysosomal sorting (61). This Ii-mediated trafficking is independent of the tyrosine-based motif and may participate in the selection of extracellular lipid antigens. The association with MHCII does not affect the intracellular localization of CD1d, but facilitates the internalization rate of the molecule from the cell surface. Ii deficiency resulted in reduced cell surface level of CD1d in MHCII^{+} cell lines, suggesting that CD1d can be complexed both with Ii and MHCII at the cell surface. MHCII/Ii recruits CD1d into membrane lipid rafts, enriched for costimulatory molecules and this makes CD1d a more potently stimulators to iNKTs (69).

2.2.1.4. CD1d trafficking during DC maturation

DCs have the ability to present lipid antigens and efficiently activate CD1-restricted T cells regardless of their maturation state, while the MHC-dependent peptide antigen presentation requires maturation of the cells and fast mobilization of MHC molecules to plasma membrane (70). Group 1 CD1 molecules continuously recycle through endocytic compartments in both iDCs and mDCs and the two DCs display similar capacity to activate reactive T cells (71). In contrast to other CD1 molecules, CD1e localization is highly affected by the maturation. In iDCs, CD1e are predominantly found in the Golgi and trans-Golgi network (72). After maturation, CD1e accumulates in the late endosomes/lysosomes, mediating lipid loading to CD1b or d. The CD1d-mediated exogenous antigen presentation is more efficient in iDCs, which actively recycle MHCII/CD1d complexes through the endocytic system, compared to

mature DCs that have stabilized MHCII expression at their surface (69). Both iDCs and mDCs present αGC, which does not require intracellular processing, although iDCs are more active in this presentation. IDCs also have the capacity to present galactosyl(1-2) galactosylceramide (αGGC) (requires lysosomal activation to generate αGC) but mDCs showed little or no ability to present this antigen (69).

2.2.2. Endogenous ligands of iNKT cells

Despite their semi-invariant TCRs, iNKTs are able to recognize a diverse set of antigens (73). INKTs were first characterized as a self-reactive T cell population, because both human and murine iNKTs react against $CD1d^+$ APCs without addition of exogenous lipids, a property defined as autoreactivity (74). iNKT-autoreactivity confirms not only the constitutive memory phenotype of these cells but also their ability to be activated in hours during immune responses. Enormous effort has been invested to find self-antigens, required for iNKT responses. These results indicated that CD1d might bind PLs (phosphatidylinositol or lysophosphatidilcholin) in the ER and PLs could be potent iNKT activator ligands in some tissues at least in mice (47). Although the complete identification of endogenous lipids mediating iNKT activation has been challenging due to poor sensitivity of assays, which are unable to detect the extreme low lipid concentrations, purified from cellular extracts.

Lysosomal glycosphingolipids (GSLs) as potent iNKT lipids has been identified by utilizing APCs lacking β-glucosylceramide, the common precursor for the majority of GSLs, because iNKT cells were not reactive to these APCs. Later the antigenicity of GSLs was confirmed in hexosaminidase B (Hex-B) deficient mice, a mouse model of a human GSL lysosomal storage disorder (75). These studies suggested that Hex-B enzyme in lysosomes was required for the generation of iNKT-selecting ligands in the thymus. Of these GSLs only isoglobotrihexosylceramide (iGb3) was immunogenic. On the contrary, evidence regarding the role of iGb3 in NKT development has been conflicting because mice deficient in iGb3 synthase, an enzyme essential for iGb3 biosynthesis, exhibited normal iNKT number or function and human iGb3 synthase gene appeared to be nonfunctional (76, 77). Subsequent studies demonstrated that mice with diverse lipid storage disorders had a general defects in iNKT development. This raised the hypothesis that the iNKT dysfunction might not be the consequence of the lack of iGb3 but rather originated by a more general defect in glycosphingolipid processing that disrupted iNKT development in these animals (78).

Previously, endogenous α-linked iNKT antigens were thought to be absent from mammalian cells and glycosphingolipids were considered to have only β-linked sugar. Later it was published that immune cells were able to produce constitutively very small quantity of αGC which served as relevant endogenous selecting lipid for iNKT development (79).

Another β-linked endogenous lipid, namely sulfatide selectively activates the type II NKT cells (80) (Figure 4).

2.2.3. Exogenous lipid antigens

Human and mouse CD1d share approximately to 65% amino acid sequence identity in their antigen binding region and bind αGC in the same orientation. The recognition properties of mouse and human iNKTs with the different lipids presented by CD1d molecules are conserved. Hence mouse and human iNKTs are highly cross-reactive and can recognize αGC regardless of the CD1d by which it is presented (81, 82).

Besides recognizing endogenous lipids, synthetic and microbial-derived antigens also activate NKTs. The first identified lipid, which activated iNKTs in the context of CD1d, was αGC, isolated from the marine sponge Agelas mauritianus (83). In this glycolipid, there are two lipid chains: an acyl chain of 26 carbone atoms (C:26) and a sphingosine chain of 18 carbon atoms (Figure 4). The hydrophilic galactose is connected to the sphingosine chain through an α-anomeric linkage (α-linked). Human CD1d crystal structure was reported in complex with or without αGC. These studies revealed that the galactose is extended above the surface of the ligand binding groove in a position suitable for recognition by the iNKT TCR. The alkyl chain fits perfectly into the A', while sphingosine chain accommodates F' "pocket" of the CD1d molecule (82). The α-linked glycan in αGC has since been shown to be a common structural motif in many identified bacterial lipids (47).

Since then, analogues of αGC have been synthetized by the modification of acyl or sphingosine chains. Some of these structural derivates trigger either Th1- or Th2-biased immune responses by iNKTs. For example αGC with a carbon-based glyosidic linkage (α-C-GC) triggers Th1-biased responses, while OHC induces Th2 responses from iNKTs (84, 85). Despite extensive research, no lipid antigens comparable potency to the prototypic iNKT cells agonist has been identified.

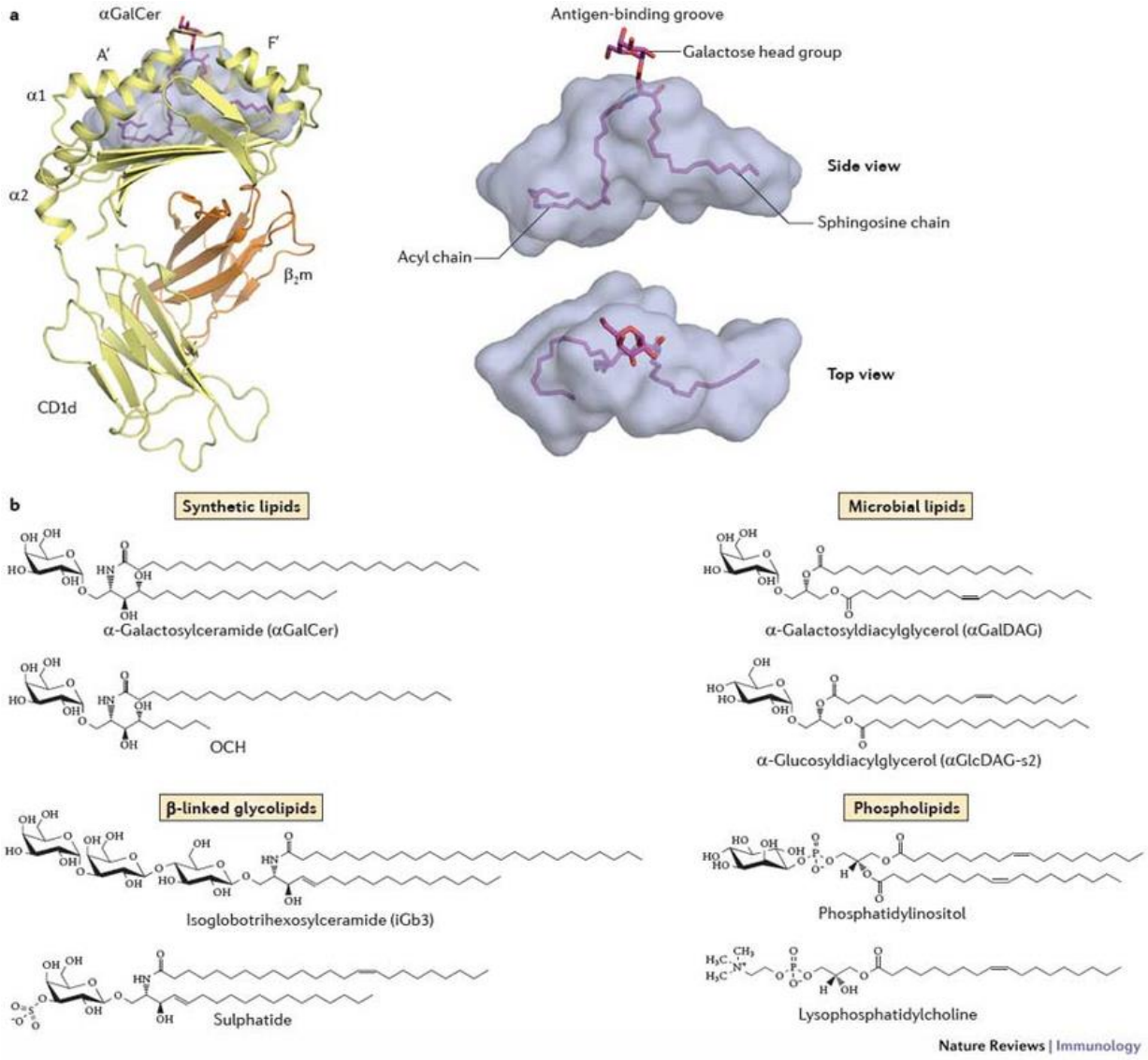

Figure 4: CD1d-dependent lipid antigen presentation. *A, The structure of human CD1d/α-galactosylceramide (αGC) complex. αGC is bound by the CD1d antigen-binding groove, which is has two lipid binding pockets: the A'-pocket and the F'-pocket. Acyl chain accommodates the A, whilst sphingosine chain fulfills the F' pocket. The α-linked galactose is surface exposed, whereas the lipid tails are loaded to the cavity. B, Chemical structures of various CD1d lipid antigens. J. Rossjohn, Nature Reviews. Immunology, Volume 12, 2012, 845-85.*

2.2.4. Lipid antigen delivery to DCs and lipid uptake by APCs

The transports of antigenic lipids are mediated by lipid transporter proteins (LTPs) that facilitate lipid trafficking to tissues and recognition by immune cells. Serum LTPs are apolipoproteins (very low-density lipoprotein (VLDL), LDL (low-density lipoprotein), high-density lipoprotein (HDL)) and the fatty acid amide hydrolase enzyme (FAAH) (86, 87). Lipoproteins are associated with apoproteins (Apo) that regulates their uptake via specific receptors expressed by DCs. The *in vivo* relevance of VLDL-dependent extracellular lipid transport has been demonstrated in $ApoE^{-/-}$ mice, because these mice had reduced numbers of iNKTs and reduced iNKT response to αGGC. DCs engulf αGGC/lipoprotein complexes by the LDL receptor (LDL-R) in ApoE-dependent manner. The lipoprotein/ApoE complexes are internalized and translocated to early endosomes. Thereafter acidic pH of late endosomes facilitates ApoE release form VLDL, association to HDL and export (86).

Based on their receptor requirement for intracellular uptake, lipid antigens can be separated into three classes: 1, LDL-R dependent lipids, such as αGGC, 2, scavenger receptor A (SR-A)-dependent lipids as *Sphingomonas*-derived α-glucuronosylceramide GSL-1 (αGluAC, PBS-29) and 3, lipids such αGC, which can be engulfed by both LDL-R and SR-A (88). In the human serum VLDL, HDL and free LTPs have been implicated in the transport of αGC. However αGC can enter into the cells *in vitro* by both LDL-R and SR-A, *in vivo* experiments with $LDLR^{-/-}$ and $SRA^{-/-}$ mice revealed that SR-A is required for αGC uptake. LDL-R deficiency in mice did not have a significant influence in the αGC-primed iNKT cytokine response and iNKT-mediated downstream adaptive $CD4^+$ and $CD8^+$ T cell responses. Deficiency in the SR-A-regulated endocytosis resulted in diminished iNKT-dependent immune responses, indicating the importance of SR-A as the main αGC uptake receptor for iNKT activation (88).

Chemical modification could alter the receptor-dependent uptake of glycolipids to DCs. Addition of one unsaturation on the acyl chain or modification of the head group such as the addition of the second galactose to αGC strongly influence the LDL-R-mediated uptake of the lipid variants and abolished their uptake via the SR-A (88).

The nature of the lipids also defines the transport to different endosomal compartments. Lipids with longer alkyl chains are sorted to late endosomes, corresponding to the localization of CD1b. Lipids that have multiple unsaturated or shorter saturated tails are directed to early- or recycling endosomes, surveyed by CD1a or c (71).

Upon intravenous injection, αGC in the serum was also associated with monomeric LTPs such as FAAH. The FAAH-transported αGC uptake was mediated by SR-A (87).

2.2.5. Lipid antigen processing and loading

Inside the cells, lipids are usually present in membranes or associate with proteins. For presentation, lipids have to be extracted from their milieu, processed and loaded into the antigen binding pocket of CD1 molecules. These processes are assisted by hydrolases and LTPs. Some lipid antigens require partial degradation to become antigenic. The synthetic glycolipid αGGC processing requires the removal of the terminal galactose of the precursor lipid to become potent αGC by α-galactosidase hydrolase enzyme, located in late endosomes (89). Lysosomal Hex-B generates immunogenic iGb3 after removal of the β-linked terminal acetylgalactosamine from isogloboside 4 (iGb4) (75). Lipid extraction to the lumen is mediated by LTPs that facilitate loading or replacement of lipid antigens to CD1 molecules in the endosomal compartments. Besides its fundamental role in endogenous lipid loading in the ER, lipid editing function of MTP is also involved in exogenous lipid presentation by replacing ER-derived lipids with lipids present in the late endosomes or lysosomes (52, 53). GM2 activator proteins participate in lipid processing as a chaperon that either extract or load lipids to CD1d (90). In addition, CD1e is also linked to the glycolipid antigen processing and transfer to CD1 molecules (72).

CD1d lipid antigens are edited by saposins (Saps), membrane-perturbing sphingolipid activator proteins (91). Active saposins (SapA-D) are generated from the precursor prosaposin in the late endosomes. This process is catalyzed by cathepsins (Cats) (92). Saposins directly bind lipid antigens, extract them from endosomal membranes, and transfer them to CD1 proteins, while the loading of the lipids onto CD1 molecules is an indirect process. The *in vivo* relevance of Sap-mediated lipid presentation was determined in $Sap^{-/-}$ mice (90). Sap deficiency leaded to defective iNKT development in the absence of prosaposin, because thymocytes of these mice failed to stimulate iNKT cells. In contrast to the impaired iNKT development, the number of the type II NKT cells was normal (93). Importantly, CD1d expression, cellular distribution and iNKT cell autoreactivity were not affected by Saps but the presentation of αGC was affected to CD1d-resticted iNKT cells (90, 91, 94). The αGC can bind to cell surface CD1d molecules without endosomal recycling, but it was shown that Saps facilitate the intracellular CD1d/αGC complex formation in lysosomes (95). Each Sap has preferences for a subset of lipids, based on their nature. SapB loads iGb3 and sulfatide onto CD1d, while αGC editing is dependent on SapA. Sap deficiency leads to dysregulated lysosomal lipid accumulation, lipid traffic and exchange between membranes. The impaired lipid metabolism results in lysosomal storage diseases which affect CD1d loading (93).

2.2.6. Lysosomal Cathepsins in DCs

Immunogenic lipid presentation is depended on proteolytic mechanism in the lysosomes of DCs. Most lysosomal proteases are known as Cats, which are essential for both peptide and lipid antigen presentation (96, 97). Cats are synthetized as zymogens, and become active after removal of their amino-terminal pro-domain, that occupies their active sites. Cysteine proteinases-mediated proteolysis is critical for the antigen-presentation in DCs, wherein controls the lipid editing by cleaving of Ii and pro-saposins in late endosomes (98). In response to maturation signals, DCs acquire higher capacity for lipid editing by enhanced lysosomal activity, characterized with elevated antigen processing and lipid/CD1 complex formation (99). This enhanced proteolytic capacity does not reflect increased protease level, because iDCs and mDCs have similar level of Cats. However, in iDCs, a substantial portion of CatL is present in proenzyme form and its activation is increased by maturation.

CatL, S, and B have shown to be expressed in DCs (100). Amongst them only CatL and S have been connected to lipid antigen-presentation to date (97, 101). In CatS deficient ($CatS^{-/-}$) mice, MHCII complexes were accumulated in endosomal vesicles, that might affect the intracellular CD1d transport to the membrane. CatS deficiency leaded to reduced level of cell surface CD1d in the thymic DCs. Moreover the intracellular trafficking of CD1d was also affected in $CatS^{-/-}$ DCs. iNKTs were functionally defective in these mice, secreting reduced amount of INFγ and were not reactive to αGC, presented by WT DCs (101). The number of iNKT cells was also reduced in $CatL^{-/-}$ mice but in contrast to $CatS^{-/-}$ animals, CatL deficiency failed to alter the CD1d level on the cell surface (97). CatL enzyme activity in thymocytes was essential for the positive selection and the enzyme was involved in the negative selection of iNKTs, mediated by APCs. In the periphery, CatL expressed by APCs was critical for the terminal differentiation of iNKTs. In both cases, the deficiency in Cat proteins appeared to impede endosomal events required for potent CD1d-mediated antigen presentation.

DCs have been reported to express lysosomal aspartic proteases such as CatD (102). Similar to cysteine proteases, CatD is synthetized in inactive form (pre-pro-CatD) and are activated by autocatalysis in ceramide-dependent manner (103). The activated CatD are abundant in lysosomes where able to cleave LTPs as prosaposin. The significance of this protease has not previously tested in the context of lipid presentation.

2.2.7. CD1d-resticted NKT cells

Unlike conventional T cells, which recognize peptide antigens, TCRs on NKTs are reactive to lipid antigens in the context of the CD1d (10, 73). CD1d-reactive T cells have been grouped according to their antigen specificity and functional properties. These unique self-reactive T cells express both NK markers and TCRs on their surface (10, 104); hence they are termed as NKTs. There are two types of CD1d-restricted T cell populations: invariant NKT (iNKT) cells, otherwise known as type I NKTs and diverse NKTs (dNKTs), which are more commonly referred as type II NKTs.

iNKTs represent a unique population of evolutionarily conserved subset of innate lymphocytes which express highly restricted set of TCR, composed of a semi invariant α chain (Vα14-Jα18 in mice and Vα24-Jα18 in humans) paired with a restricted repertoire of β chains (Vβ2, Vβ7, and Vβ8.2 in mice, or Vβ11 in humans) (10). iNKTs express a variety of homing receptors licensing them to migrate to lymphoid or into non-lymphoid organs, including skin, liver and lung (105). Moreover iNKTs acquire a constitutive memory phenotype that enables immediate reaction upon their activation (106). INFγ and IL-4 transcription is activated during iNKT thymic development, and preformed IL-4 mRNA in the cytoplasm allows the rapid cytokine secretion upon antigen stimulation (107, 108). iNKT differentiation is governed by key TFs, PLZF, TBET and RORγ, that serve as markers to define murine iNKT subtypes subdividing them into iNKT1, iNKT2 and iNKT17 cells with the secretion of key cytokines IL-4, INFγ, and IL-17, respectively (105).

In mice, iNKT comprise approximately 1 to 3% of lymphocytes in the blood and lymphoid organs, and are enriched in the liver, where they represent up to 30 % of resident lymphocytes (109). The calculated frequencies were much lower in humans (110).

In the periphery their subsequent activation results in a rapid cytokine burst within hours by which transactivates other lymphocytes. Indeed, iNKTs are involved in a wide range of immune relevant processes such as maturing DCs, activating NK or B cell or biasing T cell responses, hence iNKTs regulate both innate and adaptive immunity, modulate the ongoing immune responses, that can influence the outcome of various disease from autoimmune responses, bacterial or viral infection and cancer (111).

The potent role of iNKTs in providing tumor immune surveillance was demonstrated by αGC injection, and in several studies without administration of the antigenic lipid ligand, supporting the notion that iNKTs can recognize endogenous antigenic lipids produced by tumor cells (83, 112-115). The essential function of iNKTs was demonstrated in $J\alpha18^{-/-}$ mice, in

which adoptively transferred iNKT cells elicited protection against tumors (112). Depending on the tumor model, resident iNKT reactions can lead to effective anti-tumor immunity through down-stream activation other immune cells by initiating Th1 cytokine cascade in the tumor-associated stroma (TAS), thus orchestrating local activation of effector cells, such as NK and $CD8^+$ T cells, which ultimately kill tumor cells. As a feedback loop, iNKT activation also contributes to DC activation through the CD1d-TCR and CD40-CD40L interactions, which induce DC maturation and IL-12 expression (116). Secreted IL-12 stimulates NK and iNKT cells to produce even more INFγ, and the two cytokine together trigger NK and $CD8^+$ T cells (117-119). Co-administration of peptide antigens with iNKT agonist has adjuvant effect (116, 120). As a consequence of iNKT activation, DCs up-regulate CD70 co-stimulatory receptors, essential for cross-priming to $CD8^+$ T cells. $CD8\alpha^+$ DCs produce CCL17, which attracts $CCR4^+/CD8^+$T cells for subsequent activation and their polarization toward anti-tumor effectors (121, 122). iNKTs also alter the effects of immunosuppressive cells by reversing (myeloid-derived suppressor cell) MDSC-suppression and CD1d-dependent elimination of TAMs (123, 124).

Conversely, type II NKTs express a polyclonal TCR repertoire (125). The limited reagents to monitor type II NKTs and the absence of specific surface markers have limited the functional characterization of this NKT population. In contrast to αGC, there is not known antigen that can uniformly stimulate all type II NKTs. The immune functions of a fraction of type II NKTs can be analyzed by sulfatide/CD1d tetramers, because these complexes do not activate iNKTs (126). The frequency in number of these cells is lower than their type I counterparts in the mouse spleen but is very frequent in the human BM and liver (127).

The *in vivo* relevance of NKT activation can be characterized in $CD1d^{-/-}$ mice lacking both iNKTs and type II NKTs (128). To determine the specific function of the two NKT populations, the immunophenotype of $CD1^{-/-}$ mice have to be compared with $J\alpha18^{-/-}$ mice, which lack only iNKTs (129). These animal models have been very useful in defining the unique role of type II NKTs in several pathological conditions. Administration of sulfatide demonstrated that type II NKTs have immunosuppressive function. Once activated, type II NKTs have the capacity to override iNKT-mediated immune responses through immune cross regulation in Concanavalin A (ConA)-induced hepatitis (80). In this model, sulfatide administration resulted in preferential activation of type II NKTs. Sulfatide was presented to type II NKTs by $CD1d^+$ pDCs and facilitated the generation of IL-10 secreting regulatory cDCs. The secreted macrophage inflammatory protein-2 (MIP-2) triggered iNKT recruitment to the liver, wherein became anergized.

In contrast to the protective role of iNKTs in most murine tumor models, type II NKTs have been shown to be sufficient to suppress tumor immune surveillance and had tumor promoting activity (130-132). Sulfatide-reactive NKTs enhanced tumor burden *in vivo* and abolished the clinical effects of αGC when the two agonists were administered together, suggesting that sulfatide-reactive murine type II NKTs can antagonize the potent αGC-dependent protective iNKT responses (133). This immune regulatory axis between the two NKT cell populations and that type II NKTs favor tumor growth by releasing IL-4 and IL-13 were demonstrated in several mouse models (132, 134).

2.3. Nuclear hormone receptors

2.3.1. Classification of nuclear hormone receptors

Members of the nuclear hormone receptor superfamily display diverse roles in the regulation of development, homeostasis and immunity (135-138). As ligand-activated TFs, nuclear hormone receptors can be activated by an array of small lipophilic molecules such as steroids, retinoids and dietary lipids. These ligands are produced either intracellularly or obtained by cells from the surrounding environment. As intracellular sensors of lipophilic compounds, nuclear hormone receptors bind their activating ligands, deliver metabolic or hormonal signals directly at a transcriptional level and translate these sensed signals into physiologic effects. Human and mouse genome encode genes for 48 or 49 nuclear hormone receptors, respectively (139). Traditionally, nuclear hormone receptors are classified into three groups (Table 2). "Classic" steroid hormone receptors are activated by endocrine ligands (endocrine receptors). The ligands of these receptors had been identified before cloning of the cognate receptors. These hormones bind to their receptors with high affinity. Later by analyzing sequence similarity to previously known receptors, dozens members of the superfamily have been identified initially without physiological ligands and functions; therefore they were referred as "orphan" nuclear hormone receptors. Once their natural ligands have been identified by reverse endocrinology, corresponding orphans have considered to be "adopted". This group of nuclear hormone receptors can be activated by low-affinity endogenous ligands as dietary lipids (138, 140). Nuclear hormone receptors are conserved in all metazoan species. In 1999 the nomenclature system for the nuclear hormone receptor superfamily has been unified. The members of the superfamily have been categorized into six distinct groups according to sequence homology and phylogenetic analysis, identifying each nuclear hormone receptors with less ambiguity (141).

2.3.2. Structure of nuclear hormone receptors

Nuclear hormone receptors share a common domain organization (142, 143) (Figure 5). A typical nuclear hormone receptor consists of five-six functional regions. The variable N-terminal domain (NTD or A/B domain) is the most diverse domain among these receptors. "Classic" hormone receptors have the largest A/B domains, ranging from 400 to 600 amino acids, while A/B domains of non-steroid receptors are much shorter (144, 145). Most A/B domains include activation function-1 (AF-1) region which can mediate ligand-independent

transcriptional activation. The highly conserved DNA binding domain (DBD or C region) contains two typical cysteine-rich zinc finger motifs, targeting the receptor to specific hormone response elements (HREs) which are *cis*-regulatory DNA sequences in the enhancer of target genes (146). The first zinc finger contains the proximal- or P-box, a highly conserved section region, which determines the sequence specificity of the receptor-DNA binding (147). The distal- or D box in the second zinc finger determines the half-site spacing and allows the ligand binding domain (LBD or E domain) to hetero- or homodimerize (148-150). The hinge or D domain is a poorly conserved segment and behaves as a flexible bridge between DBD and LBD. LBD domain contains four functionally interacting but structurally distinct surfaces: 1, dimerization interfaces; 2, activation function-2 (AF-2) region, required for the ligand-dependent transcriptional activation; 3, ligand binding pocket (LBP) that specifies the ligand binding to the receptors; 4, cofactor-binding surfaces that mediate recruitment of co-activator or co-repressor complexes to the receptor (138, 151, 152). The size of the LBP varies between nuclear hormone receptors. Steroid hormone receptors have a relatively small so called ”tight-fitting” LBPs and their ligands bind to LBDs with high specificity and affinity, while other receptors such as peroxisome proliferator-activated receptors (PPARs) own large LBPs accepting more, structurally divers activating ligands with lower specificity and affinity (151, 153, 154). The C-terminal F region is not present in all receptors, and its function is poorly characterized.

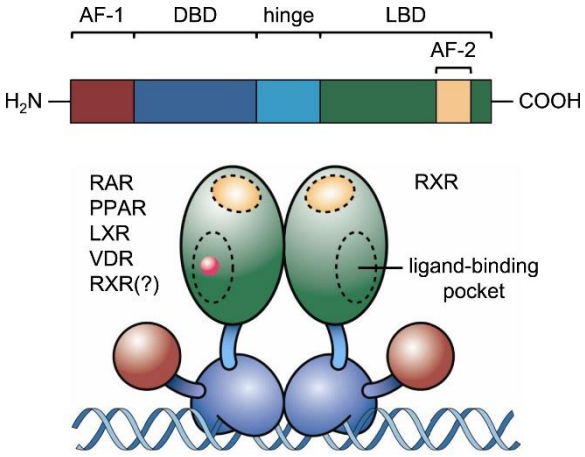

Figure 5: Functional domains of nuclear hormone receptors*. Nuclear hormone receptors consist of 5-6 functional domains: N-terminal A/B region is the ligand-independent activation domain (including activation function-1 (AF-1)), C region (DNA binding domain (DBD)) defines DNA-binding, the D region acts as a hinge, while the E (ligand binding domain (LBD)) is responsible for the ligand-dependent transactivation domain. M. Kiss, Journal of Allergy and Clinical Immunology, Volume 132, 2013, 264-286.*

As TFs, nuclear hormone receptors rely on sequence-specific binding to regulate their target genes (155). Majority of nuclear hormone receptors bind to HREs as monomers, homo- or heterodimers with the retinoid X receptor (RXR). Sequence specific HREs consist of one or two hexa-nucleotide half-sites. The consensus sequence motif of the non-steroid nuclear hormone receptor is AGGTCA or its variants, separated from each other by a spacer with variable length. The binding specificity of the receptors is largely directed by the spacing, sequence and the orientation of the two half-sites. Recognized half-sites can be configured as direct repeats (DRx, AGGTCA-Nx-AGGTCA, where N is any nucleotide and x is the number of spacer nucleotides, present between the two half-sites), everted repeat (ERx, ACTGGA-Nx-AGGTCA) or inverted repeat (IRx, AGGTCA-Nx-ACTGGA). Classic steroid receptors as homodimers recognize inverted repeats (IR), while non-steroid nuclear hormone receptors bind to high-affinity DRs with distinct half-site spacing (i.e. PPARs-DR1, liver X receptors (LXRs)-DR4, retinoic acid receptors (RARs-DR2-DR5) or IRs as farnesoid X receptor (FXR)-IR1). The pattern of half-site selectivity is based on the receptor-specific spacing of DRs, an axiom that was became known as 1–5 rule (138, 142, 152, 155-157). Orphan receptors recognize HREs as monomers, dimers or heterodimers with the exception of DAX1 and SHP atypical nuclear hormone receptors , which lack DBD, bind to AF-2 of other nuclear hormone receptors, prevent co-activator binding or recruit co-repressor complexes, leading to transcriptional repression (158).

The “classic” steroid hormone receptors such as glucocorticoid receptors (GR) are located in the cytoplasm in the absence of ligands. They form complexes with chaperons including heat shock proteins (159). Upon ligand binding they release from chaperons, translocate to the nucleus and bind to their HREs. Other receptors in the “classic" group such as vitamin D receptor (VDR) and RARs form heterodimers with RXR, allowing a more complex and combinatorial regulation of their target genes by integrating different signaling networks. These heterodimers are located in the nucleus and regulate (either promoting or repressing) gene expression by different mechanisms. Generally, in the absence of ligand, nuclear hormone receptors bind to HREs and held inactive by co-repressors, such as silencing mediator of retinoid and thyroid signaling (SMRT) and nuclear receptor co-repressor (NCoR) in association with histone deacetylases (HDAC3) (160-163). Deacetylation leads to chromatin compaction and suppression of basal transcriptional activity, mediating the process called direct repression. Upon ligand binding, a conformational change occurs in the receptors facilitating co-activator complex recruitment and co-receptors releasing. These co-factor changes direct local covalent histone modifications and chromatin remodeling at their associated target genes to induce

chromatin decompaction and gene activation. Among these co-activators, the members of p160 recruit immediately to the nuclear hormone receptors and CBP/p300 family harbor histone acetyltransferase activity (HAT), whereas co-activator-associated arginine methyltransferase 1 (CARM1) histone methyltransferase modify the chromatin template by arginine and lysine methylation (164, 165). These initial chromatin-modifying steps are followed by the actual recruitment of the RNA polymerase II holoenzyme and components of the basal transcription machinery. In some cases, nuclear hormone receptors also can mediate transcriptional repression when co-repressors bind to RXR heterodimers in ligand-dependent manner. Finally, certain heterodimers such as PPARγ interfere with gene expression in ligand-specific, but sequence-independent manner. In the process of transrepression, nuclear hormone receptors prevent transcriptional activation of other signal-induced TFs such as nuclear factor κB (NF-κB) or activator protein-1 (AP-1), by stabilizing formation of a co-repressor complex at target regulatory elements, thus nuclear hormone receptors have the ability to integrate and co-regulate diverse signaling pathways and modulate the activities of other major signaling cascades (166).

Nuclear hormone receptor superfamily		
Endocrine receptors	**Adopted orphan receptors**	**Orphan receptors**
Steroid receptors	RXRα,β,γ 9-*cis* retinoic acid	DAX-1
GR glucocorticoid	PPARα,β,γ fatty acids	SHP
ER estrogen	LXRα,β oxysterol	NR4Aα,β,γ
MR mineralocorticoid	FXR bile	Rev-erbα,β
PR progesterone	PXR xenobiotics	COUP-TFα,β,γ
AR androgen	CAR androstane	
RXR heterodimers	RORα,β,γ retinoic acid	
TRα,β thyroid hormone	ERRα,β,γ estrogen?	
RARα,β,γ retinoic acid		
VDR vitamin D		

Table 2: *Classification of the nuclear hormone receptor superfamily. Receptors and their representative ligands are listed. Based on (167).*

2.3.3. Nuclear hormone receptors in human mo-DCs

A global gene expression analysis revealed that some nuclear hormone receptors including PPARγ and LXRα are expressed and induced in differentiating DCs (168). Later our microarray profiling demonstrated that 20 out of the 48 nuclear hormone receptors are expressed in human mo-DCs (169). These findings suggested that non-steroid nuclear hormone receptors may have potent functions in DC development and functions. RXRs are unique nuclear hormone receptors with the ability to form heterodimers with one third of the nuclear hormone receptor family (170, 171). In most cases, RXRs act as obligate partner for high affinity binding to corresponding HREs for transactivation (138). RXR heterodimers are classified into functionally distinct non-permissive and permissive subgroups. Non-permissive heterodimers (RAR/RXR) are unresponsive to the activation from the RXR side and can be activated only by the partner receptor's agonists (171). Ligand–induced activation of RXR is prevented by the partner receptor through blocking the ligand binding to the RXR. This phenomenon is referred as "silencing" and RXR is considered as a "silent partner" in these heterodimers (172, 173). RXR can be activated in the RAR/RXR heterodimer in the presence of RAR ligands and simultaneous activation of RXR and RAR enhances the transcriptional response to the RAR ligand. In contrast, (PPAR/RXR) permissive heterodimers can be activated by either RXR ligands or a NR partner's agonist and heterodimers activation in the presence of both ligands results in a co-operative, synergistic response compared to that resulting from binding of only a single receptor ligand. Moreover, RXR can form heterodimers with Nurr77 and Nurr1 with atypical LBD, unlikely to be occupied by any ligand (174).

Recently we have surveyed the expression pattern of each potential RXR partners and RXRs in human developing mo-DCs to explore the full map of RXR heterodimers in these cells (175). These data confirmed our previous results that the dominant RXR subtype is the RXRα in these cells. Among RXR partners, LXRα, PPARγ, PPARδ/β, VDR and RARα are highly expressed in mo-DCs and are robustly induced at transcriptional level during DC differentiation, while the expression of LXRβ is decreased. Nur77 and Nurr1 are expressed in freshly isolated monocytes but during the first day of the differentiation, their expression levels were reduced dramatically. Other potent RXR partners (such as RARβ) are not expressed or are detectable at very low level in this cell type. Based on our global gene expression and pharmacological analyses, RXRs may act as homodimers or may be as a potent functional partners for PPAR (γ, δ), LXR (α, β) (permissive heterodimers) and for VDR, RARα (non-permissive heterodimers) in differentiating mo-DCs. Among RXR partners, the role of PPARγ/RXR and RARα/RXR

heterodimers in developing mo-DCs will be introduced in the next chapter as the activation of these receptors leads to phenotypic and functional changes in DCs by co-ordinate regulation of a set of their responding genes (175).

2.3.4. The role of retinoid acid receptors in DC biology

Vitamin A/retinol and its derivatives are collectively known as retinoids. The essential function of vitamin A has been identified in vision, embryonic development, immune competence and reproduction (176-179). Deviation from optimal retinoid level is associated with a variety of human diseases including visual disorders, infectious diseases and cancer (176, 178, 180). All-*trans*-retinoic acid (ATRA), the highly potent biologically active metabolite of retinol, prevents and rescues the main defects caused by Vitamin A deficiency in adult animals, while 11-*cis*-retinaldehyde displays a key role in visual function (137, 176).

Retinoids exerts their pleiotropic effect in target cells by inducing the transcriptional activity of the nuclear retinoid receptors (181). RARs consist of three subtypes involving RARα (NR1B1), RARβ (NR1B2) and RARγ (NR1B3), which molecules are encoded by separate genes and the isoforms of all receptor subtype are generated by alternative splicing. RARs form heterodimers with RXRs, which also have three subtypes, RXRα (NR2B1), RXRβ (NR2B2) and RXRγ (NR2B3) (182) . Although both ATRA and 9-*cis* retinoic acid activate RARs, RXR binds 9-*cis* retinoic acid only (183). 9-*cis* retinoic acid, docosahexaenoic acid and phytanic acid have been identified as putative natural RXR activators but none of these compounds have been evidenced as an endogenous ligand *in vivo* (reviewed in ((184)). The rexinoids are synthetic RXR activators with receptor isoform selectivity give raise the possibility to assess the contributions of each RXR isoforms to retinoid signaling pathways (185).

2.3.4.1. Source of retinoids

Vertebrates do not have the ability for *de novo* retinol synthesis but can obtain this vitamin from the diet as retinyl ester or carotenoids (186, 187). Retinyl esters are hydrolyzed in the intestinal lumen by pancreatic lipase and phospholipase B, incorporated with carotenoids into mixed micelles and absorbed by enterocytes (188-191). In enterocytes, carotenoids are metabolized to retinyl esters and secreted into the lymph in chylomicrons, transported predominantly to the liver, the main retinoid store in the body (192, 193). Retinyl esters are

continually hydrolyzed into retinol from the liver store, binds to Retinol binding protein 4 (RBP4), which delivers it to target tissues (194).

2.3.4.2. Retinoids in target cells (cellular up-take and transport)

Retinol target cells express a highly conserved multi-transmembrane domain protein, the stimulated by retinoic acid-6 (STRA6) transporter (195), that mediates the binding of RBP-retinol and facilitates retinol uptake to the cells. Cells may take up retinol through the recently identified RBP4 receptor-2 (RBPR2) transporter. The structure of RBPR2 is related to human and murine STRA6 and therefore the receptor may be an alternative retinol transporter for STRA6 negative cells (196).

Within the cell, retinoids are bound by cellular retinol binding proteins (CRBPs) that solubilize retinoids in the hydrophilic nature and protect them from oxidation and isomerization (197). CRBP1 targets retinol for storage or toward metabolic enzymes such medium-chain alcohol dehydrogenases (ADHs) or short-chain dehydrogenase/reductases (RDHs) that convert retinol to retinal (Figure 6). Subsequently, retinal dehydrogenase (RALDH) enzymes synthetize ATRA form retinal (198). ATRA associates with cellular retinoic acid-binding protein 1 (CRABP1), CRABP2 or fatty acid-binding protein 5 (FABP5) transporters (199). Upon binding of ATRA, cytosolic CRABP2 delivers ATRA directly to RARs through direct protein-protein interactions and enhances the transcriptional activity of the receptors (200). Interestingly, CRABP2 does not contain recognizable nuclear localization signal (NLS), but during ligand binding a conformational change is induced in the protein and CRABP2 becomes recognizable by nuclear import proteins such as importin-α (201). During embryonic development both CRABP1 and 2 molecules are widely expressed in the embryo but usually localized in different cells (202, 203). In adults, CRABP1 is widely expressed, while the expression of CRABP2 is restricted to the liver, skin, testis, uterus, ovary and the choroid plexus (204-208). The altered expression profiles reflect distinct function of CRABP1 and CRABP2 in retinoid biology.

CRABP1 moderates the cellular response to ATRA by transporting it to enzymes involved in the ATRA catabolism (199). Intracellular ATRA level is tightly regulated by the members of cytochrome P450 gene family: CYP26A1, CYP26B1 and CYP26C1 (209-211). Polar metabolites generated by these catabolic enzymes are more easily excreted from cells. $Cyp26A1^{-/-}$ mice confirmed the importance of ATRA degradation in cells to protect against teratogenic exposure of retinoids (212). Importantly, the proximal upstream promoter region of

the *Cyp26a1* gene contains a functional retinoic acid response element (RARE), therefore *Cyp26a1* gene expression is directly regulated by RARs (213).

FABP5 transfers ATRA to PPARβ/δ and activates PPARβ/δ-mediated transcription. This selective ATRA delivery, mediated by binding proteins, provides a mechanism to induce dissimilar ATRA actions (214).

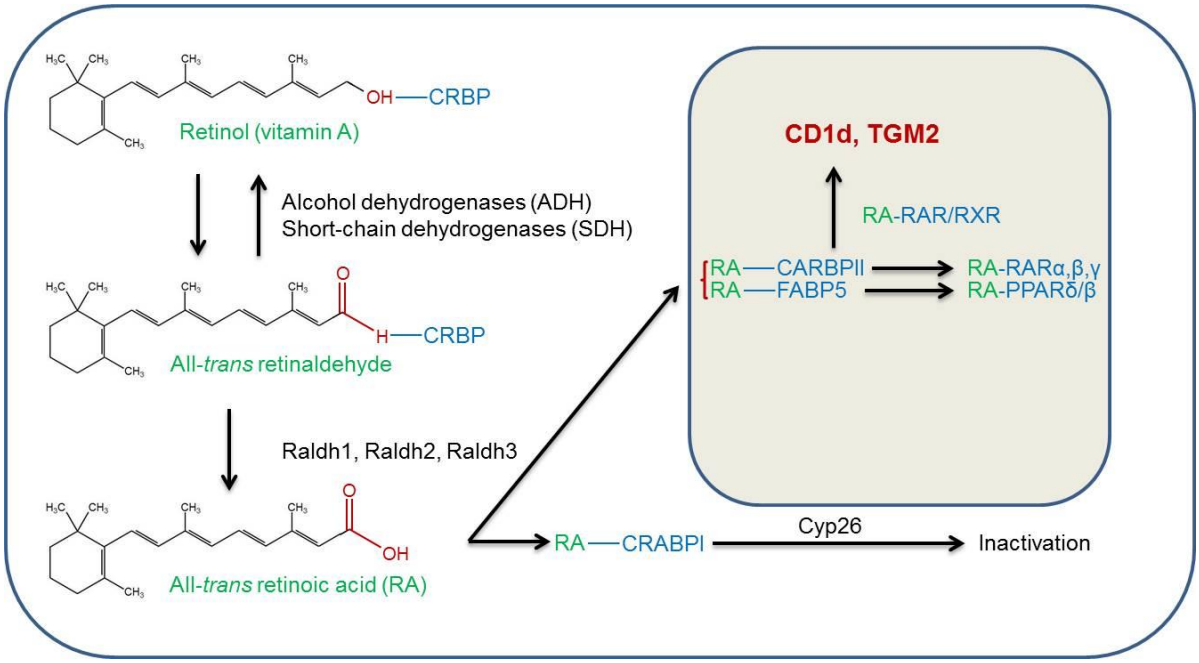

Figure 6: Component of the cellular retinoid metabolism. *Retinol is converted to all-trans retinaldehyde by alcohol dehydrogenases (ADHs) or short-chain dehydrogenase/reductases (SDRs). The second enzymatic step of this metabolic pathway is mediated by retinaldehyde dehydrogenase (RALDH) enzymes generating all-trans retinoic acid (ATRA). ATRA is transported to the nucleus by fatty acid-binding protein 5 (FABP5) and* cellular retinoic acid-binding protein 2 (*CRABP2) to RAR. ATRA is inactivated by cytochrome p450 26 (Cyp26) enzymes.*

2.3.4.3. Retinol metabolism

For exerting physiological function, retinol obtained either from the diet, liver deposit or bile, and has to be converted during two consecutive oxidative reactions for metabolic activation (Figure 6). In the first rate-limiting oxidative step retinol is converted to retinal. This enzymatic reaction can be catalyzed either by alcohol dehydrogenases (ADH1, ADH3, and ADH4), members of the medium-chain dehydrogenase/reductase (MDR) superfamily or by retinol dehydrogenases that are members of the short-chain dehydrogenase/reductase superfamily

(SDR) (retinol dehydrogenase 1 (RDH1) and RDH10) (215-218). Due to the reversible nature of these reactions, retinal can be reduced back to retinol through the action of some RDHs such as DHRS3 (219). It was demonstrated in studies utilizing retinol/CRBP1 as a substrate, that 80-94% of cellular retinal-generating capacity resided in the microsomes (intracellular localization of RDHs), rather than the cytosol (site of ADHs) (220). Currently at least three RDHs are seem to be physiologically participating in converting retinol to ATRA: RDH1, RDH10 and DHRS9 (221). DHRS9 have all-*trans* or *cis*-retinol dehydrogenase activity *in vitro* and are contributed to ATRA metabolism in transient transfection systems. RDH10 specifically oxidize**s** all-*trans*-retinol as substrate. RDH10 was identified as all-*trans* retinol dehydrogenase in the RPE BX and was purified from the microsomal fraction of rMC-1 cells (222, 223). The role of RDH10 for embryonic ATRA synthesis was identified by N-ethyl-N-nitrosuera (ENU)-induced forward genetic screen method (217). The missense point mutation in *Rdh10* generated by Ethylnitrosourea eliminated the RDH10 retinol dehydrogenase activity in mice. These trex/Rdh10 mutants had severe organ abnormalities and an embryonic lethal phenotype at embryonic day 13.5. Retinal supplementation between gastrulation and early fatal stage leaded to viable $RDH10^{-/-}$ mice however, these animals still suffered from severe developmental abnormalities (224). The fundamental role of RH10 in embryonic development has been confirmed utilizing $RDH10^{-/-}$ mice, carrying the *RARE-lacZ*-reporter transgene, which monitor endogenous sites of retinoid signaling (217, 225).

The second enzymatic step is the irreversible oxidation of retinal to ATRA, mediated by RALDH1/ALDH1A1, RALDH2/ALDH1A or RALDH3/ALDH1A3, members of the aldehyde dehydrogenase family (198, 226). Genetic deletion experiments in mice have established the physiological contribution of RALDH isoforms to ATRA production and vital functions of RALDH2 during the embryonic development (221, 227, 228). $RALDH2^{-/-}$ mice showed early lethality suggesting that this enzyme was essential for embryonal ATRA production (229). These experiments also indicated that the sites of RDH10 expression overlapped with RALDH2 sites suggesting that co-expression of the two metabolic enzymes was required for active ATRA generation in developing embryos.

2.3.4.4. The effects of retinoids on DCs

Retinoids also have potent immune modulatory capacity and exert their effects on multiple immune cells. The ability of retinoids to promote myeloid cell differentiation was demonstrated by extensive research of acute promyelocytic leukemia (230). *In vitro* data showed that Vitamin

A enhances T and B cell proliferation and survival and 9-*cis* retinoic acid effectively prevented activation-induced apoptosis in T cells (231-234). Furthermore, it has been demonstrated that retinoids regulated DC differentiation and immunogenicity by activation retinoid receptors (235, 236).

The expression of RARs was examined in murine Sp-DCs, which express all RAR subtypes (α, β and γ), in LP- and colonic DCs expressing predominantly RARα (237, 238) . Our previous results assessed the transcript levels of retinoid receptors in human mo-DCs (239). Based on microarray analysis, real time quantitative PCR (RT-qPCR), Western blot and IHC data we concluded that the RARα/RXRα is likely to be the dominant heterodimer in developing mo-DCs.

Retinoids play an important role in the development of mouse BM-DCs in the presence of GM-CSF. Depleted serum retinol decelerated the differentiation of DCs, whereas ATRA or 9-*cis* retinoic acid supplementation significantly restored the number of DCs and inhibited the granulocyte development. These results indicated that retinoic acid supported the differentiation of myeloid progenitors to iDCs instead of granulocytes when dietary retinol was adequate. Interestingly, retinol significantly reduced the DC development in Flt3L treated cells (240).

The retinoid-mediated effects on DC homeostasis have also been demonstrated in humans. ATRA modified the differentiation of DCs from circulating peripheral blood monocytes (ATRA-DCs). ATRA-DCs exhibited DC morphology and iDC phenotype. The retinoid also up-regulated the cell surface levels of co-stimulatory molecules (CD40, CD80 and CD86) and enhanced the proliferative capacity of naïve $CD4^+$ T cells primed by ATRA-DCs. Although ATRA-DCs retained their antigen-capture capacity, they secreted interleukin IL-12 without addition of any maturation agent. In addition, ATRA-DCs could drive the differentiation program of T cells towards an IL-12-dependent Th1 response with INFγ secretion (241). A subsequent study characterized further the function of retinol and ATRA in mo-DCs. Retinoids induced dose-dependent increase in the membrane expression of CD86 and induced MHCII translocation from cytoplasmic compartments to the cell surface in the presence of TNFα. ATRA co-operated with inflammatory cytokines, increased the DNA binding activity of NF-κB and enhanced the antigen specific T cell response triggered by DCs (236). Moreover, ATRA increased the migratory capacity of DCs to reach the nearest lymph node by upregulating the secretion of matrix metalloproteinase 9 (MMP9) and 12 and inhibiting that of tissue inhibitors of matrix metalloproteinases (TIMPs). Mature DCs showed increased migration capacity in matrigel toward the lymphoid chemokines CCL19 and CCL21, due to the enhanced capacity of

these cells to degrade the extracellular matrix (242). The physiological function of retinoids in the immunogenicity of DCs was demonstrated in case of epidermal LCs. Activation of LCs after topical administration of ATRA enhanced the LC antigen presentation capacity to $CD4^+$T cells (243). Moreover, retinoid treatment restored the aberrant distribution of LCs in psoriatic epidermis of patients (244). The homeostasis of developmentally related splenic $CD11b^+/CD8a^-/Esam^{high}$ DCs and intestinal LP-$CD103^+/CD11b^+$ DC subset is critically controlled by the retinoid signaling (245). Both DC populations were reduced in mice with chronic vitamin A deficiency (VAD) indicating that VAD causes significant reduction of DCs not only in the intestine but also in the central lymphoid organ. A reduced DC number could also be observed after total body irradiation (TBI), which exerted significant injury in the small and large intestines. This injury leaded to failure of retinol absorption and VAD in treated patients. It was also shown that TBI followed by ATRA administration enhanced the MHCII-mediated antigen presentation capacity of DCs and increased their $CD4^+$ T cell-dependent antitumor immunity and autoimmune responses in mice, correlating with the restored level of $CD11b^+/CD8a^-$ Sp-DC subset. Similar positive effect of dietary retinoids has been examined mice fed with a diet containing vitamin A acetate (VAA) and 13-*cis*-RA. Beside increased number of accessory cells in the paracortical region of the LNs and in splenic marginal zone, DC cells had enhanced antigen-presenting cell function evidenced by both alloproliferative and allocytotoxic T cell responses *in vitro* (245).

However, in contrast to their above mentioned positive effects, retinoids can modulate the DC-mediated immunity negatively as well. Retinoids induced the apoptosis of DC through caspase dependent/FasL-independent pathways in iDCs (236). The apoptotic effect of retinoids was transduced through RARα/RXR-dependent signaling and was restricted to iDCs because neither monocytes nor mDCs showed cell death upon retinoid treatment. ATRA reduced the allogeneic stimulatory effect of Sp-DCs in *in vitro* mixed leucocyte reaction (MLR) (246). Moreover, DCs isolated from mice kept on VAA-enriched diet have reduced capacity to stimulate allogeneic T cells.

The effects of ATRA on DCs derived from human cord blood monocytes helped to clarify the role of retinol on immune functions in children (247). Monocytes differentiated *in vitro* to DCs yielded a reduced number of mo-DCs with significantly lower IL-12 secretion. ATRA-treated DCs favored Th2 polarization with higher IL-4, IL-10 and lower INFγ cytokine secretion. The negative function of ATRA on DC differentiation and maturation has been further supported recently on mo-DCs. These DCs produced a low level of IL-12 and high amount of IL-10 by which triggered Th2 and Treg differentiation (248). Activation of Sp-DCs

by the TLR2 ligand zymosan leaded to extracellular signal-regulated kinase (ERK) activation and RALDH2 expression in DCs (249). DCs utilizing retinol metabolized ATRA which exerted an autocrine effect on DCs, triggering suppressor of cytokine signaling-3 (SOCS3) via RAR and RXR receptors. SOCS3 attenuated p38 MAPK activation and secretion of pro-inflammatory cytokines (IL-12, IL-6, IL-23 and TNFα). In contrast, zymosan induced robust IL-10 production. ATRA and IL-10 synergistically educated DCs to induce Treg cells (with TGFβ) or IL-10 secreting Type 1 regulatory T cells (Tr1) (without TGFβ) differentiation via autocrine feedback loop (249).

9-*cis* RA and fenretinide (4-HPR) rexinoid specifically inhibited the functional up-regulation of CCR7 on human mDCs and on murine BM-DCs; 4-HPR also reduced the expression of CXCR4, therefore, inhibiting *in vitro* migration of human DCs toward CXCL12. *In vivo* experiences showed that, 4-HRP also impaired CCR4-mediated DC mobility (250).

2.3.4.5. ATRA synthesis in DCs

Numerous data have demonstrated that multiple factors including ATRA, retinol, GM-CSF, IL-4, TLR ligands can promote or in case of prostaglandin E2 (PGE2) can inhibit the ATRA synthesis in the cells (239, 249, 251, 252). These imprinting factors promote the expression of *Raldh* genes, indispensable markers for active ATRA synthesis in DCs. First, Iwata demonstrated that PP- and MLN-DCs synthetized ATRA from retinol and released ATRA enhanced the expression of CCR9 and integrin α4β7 gut homing markers on responding $CD4^+$ T cells which effect was suppressed by citral (RALDH inhibitor) and LE135 (RAR antagonist) (253). According to their results, *Adh5* was expressed ubiquitously and PP-DCs expressed *Adh1* and *4*, suggesting that these enzymes might be responsible for retinol to retinal conversion in adult mice. For the retinal to ATRA oxidation step, PP-DCs expressed *Raldh1* and to a lower extent *Raldh2*, while MLN-DCs expressed *Raldh2* (253). Subsequent studies demonstrated, that *Raldh2* expression in GALT-associated DCs was enriched in $CD103^+$ DC subsets, by which triggered $\alpha_4\beta_7$ and CCR9 more potently than their $CD103^-$ DC compartments (32, 251, 254). It soon became evident that ATRA synthesis is not a universal DC property and only certain DC subsets acquire the ability to produce this retinoid. Enormous research effort has been taken to identify those factors that determine ATRA synthesis capacity in DCs. One hypothesis suggested that RALDH expression is defined by an intrinsic developmental program, restricted to lineage specific DCs. Because common DC progenitors, under the

control of IFR8 and BATF3 TFs, gave rise developmentally related RALDH active ($CD103^+$) and also RALDH negative DCs in the periphery, therefore this idea was excluded (22, 27, 255). However, it is more likely that DCs become imprinted to express RALDHs after migrated into peripheral tissues such as the gut.

ATRA and retinol are pivotal among multiple physiological factors intrinsic to the local intestinal microenvironment (238, 251, 256)**.** The concentration of retinol is significantly higher in the small intestine and MLNs than in the colon, spleen in the steady state and can be reduced in mice kept on VAD diet (238, 257). Small intestine receives retinol also from the bile, which contains significantly higher retinol level than the serum (238). As intestinal epithelial cells (IECs) strongly express *Raldh1*, they may convert ATRA from dietary-, blood-derived- or bile retinol (258). The biologically active metabolites can be provided to adjacent DCs, which constitutively receive ATRA signals from stromal cells (expressing *Raldh1*, *Raldh2*, and *Raldh3*), or intestinal macrophages as well (253, 256, 259, 260). $CD11c^+$ cells in the MLNs of VAD mice displayed dramatically inhibited *Raldh2* expression and RALDH activity that was restored with oral retinol or ATRA supplementation (238, 251, 256, 257, 261). Furthermore, ATRA enhances the ability of DCs to differentiate gut tropic T cells and Tregs and directly regulates the *Raldh2* gene, suggesting that ATRA triggers its own metabolism (238, 256, 257, 261).

BM-DC differentiated in the presence of GM-CSF expressed *Raldh2* and the growth factor had similar positive effect in case of Sp- or Flt3L-differentiated BM-DCs, which originally did not express detectable RALDH2 enzyme (251). The physiological effect of GM-CSF has been confirmed in $CsFR2^{-/-}$ mice, lacking the common GM-CSF/IL-3/IL-5 subunit of the receptor. These mice had decreased number of DCs in LNs and the isolated MLN- and PP-DCs showed markedly lower RALDH activity. GM-CSF was also critical for maintaining RALDH2 expression in cultured BM-DCs. GM-CSF-mediated effects were inhibited by RAR inhibitor, suggesting that ATRA-mediated signals might contribute to the *Raldh2* expression. Other cytokine which triggers DC *Raldh* expression *in vitro* is IL-4 since IL-4-treated Flt3L-BM-DC and Sp-DC expressed *Raldh2* mRNA and had RALDH activity. Intestinal DCs, obtained from $IL\text{-}4R^{-/-}$ mice, lacking the common subunit of IL-4 and IL-13 receptors, displayed similar RALDH activity as compared to wild type (WT) mice. Due to the fact that IL-13 induced the *Raldh2* expression in Flt3L-BM-DCs, this phenomenon might be explained with the presence of IL-13 in the intestinal environment. Interestingly, IL-4 and GM-CSF synergistically primed BM-DCs to generate ATRA *in vitro*, moreover the additive effects of the cytokines was further increased by TLR ligands. This synergistic effect might be important in term of human mo-

DCs, because DCs generated with GM-CSF and IL-4 are widely used for research or therapeutic purposes (251).

Beside cytokines, several TLR ligands were shown to trigger *Raldh2* expression and RALDH activity in Sp-DCs, including zymosan (TLR2), Pam3CSK4 (TLR1/2), Pam-2-cys and follistatin-like 1 (TLR2/6) (249, 257, 262, 263). The Pam3CSK4-triggered *Raldh2* expression was mediated by C-Jun N-terminal kinase (JNK)/mitogen-activated protein kinase signaling downstream of TLR1/2 (263). DCs from TLR2-, TLR6-, or ERK1 deficient mice showed significantly reduced levels of RALDH enzymes in response to zymosan treatment. Moreover, $CD103^+$ MLN-DCs from $TLR2^{-/-}$ mice and mice treated with pan-JNK inhibitor displayed reduced retinol metabolizing activity and lower capacity to induce gut homing receptors on responding T cells (263). The other intracellular signaling pathway that can be required for the retinoid-producing capacity of intestinal APCs is the WntT-β-catenin-mediated cascade, which is constitutively active in intestinal LP-DCs and macrophages. Both LP-DCs and LP-macrophages, obtained from $\beta\text{-catenin}^{-/-}$ mice expressed lower amount of RALDH1 and RALDH2 enzymes. Activation of β-catenin pathway by E-cadherin, TLRs or Wnt ligands in DCs promoted IL-10 and TGFβ secretion, critical for promoting Treg response and for limiting inflammatory responses (264).

PGE2 have been described as an environmental factor which suppresses the retinol metabolizing activity during DC differentiation both in mice and human (252). PGE2 suppressed *Raldh2* expression in BM-DCs *in vitro* through its receptor, prostaglandin E2 receptor 4 (EP4), whereas reduced RALDH activity via activating EP2 or EP4-coupled signaling cascades in mo-DCs. The negative effect of PGE2 in *Raldh2*/*RALDH2* expression was mediated by the inducible cAMP early receptor (ICER) which seemed directly down-regulated RALDH2 transcription because its promoter contains multiple CRE-binding sites (265).

The relevance of examining intestinal retinoid metabolism in DCs was further intensified by the detection of $CD103^+$ DCs in human MLNs. These cells displayed a more mature phenotype by the cell surface expression of CD83 as compared with their $CD103^-$ counterparts and induced α4β7 or CCR9 expression on responding $CD8^+$ T cells efficiently. The DCs-mediated gut-homing expression could be inhibited by LE540 (RARα antagonist), suggesting that human DCs similarly to mouse cells acquire active ATRA metabolic capacity in the gut (266). Furthermore, unique APCs within the LP, with macrophage-like morphology and co-expressed macrophage (CD14) and DC (CD209) markers, elicited potent antigen-specific immune responses through ATRA-mediated signals. These cells express RDH10 and RALDH2,

suggesting that at least some *in vivo* APCs may produce ATRA by utilizing these oxidizing enzymes (267).

Finally, a comprehensive analysis demonstrated that ATRA metabolism could be detected also in extra intestinal tissue-derived DC such as lung and skin DCs by using a flow cytometry-based detection assay. Unexpectedly, the RALDH activity was detected in $CD103^-$ skin migratory DCs, while ATRA producing cells in the lung contained both $CD103^+$ and $CD103^-$ subsets (262). These data collectively demonstrated that ATRA synthesis capacity is not restricted to intestinal DCs and at least some migratory DC subsets in the peripheral tissue produce ATRA under a complex control of imprinting factors including cytokines, signaling pathways and cell-derived lipid mediators.

2.3.5. PPARs in DC biology

DCs express PPARs that also control a broad range of cellular responses in the human body including cell differentiation, proliferation, cell death and inflammation (reviewed in (184)). The PPAR family consists of three isotypes: PPARα (NRC1C1), PPARδ/β (NR1C2) and PPARγ (NR1C3), each of them is encoded in a separate gene. These receptors show distinct tissue-specific distribution with different physiological functions. PPARα is abundantly expressed in tissues characterized by high metabolic activity (liver, skeletal muscle, kidney, heart) and regulates fatty acid oxidation and lipid transport (268, 269). PPARδ/β shows a ubiquitous distribution, while PPARγ expression can be detected in various cell types like adipocytes, macrophages and DCs (168, 268, 270, 271). PPARγ has two full-length isoforms of which PPARγ2 is highly detectable in the adipose tissue, while PPARγ1 has a border expression pattern in the body (270, 272). The PPARγ receptor was initially described in mouse adipose tissue as a master regulator of adipogenesis and also required for the maintenance of adipocyte specific functions (270, 273). $PPAR\gamma^{-/-}$ mice are lipodystrophic and die of placental defects showing the essential regulatory function of the receptor in the control of embryonic differentiation (274). Genetic variants of PPARγ in humans are also associated with lipodystrophy and insulin resistance, providing genetic evidence for the receptor in adipogenesis and glucose homeostasis (275).

In the nucleus for direct transcriptional activation, PPARs heterodimerize with RXRs and bind to their receptor-specific response elements (PPREs) in the promoter or enhancer regions of their target genes (276). The PPRE contains direct repeat sequences separated by one base

pair (DR1). PPARγ can be activated by selective natural ligands, such as the components of the oxidized low-density lipoprotein (oxLDL) and prostaglandin derivate 15d-PGJ2 (277, 278). To date, a wide range of synthetic ligands have been identified. Amongst them, Avandia (Rosiglitazone/RSG) or pioglitazone have been utilized in the therapy of Type II diabetes mellitus (279). Due to the importance of these ligands in the treatment of this disease, PPARγ is the most intensively characterized PPAR isotype.

The PPARγ receptor is expressed in different lineages of immune cells. PPARγ influences myeloid development and macrophage functions as well (277). Ligand activation of the receptor up-regulates the CD36 scavenger receptor, which in turn leads to oxLDL uptake by macrophages. OxLDL delivers even more receptor selective PPARγ activator ligands to the cells that subsequently activate lipid metabolic pathways (135, 280, 281). The altered lipid metabolism through lipid accumulation leads to foam cell formation in atherosclerotic vessels.

Beside this fundamental role in metabolism, the receptor is involved in the regulation of immune responses. Studies on macrophages revealed that PPARγ can be considered as an anti-inflammatory TF but the exact molecular mechanism is still elusive (282). The receptor can attenuate the transcriptional activity of other TFs including NF-κB, AP-1 or NFAT involved in pro-inflammatory signaling pathways, a mechanism known as transrepression, by which inhibits the expression of a various proteins with pro-inflammatory properties such as cyclooxygenase-2 (COX2), inducible nitric oxide synthase (iNOS) and a variety of cytokines. The treatment of cells with PPARγ ligands enhanced the differentiation of classically activated/M2 macrophages with distinct secretory and functional capacity, attenuating inflammatory responses (reviewed in (184)).

The idea that PPARγ might transcriptionally integrate lipid metabolism and inflammatory responses in DCs was supported by increasing amount of evidence. There are several tissues or tissue compartments in the human body wherein DCs are lightly to sense environmental lipids (184, 283). Several lines of *in vitro* experiments presented that the receptor was functional in DCs, contributing the subtype- and functional specification and immune phenotype of the cells (49, 169, 239, 284-289). However, the receptor was not expressed in all DCs but at least in a subset of these immune cells *in vivo* (49, 288-290) . The expression of PPARγ was demonstrated first in murine Sp-DCs (284). Activation of the receptor with the synthetic ligand RSG did not alter the mature phenotype of Sp-DCs *in vitro* and injection of antigen-pulsed, RSG-treated DCs into the footpads of mice did not alter the antigen presentation property of the cells. Activated T cells secreted both Th1 and Th2 type cytokines (INFγ and IL-4, IL-5, IL-10) regardless of PPARγ ligand treatment (284).

Conversely, it was also shown that there was a PPARγ-inhibited IL-12 secretion by iDCs and mDCs. DC-derived IL-12 was indispensable for Th1 promotion and $CD8^+$ T cell activation, suggesting that PPARγ might affect the polarization of DC-directed immune responses (284). First, an extensive microarray analysis revealed that PPARγ gene was up-regulated during human monocyte-to-DC development (168). Subsequently, the expression of PPARγ at mRNA and protein level was confirmed by other investigators (285, 286). These studies demonstrated that synthetic PPARγ ligands and natural agonist upon DC maturation directed developing DC to have a less matured phenotype, characterized with decreased cell surface expression of CD80 and elevated MHCII and CD86 levels.

Similarly to murine Sp-DCs, PPARγ active mo-DCs had altered cytokine secretion pattern, secreting lower amount of IL-12, while the concentration of IL-6 and IL-10 in cell supernatant were unchanged as compared to mo-DCs with lower PPARγ activity. mDCs secreted reduced amount of chemokines involved in the recruitment of Th1 lymphocytes (CXCL10, CCL5 MIP-1a) but PPARγ signaling did not affect the producing of Th2 attracting chemokines (CCL17 and CCL22) (285). The inhibitory effect of PPARγ activators in line with the less matured phenotype of cells resulted in a reduced immunogenicity of DCs (286). However, IL-12 administration to DC/peripheral blood mononuclear cells (PBMC) co-cultured samples failed to revert the reduced level of T cell proliferation, suggesting that the impaired T cell activation of mDCs was not only due to lack of IL-12 but also to other effects that modulate DC maturation process (286). These results suggested that PPARγ active DCs might prime less potently the Th1 cell differentiation and recruitment, and DCs may favor Th2 immune responses. In contrast to this hypothesis, no one has been able to found any Th2 response upon activation of PPARγ in DC/leucocyte co-culture experiments so far.

DCs have to migrate from the peripheral tissues to LNs for effective T cell priming. RSG supplementation dumped the migration capacity of BM-DC through the down-regulation of CCR7 (288). Following intratracheal injection, PPARγ ligands impaired the migration of murine DCs to LNs and reduced DC motility *in vitro* towards CCL19 chemokine. Moreover, RSG-treated and OVA-pulsed DCs reduced the proliferation of responding T cell in LNs (291). The detrimental effect of PPARγ was further supported in other experimental murine models of LC migration. RSG inhibited the TNFα-triggered emigration of LC from the epidermis in receptor-dependent manner (288). Importantly, PPARγ reduced the steady-state motility of DCs from the mucosal area to the thoracic LNs as well. Furthermore, RSG prevented the initiation of allergic responses and the early development of atopic dermatitis (AD) in NC/Tnd mice, a model for human AD (292). In this model the synthetic agonist reduced the

accumulation of Langerin$^+$ DCs in skin lesions and migration of DCs to LNs. In addition, systemic administration of pioglitazone into mice provided protection from lethal H5NI influenza infection (293). During influenza infection, the PPARγ ligand pioglitazone reduced the migratory and the antigen-specific CD8$^+$ CTL activating capacity of tip-DCs against influenza-virus-generating epithelial cells in the respiratory tract indicating that pioglitazone might impede DC mobility via receptor specific effects. As PPARγ ligand treatment reduced the CCR7 expression, this might be partly responsible for the impaired tip-DC accumulation.

Collectively these *in vitro* and partly *in vivo* experimental data suggested that PPARγ acts as a suppressive TF in DCs that inhibits murine and human DCs immunophenotype at multiple levels. The anti-inflammatory effects of PPARγ receptor has partly been characterized at molecular level in LPS-matured DCs (287). PPARγ activation impaired the MAP kinase and NF-κB pro-inflammatory signaling pathways, probably due to transrepression mechanism that subverted IL-12 expression.

Besides the aforementioned negative effects of PPARγ activation on DCs selective agonist of PPARγ enhanced the internalizing capacity of the cells (49). In response to selective activator ligands, DCs had higher capacity to endocytose FITC-dextran, which was mainly mediated by mannose receptor (MR). MR was up-regulated by PPARγ in BM-DCs, mediating Ova antigen uptake and elevated cross presentation of the model antigen by MHCI molecules. In contrast to these results, our laboratory could not detect induced MR expression on the cell surface of RSG-treated human mo-DCs (49). Furthermore, PPARγ activation induced the expression of CD36 receptor. The receptor CD36 has been supposed to be involved in apoptotic cell uptake by human DCs and in mediating cross-presentation of antigens to CD8$^+$ T cells however, in CD36 deficient mice, this receptor was not essential for CD8a$^+$ murine DCs-mediated cross-priming (294, 295). In line with this murine data, a detailed analysis of CD36 expression and increased latex bead uptake for estimating phagocytosis revealed, that PPARγ-regulated increased internalization capacity of the cells is independent of CD36 in our model (49). We could not detect any differences in MHCI expression, suggesting that the MHCI-mediated peptide antigen presentation capacity of the cell was probably not affected.

Interestingly, our laboratory has also demonstrated that PPARγ highly up-regulated ATP binding cassette subfamily G member 2 (ABCG2), a member of ATP-binding cassette transporters in developing DCs (296). These results also confirmed that ABCG2 gene expression was directly regulated by the receptor. ABCG2 had important function in tumor drug resistance by exporting a variety of anticancer drugs including mitoxantrone. In line with

this property of the transporter we found, that RSG-treated cells accumulated less mitoxantrone compared to control DCs, thus the PPARγ might confer protection form anticancer drugs.

For further characterization of the role of PPARγ on human DC functions, a suitable *in vitro* model system is required in which DCs express the receptor. Human DCs can be differentiated either from $CD34^+$ hematopoietic stem cells, from $CD14^+$ peripheral monocytes or from myeloid $CD1c^+$ blood DCs (297). According to previous results of our laboratory, PPARγ expression was immediately induced in a narrow developmental period during the monocyte-to-DC differentiation (49). Freshly isolated monocytes failed to express the receptor, while the PPARγ protein was detectable after 4 hours in cultured cells. The receptor was active in this *in vitro* DC model, because synthetic and natural agonists induced the expression of its bone fide target gene FABP4. To assess the global PPARγ-dependent gene expression profile during DC differentiation we utilized microarray experiments (169). These results revealed that PPARγ was not a simple inhibitory TF of the DC development because more than 1000 transcripts were regulated by the receptor and the half of these transcripts was up-regulated in the RSG-treated samples. PPARγ-activated genes in the first 6 hours of the differentiation program were involved primarily to the lipid metabolism and transport (FABP4, CD36, LXR, and PGAR) and were most likely directly/transcriptionally regulated by the receptor. Conversely, immune function-related genes were regulated in the later developmental period by the receptor, suggesting that PPARγ might alter the DC immune phenotype indirectly through activation of intracellular lipid metabolism and signaling pathways.

2.3.6. Co-ordinated regulation of retinoid signaling by RARα and PPARγ in DCs

PPARγ and RARα regulate the expression of genes participating in lipid antigen presentation (*CD1a, CD1d*) in mo-DCs. We confirmed that both receptors could regulate the mo-DCs-mediated lipid antigen presentation through up-regulated CD1d expression in cultured DCs (49, 239).

Based on literature data, endogenous serum derived lipids skewed mo-DC development to the generation of $CD1a^-$ cells (298). Lysophosphatidic acid and cardiolipin were identified as lipids present in normal human serum that could potently modulate the expression profile of Group 1 CD1 molecules but not that of CD1d. The control of CD1 mRNA expression was regulated by PPARγ. DCs differentiated in human serum-supplemented medium expressed CD1d in PPARγ-, and RAR-dependent manner (239). Administration of lipoproteins during the

DC development also affected the CD1 profile of the cells, suggesting that the uptake of lipids resulted in intracellular endogenous PPARγ agonists that induced transcriptional events, co-ordinating lipid metabolism, expression of CD1 molecules and DC immune functions (239, 289).

Monocytes express cell surface CD1d at high levels which was rapidly down-regulated after the induction of mo-DC differentiation (49). In contrast to CD1d, monocytes did not express CD1 group 1 molecules (CD1a, b, c) but the CD1a protein was up-regulated on the surface of the cells. PPARγ agonist treatment induced the expression of CD1d molecules along with the down-regulation of CD1a at both mRNA and protein levels. We established that PPARγ triggered indirectly the CD1d expression by turning on endogenous lipid ligand synthesis in developing mo-DCs (239). Utilizing global gene expression analysis, we compared the expression pattern of genes in control samples and in PPARγ-ligand treated samples, which might be involved in retinol and retinal metabolism and endogenous ATRA production from retinol. We found that members of SDRs (required for retinol to retinal conversion), RDH10 and DHRS9 were up-regulated by PPARγ during mo-DC differentiation. Furthermore, RSG-treatment induced RALDH2 expression, an essential retinal converting enzyme in intestinal DCs. The microarray results were validated by RT-qPCR and IHC. We determined the intracellular ATRA concentration in RSG-treated differentiated DCs by LC-MS analysis. The co-treatment of DCs with RSG and DEAB (RALDH inhibitor) to probe the contribution of these enzymatic steps in the regulation of gene expression of PPARγ-regulated genes confirmed, that PPARγ-triggered ATRA synthesis was mediated by RALDH activity. The accumulation of ATRA resulted in the induction of retinoid response by the RARα/RXR heterodimer. We also found that approximately the 30% of all PPARγ-responsive genes are regulated via the induction of retinoid signaling (239).

We characterized the functional consequences of the PPAR-induced, ATRA-regulated CD1d expression on DC surface. Both PPARγ and RARα activation leaded to iNKT expansion (49, 239). Nuclear hormone receptor instructed DCs were pulsed with synthetic iNKT ligand, αGC. These DCs triggered selective induction of iNKT proliferation and INFγ secretion in autologous MLR cultures. As iNKT cell activation was restricted to CD1d-dependent lipid antigen presentation, we concluded that PPARγ-induced CD1d expression could be translated to efficient lipid presentation by DCs and to enhanced iNKT activation under these *in vitro* conditions. These results linked PPARγ and RARα to iNKT-mediated immune responses. PPARγ-altered lipid metabolism would allow DCs to respond to altered lipid homeostasis by changing CD1 gene expression and lipid antigen presentation. Moreover, synthetized lipid

mediators such as ATRA, if exported, might also influence the functions of neighboring cells in the peripheral tissues.

3. AIMS

During the process of DC differentiation many genes in these cells become up-or down-regulated. The regulation of gene expression requires a complex network of growth factors, signaling pathways and TFs. Environmental factors such as lipids induce signal transduction pathways that act on TFs, which have a fundamental role in controlling and co-ordinating of the expression of multiple genes that regulate physiological functions of DCs. We demonstrated that PPARγ signaling axis altered the lipid metabolism through the activated endogenous ATRA synthesis in mo-DCs, leading to subsequent cell type specification, characterized by enhanced lipid antigen presentation capacity of the cells. Despite of enormous scientific effort, the identity of permissive cell types, the required components of the biological active ATRA synthesis and the steps of lipid antigen processing for CD1d-mediated lipid presentation in DCs are still not characterized to date.

Therefore the objectives of our studies:

1, Identification of permissive murine DC subtypes by characterization of the expression of genes required for retinol uptake, ATRA production and signaling.

2, Systematical survey of human DC subtypes for ATRA biosynthesis and signaling.

3, Functional validation of our human mo-DCs as a suitable model to characterize the required steps for PPARγ-regulated ATRA synthesis, retinoid signaling and lipid antigen presentation.

4, Determination whether PPARγ also stimulates retinoid signaling through the ATRA transport.

5, Characterization of the PPARγ-regulated ATRA signaling in human tissues.

6, Providing functional evidence by gene specific silencing and lipid antigen presentation assay that beside RALDH2, PPARγ-activated RDH10 and CRABP2 are also mechanistically indispensable for the retinoid signaling axis-mediated gene expression.

7, Determination whether PPARγ stimulates the iNKT expansion capacity of DC through a novel signaling axis.

4. MATERIALS AND METHODS

4.1. Ligands

Cells were treated with the following ligands: rosiglitazone (RSG) and GW9662 (Alexis Biochemicals, San Diego, CA, USA), ATRA (Sigma-Aldrich, St. Louis, MO, USA), AGN193109 a gift from Roshantha A. S. Chandraratna, (Allergan Inc. Irvine, CA, USA), AM580 (Biomol, Hamburg , Germany), 4-diethyl amino-benzaldehyde (DEAB) from Fluka (Honeywell, Morris Plains, NJ, USA) pepstatin A and OVA 257-264 peptide (Innovagen, Lund, Sweden), bafilomycin (Sigma-Aldrich). α-galactosylceramide (αGC) was obtained from Kirin Brewery Ltd. (Gunma, Japan), galactosyl(1-2) galactosylceramide (αGGC) from P.A. Illarionov (School of Bioscience, University of Birningham, Edgbaston, UK). The vehicle control (1:1 of dimethyl sulfoxide/Ethanol) had not detectable effect on the cell differentiation (data not shown).

4.2. Generation of bone marrow-derived dendritic cells (BM-DCs)

BM cells were isolated from the femur of C57BL/6 mice. Animals were housed under specific pathogen free conditions and the experiments were carried out under institutional ethical guidelines and licenses (license number: 21/2011/DEMÁB). BM cells were differentiated to BM-DCs in RPMI 1640 culturing medium (Sigma-Aldrich) supplemented with 10% Fetal bovine serum (FBS) (Invitrogen, Thermo Fisher scientific, Waltham, MA, USA), 500 U/ml penicillin/streptomycin (Invitrogen, Thermo Fisher scientific), 2 nM L-glutamine (Invitrogen), 20 ng/ml GM-CSF (Peprotech EC, London, UK)) and 20 ng/ml IL-4 (Peprotech) or 20 ng/ml GM-CSF alone for 9 days. Cytokine treatment was repeated at day 3 and 6 (299). After 9 day of culturing period, cells were harvested in Trizol reagent (Invitrogen, Thermo Fisher scientific) for RNA isolation.

4.3. Splenic (Sp-DC) and Mesenteric lymph node-dendritic cell (MLN-DC) separation

$CD11c^+$ MLN-DCs were obtained from B16-Flt3L tumor cell-injected C57BL/6 mice (300). Pooled spleens and MLNs of male C57BL/6 mice were cut into small fragments and digested with Collagenase D (Roche, Basel, Switzerland) for 40 minutes at 37°C. Solutions were passed through a nylon mesh and washed. Cell suspension was pre-incubated for 10 minutes at 4°C

with anti-mouse CD16/CD32 Mouse BD FC Block antibody (BD Biosciences Pharmingen, San Diego, CA, USA). $CD11c^+$ cells were obtained followed by anti-CD11c MACS bead (Miltenyi Biotec, Bergisch Gladbach, Germany) separation. $CD103^+$ and $CD103^-$ DCs were separated by labeling the cells with anti-CD11c-APC and anti-CD103-PE (BD Biosciences Pharmingen) antibodies and subsequent sorting on FACSVantage (BD Biosciences, San Hose, CA, USA) (32, 254). Cells were harvested in Trizol reagent (Invitrogen, Thermo Fisher scientific) or were utilized in co-culture experiments.

4.4. DC/Splenocyte co-culture experiment

Pooled MLN $CD103^+$ DCs were obtained as described above (4.3.). Splenocytes were purified from pooled spleens of BALB/c mice. Spleens were placed in Petri dish containing RPMI 1640 medium supplemented with 10% FBS (Invitrogen, Thermo Fisher scientific). Cells were squeezed out with glass plunger. After washing, Lysing Buffer (BD Pharm Lyse, BD Biosciences) was applied against red blood cells. The cell suspension was plated in Petri dishes for 12 hours to attach splenic DCs. Co-culture experiments were set in 12-well plates. The DC/Splenocyte ratio was 1:20, corresponding to 1:10 DC: T cell ratio in 2 ml culturing medium/well. After 72 hour incubation at 37ºC, MLN $CD103^+$ DCs were separated by labeling cells with anti-CD11c-APC and anti-CD103-PE (BD Bioscences Pharmingen) antibodies and subsequent sorting on FACSVantage (BD Biosciences). Cells were harvested in Trizol reagent (Invitrogen, Thermo Fisher scientific).

4.5. DC/$CD8a^+$ T cell co-culture experiment

$CD8a^+$ T cells were obtained from OTI-I mice (as a gift of Dr. Zoltan Pós). Single-cell suspension from spleens of OT-I mice were prepared using gentleMACS Dissocator (program: m. spleen 01.01 for 1-2 spleens) (Miltenyi Biotech). After washing, $CD8a^+$ cells were obtained followed by the $CD8a^+$ T Cell Isolation Kit II (Miltenyi Biotech), by autoMACS Separator (Deplete program) (Miltenyi Biotech). Pooled $CD103^+$ MLN-DCs were isolated as described above (4.3). $CD103^+$ DCs were loaded with 20 pM OVA 257-264 peptide (Innovagen). Co-culture experiments were set in 24-well plates. The DC/T cell ratio was 1:2. After 72 hour incubation at 37ºC, $CD103^+$ MLN-DCs were separated by labeling cells with anti-CD11c-APC and anti-CD103-PE (BD Biosciences Pharmingen) antibodies and subsequent sorting on

FACSVantage (BD Biosciences). Cells were harvested in Trizol reagent (Invitrogen, Thermo Fisher scientific).

4.6. Human monocyte-derived dendritic cell (mo-DC) culture

Human monocytes (98% $CD14^+$) were isolated from Buffy coats of healthy volunteers, obtained with the Regional Ethical Board permit from the Regional Blood Bank, by Ficoll gradient centrifugation (Amersham Biosciences, Uppsala, Sweden), followed by magnetic bead separation using anti-CD14-conjugated microbeads (Miltenyi Biotech). Monocytes were differentiated to DCs in multiwell culture plates at the density of 1.5 x 10^6 cell/ml in RPMI 1640 medium (Sigma-Aldrich) supplemented with 10% FBS (Invitrogen, Thermo Fisher scientific), 500 U/ml penicillin/streptomycin (Invitrogen), 2 nM L-glutamine (Invitrogen, Thermo Fisher scientific), 800 U/ml GM-CSF (Gentaur Ltd. London, UK) and 500 U/ml IL-4 (Peprotech). Cells were cultured for 5 days. Ligands or vehicle control were added to the cell culture at day 0 and at day 3.

4.7. Flow cytometry

Cells were harvested and washed in 1X buffered (phosphate buffered saline) PBS and stained in 1X PBS supplemented with 0.5% bovine serum albumin (BSA) (Sigma-Aldrich) for 40 minutes at 4ºC. Cell staining was performed using PE- or FITC- conjugated antibodies: anti-CD14-FITC, anti-F4/80-FITC, anti-CD11c-PE, anti-CD1d-PE, anti-CD1a-FITC, anti-CD11c-FITC, anti-CD209-PE (BD Biosciences Pharmingen) and anti-Vα24-FITC, anti-Vβ11-PE (Immunotech, Marseille, France) and appropriate isotype-matched controls (BD Biosciences Pharmingen, Immunotech). Analysis of cell surface expression of proteins was performed using a FACSCalibur (Beckman Coulter, BD Biosciences, San Jose, CA, USA) and analyzed by CellQuest software.

4.8. Microarray analysis

The generation of the microarray data used for Figure 18 and 20 (DC subtypes) was described in Széles et al. (175). We assessed the genes are expressed in mo-DCs and other DC types. Using Affymetrix microarray data of human Langerhans cells (LC), dermal DCs, tonsillar $CD1c^+$ DCs, blood $CD1c^+$ DCs, blood plasmacytoid DCs (pDCs) along with mo-DCs (169, 175, 301, 302). The generation of the microarray data of human mo-DC used for Figure

18 and 20 was described in Szatmári et al (169). Briefly, mo-DCs were cultured with or without the PPARγ agonist RSG and RNA was isolated at 6 h, 24 h, or day 5 of the culture. Hybridization of the RNA samples was carried out at the Microarray Core Facility of the European Molecular Biology Laboratory (Heidelberg, Germany). Analysis was carried out using GeneSpring GX7.3.1 software (Agilent Technologies, Santa Clara, CA, USA). Raw data (cell files) were analyzed by the GeneChip robust multiarray analysis algorithm (GC-RMA) and raw signal intensities were normalized per chip (to 50th percentile). All microarray data are available in the public Gene Expression Omnibus database (GEO) under accession no. GSE23618 (DC subtypes and in ArrayExpress database, accession no E-TABM-34), accession no. GSE8658 (mo-DC differentiation). For a full description of cell culture and differentiation, RNA isolation, hybridization, and data analysis, see Szeles et al. (175) and Szatmari et al. (169).

4.9. Real time quantitative PCR (RT-qPCR)

Total RNA was isolated from cells using Trizol reagent (Invitrogen, Thermo Fisher scientific). 1000 ng of total RNAs were reverse transcribed with SuperScript II reverse transcriptase (Invitrogen, Thermo Fisher scientific) and random primers (Invitrogen, Thermo Fisher scientific). This was performed at 42^{o}C for 2 hours, and 72^{o}C for 5 min. Quantitative PCR was performed on LC480 platform (Roche), 40 cycles of 95^{o}C for 10 sec and 60^{o}C for 30 sec for Taqman assays (Applied Biosystems, Thermo Fisher scientific, Waltham, MA, USA) or 95^{o}C for 10 min, 40 cycles of 95^{o}C for 10 sec and 60^{o}C for 30 sec using Sybr green. The sequences of primers and probes used in transcript quantification are listed in Table 1. Gene expression was quantified by the comparative threshold cycle method and normalized to human or mouse *Cyclophilin A* (*PPIA* and *Ppia*) expression as housekeeping gene. All PCR reactions were performed in triplicates. Values are expressed as means ± SD. In addition, TaqMan low-density arrays (TLDAs) (Applied Biosystems, Thermo Fisher scientific) were used according to manufacturer's instructions. For TLDA analyses a high capacity cDNA archive Kit (Life Technologies, Thermo Fisher scientific) was used. RT-qPCR was performed using real-time PCR (ABI Prism 7900, Applied Biosystems, Thermo Fisher scientific).

Gene symbols	**Primer sequences and Taqman probes**	**Pre-designed gene expression assays/TLDA**
Cd1d1	Fw gggccccatcttggttaga Rev ggttgcacttgtcccttgatc Sybr green	
Crabp1	Fw tgtgcagtgaatcttgttctca Rev aaggtcggagagggcttc Sybr green	
Crabp2	Fw tcctgtttgatctcgactgct Rev ttcaggaaatgctaaaagc Sybr green	***Crabp2*-Mm00801691_m1/TLDA**
Cyp26a1	Fw ccggcttcaggctacaga Rev ggagctctgttgacgattgtt Sybr green	***Cyp26a1*-Mm00514486_m1/TLDA**
Ppia/Cyclophillin A	Fw cgatgacgagcccttgg Rev tctgctgtctttggaacttgtc Sybr green	***Ppia*-Mm02342429_g1/TLDA**
Rbpr2	Fw cggagacaaagagatgaca Rev gtccccacgaagtccaga Sybr green	
Rdh10	Fw tcgtcaaaacccacaactcc Rev ctccctgggactgttcagc Sybr green	***Rdh10*-Mm00467150_m1/TLDA**
Raldh2/Aldh1a2	Fw gcgcatttaaggcattgtaac Rev catggtatcctccgcaatg Sybr green	***Raldh2*-Mm00477463_m1/TLDA**
Rara		***Rara*-Mm00436264_m1/TLDA**
Rarb		***Rarb*-Mm01319674_m1/TLDA**
Rarg		***Rarg*-Mm00441091_m1/TLDA**
Rxra		***Rxra*-Mm00441182_m1/TLDA**
Rxrb		***Rxrb*-Mm00441193_m1/TLDA**
Stra6	Fw cctgggagtgatggatagtga Rev ggtctggcttccattctcag Sybr green	
Tgm2	Fw tccctcctccacattgtca Rev ctcacgttcggtgctgtg Sybr green	***Tgm2*-Mm00436980_m1/TLDA**
CATD	Fw tggatccaccacaagtacaaca Rev cgagccatagtggatgtcaaa Probe FAM-gacaagtcccagcacctacgtt	
CATL	Fw agaaatgggccccacagtt Rev ggctttgtggacatccctaag Probe FAM-gaggagaaggccctgatgaag-TAMRA	
CD1D	Fw gtcagggaagtcggaactga Rev atcctgagacatggcacacc Sybr green Probe FAM-tggccattcaagtgctcaaccagg-TAMRA	
CRABP2	Fw atgctgaggaagattgctgtg	

	Rev tccctcctgtttgatctcca Sybr green
FABP4 *FABP4*	Fw ggatggaaaatcaaccacca Rev ggaagtgacgcctttcatga Sybr green Probe FAM-attccaccaccagtttatcatcctctcgtt-TAMRA
INKT	Fw agcgattcagcctcctacatct Rev gtcaactgagttcctcttccaag Probe FAM-tgtggtgagcgacagaggctcaa-TAMRA
PPARG *PPARG*	Fw gatgacagcgacttggcaa Rev cttcaatgggcttcacattca Sybr green Probe FAM-caaacctgggcggtctccactgag-TAMRA
PPIA/CYCLOPHILLIN A	Fw acggcgagcccttgg Rev tttctgctgtctttgggacct Sybr green Probe FAM-cgcgtctcctttgagctgtttgca-TAMRA
RALDH1/ALDH1A1	Fw aattgctatggcgtggtaagt Rev accgtactctcccagttctctt Sybr green
RALDH2/ALDH1A2	Fw aggccctcctcgctcac Rev tgccccagaatgagctca Sybr green
RALDH3/ALDH1A3	Fw aacccctgcstcgtgtgt Rev tggttgaagaacactccctga Sybr green
RBPR2A	Fw gcattgaagtcggcctgt Rev agcccaagatggagctgac Sybr green
RBRP2B	Fw accctgtgcttgtcagcttt Rev gcaccagtatttggtgctctg Sybr green
RDH10	Fw cagaggctGCCGAATCAG Rev ggcctgcttcacacagttatc Sybr green
STRA6	Fw ctctggcctgactgtgtgc Rev tgtccccagccaagaaatc Sybr green
TGM2	Fw ctgggccacttcattttgc Rev actactgccgctcctcttc Sybr green Probe FAM-tccaggtacacagcatccgctggg-TAMRA

Table 3: *The sequences of primers, probes and pre-designed gene expression assays used in transcript quantification. Fw: forward primer, Rev: reverse primer.*

4.10. RNA interference

Small interfering RNA (siRNA) delivery was performed using electroporation of monocytes as described earlier (303). Monocytes were counted and resuspended in Opti-Mem (Invitrogen,

Thermo Fisher scientific) without phenol/red at the density of 4 x 10^7 cell/ml. For silencing of RDH10, RALDH2, CRABP2 or FABP4 expression, the following siRNA oligonucleotides were used: On-Target*plus* SMART pool siRNA against human *RDH10*, *RALDH2*, *CRABP2*, *FABP4* or On-Target*plus* non-targeting control siRNA pool (non-silencing (NS)) (Dharmacon, Lafayette, CO, USA). Non-silencing (NS=scrambled control) siRNA and siFABP4 were used, that did not altered the normalized mRNA level of the examined genes. Oligonucleotides were transferred to a 4-mm cuvette (Bio-Rad Laboratories, Hercules, CA, USA) at 3 μM final concentration. 100 μl cell suspension was added, gently mixed (avoiding bubbles) and incubated for 3 minutes at room temperature. Electroporation was performed using a Gene Pulser Xcell (Bio-Rad Laboratories). Pulsing conditions were square-wave pulse, 500 V, 0.5 ms. After electroporation, cells were transferred into RPMI 1640 medium supplemented with 10 % FBS, 500 U/ml penicillin/streptomycin, 2 nM L-glutamine, 800 U/ml GM-CSF and 500 U/ml IL-4. Silencing efficiency was assessed on day 1 and day 2 post electroporation. The average siRDH10 efficiency was 48.58± 8.44%, in the case of siRALDH2 the efficiency was 39.22± 10.81% and the average siCRABP2 efficiency was 44.22± 9.25%.

iDCs were harvested at day 3, washed once with unsupplemented RPMI 1640 and PBS (room temperature). Cells were resuspended in Opti-Mem without phenol/red (Life Technologies, Thermo Fisher scientific) at the density of 4 x 10^7 cell/ml. The expression of *PPARG* was silenced with Qiagen siRNA against *PPARG*, On-Target*plus* SMART pool siRNA against human *CATD* or On-Target*plus* non-targeting control siRNA pool (non-silencing (NS)) (Dharmacon). Electroporation was performed using a Gene Pulser Xcell (Bio-Rad Laboratories). Pulsing condition was identical to that was used for monocyte samples. *PPARG* and *CATD* were silenced at an efficiency approximately 60%.

4.11. Aldefluor assay

Aldehyde dehydrogenase activity of mo-DC was determined by ALDEFLUOR Kit (StemCell Technologies Germany, Cologne, Germany). The RALDH activity measurement was carried out according to manufacturer's instructions. Briefly, cells were incubated at the density of 1 x 10^6 cell/ml in ALDEFLUOR assay buffer containing activated ALDEFLUOR substrate with or without DEAB for 40 minutes at 37°C. ALDEFLUOR reactive/positive cells were determined in FL1-chanel of FACSCalibur (Beckman Coulter, BD Biosciences), compared to DEAB-treated control samples.

4.12. Expansion of iNKT cells

mo-DCs were differentiated for 5 days. Cells were treated with 100 ng/ml αGC or αGGC for 48 hours to obtain αGC- or αGGC-pulsed DCs. Lipid-loaded DCs (1 x 10^5) were co-cultured with monocyte-depleted autologous peripheral blood mononuclear cells (PBMCs) (1 x 10^6) for 5 days in 24-well plates (1:10 DC/PBMC cell ratio). In CatD inhibition experiments, DCs were treated with 1 or 10 μM pepstatin A (Sigma-Aldrich) at day 3. Prior to co-culture, DCs were washed extensively and resuspended in fresh RPMI 1640 medium supplemented with 10 % FBS, 500 U/ml penicillin/streptomycin, 2 nM L-glutamine, 800 U/ml GM-CSF and 500 U/ml IL-4. PBMCs were stained with anti-TCR Vα24-FITC and anti-TCR Vβ11-PE monoclonal antibodies (Immunotech) and double-positive iNKT population was monitored by flow cytometry using FACSCalibur (Beckman Coulter, BD Biosciences). Additionally, the invariant Vα24-Jα18 (iNKT) TCRα chain was quantified by using RT-qPCR. In lysosomal acidification inhibition experiments, DCs were differentiated in the presence of RSG. Cells were treated with 50 nM bafilomycin at day 4.

4.13. Western blot analysis

20 μg protein from whole cell lysate was separated by 12.5% polyacrylamide gel and transferred to PVDF membrane (Millipore, Merck, Darmstadt, Germany). Membranes were probed with anti-CRABP2 (208) antibody, kindly provided by Cecile R.-Egly (IGBMC, INSERM, Illkirch-Graffenstaden, France France), and then the membranes were stripped and re-probed with anti-GAPDH antibody (ab8245-100; Abcam, Cambridge, MA, USA) according to the manufacturer's recommendations. In addition, 50 μg protein whole cell lysate was separated by 12.5% PAGE before being transferred onto PVDF membrane (Bio-Rad Laboratories). Membranes were blocked using 5% nonfat dry milk in tris-buffered saline (TBS)+ Tween 20 (TBST) at 4°C overnight before being probed with anti-CatD antibody (R20, sc-6487; Santa Cruz Biotechnology, Paso Robles, CA, USA), and then membranes were stripped and reprobed with anti-GAPDH (ab8245-100; Abcam).

4.14. Immunoperoxidase staining

For immunohistochemistry (IHC), monocytes, vehicle-treated DCs, or RSG-treated DCs (6 x 10^6 cells/group) were pelleted and fixed in 4% buffered paraformaldehyde for 24 hours at 4°C. Cell blocks were embedded into paraffin. After deparaffinization and dehydration, sections (4 μm from each group) were mounted on glass slides and were used for peroxidase-based indirect IHC. In brief, sections were treated with 3% H_2O_2 in methanol for 15 minutes at room temperature to block the endogenous peroxidase. For antigen unmasking, sections were heated in antigen retrieving citrate buffer (pH 6.0, Dako, Thermo Fisher Technologies) for 2 minutes at 120°C using a pressure cooker. Immunostaining of the cells for CRABP2 were carried out using the standard ABC technique utilizing the primary antibody-specific biotinylated secondary antibodies (Vectastain kits, Vector Laboratories, Burlingame, CA, USA). After blocking the non-specific binding sites, sections were incubated with the primary anti-CRABP2 (208) antibody at dilutions of 1 x 1/50 for 1 hour at room temperature prior to use the biotinylated secondary antibodies. The peroxidase-mediated color development was set up for 5 minutes using the VIP substrate (Vector Laboratories). Finally, the sections were counterstained with methyl green.

4.15. Double immunofluorescence

Double immunofluorescence (DI) was performed on formalin-fixed, paraffin embedded intestinal tissue sections obtained from the archives of surgical specimens of the Department of Pathology, University of Debrecen as described earlier (289). Briefly, following antigen-retrieving and peroxidase block (described above), the first primary antibody was visualized with antibody-matched peroxidase-conjugated IgG followed by tetramethyl-rhodamine (TMR) tagged tyramide (PerkinElmer, Waltham, MA, USA) treatments (red fluorescence). After washing and blocking the non-specific binding sites, sections were incubated with the second primary antibody which was then developed with the use of matched biotinylated secondary antibody (IgG$[Fab]_2$) and streptavidin-FITC (fluorescent isothiocyanate, Vector Laboratories,) resulting in green fluorescence. After thorough washings, nuclear counterstaining was made with 4',6-diamidino-2-phenylindole (DAPI) containing the mounting medium (Vector Laboratories). To check the staining specificities, positive and negative controls were included for each IF reaction as described earlier (289) and as indicated in the result section (Figure 26).

In Figure 35, monocytes, DC, or RSG-treated DCs (6×10^6 cells/group) were pelleted and fixed in 4% paraformaldehyde (pH 7.3) for 24 hours at 4ºC. Cell blocks were then embedded in paraffin followed by serial sectioning (4 μm thick). After deparaffinization and dehydration, sections from each group were mounted on the same glass slides and subjected to sequential DI staining for detection of PPARγ and CatD protein expressions, respectively. The following primary antibodies were used: anti-PPARγ (clone E8; Santa Cruz Biotechnology) at 1:75 dilution and polyclonal goat anti-CatD (clone C20; Santa Cruz Biotechnology) at 1:100 dilution. In brief, PPARγ was detected by incubating sections 1 hour at room temperature with primary antibody followed by HRP-labeled anti-mouse secondary (IgG[Fab]$_2$) and FITC-conjugated tyramide (PerkinElmer Life Science, Boston, MA, USA) treatment. Following extensive washing and blocking, CatD protein expression was detected by 1 h incubation with primary antibody followed by biotinylated rabbit anti-goat (IgG[Fab]$_2$) and streptavidin-Texas Red (Vector Laboratories). DAPI was used for nuclear counterstaining (Vector Laboratories). For negative controls, isotype-specific control IgG Abs (Dako, Thermo Fisher Technologies) or a mixture of monoclonal antibody to PPARγ and a specific blocking peptide were applied on separate slides in replacement of primary antibodies. Normal human adipose tissue was included as positive control. Fluorescence microphotographs were captured using an Olympus BX51 microscope (Tokyo, Japan) equipped with a tricolor excitation filter and an Olympus DP50 digital camera. For transferring and editing images for documentation, Viewfinder and Studio Lite software version 1.0.136 of 2001 Pixera (Pixera UK Digital Imaging Systems, Bourne End, UK) and Adobe Photoshop version 8.0 were used.

4.16. Mixed leucocyte reaction (MLR)

Mo-DCs were harvested on day 5 and used as stimulator cells. To obtain mDC, iDCs were treated with a mix of cytokines: 10 ng/ml TNFα, 10 ng/ml IL-1β, 1000 U/ml IL-6 (Pep Rotec), 1 μg/ml PGE2 (Sigma-Aldrich), and 800 U GM-CSF for 24 hour. Allogeneic PBMCs were labeled in PBS supplemented with 10 μM Carboxyfluorescein succinimidyl ester (CFSE) (Molecular Probes, Thermo Fisher Technologies) at 37ºC for 15 minutes. CFSE-labeled PBMCs (2×10^5 cell/ml) and immature or mature DCs (1×10^4 cell/ml) were co-cultured in 96-well flat-bottom tissue culture plates (1:20 DC/PBMC cell ratio). Cell proliferation was quantitated on day 5 by FACSCalibur (Beckman Coulter, BD Biosciences).

4.17. Statistical analyses

Samples for each experiment were performed in triplicate (n=3). Biological repeats for each experiment were performed at least three times. Statistical significance was determined using the GraphPad Prism (GraphPad Software, La Jolla, CA, USA) program. Probability of significance was determined using the two-sample Student *t* test. The results were considered significant at the level of $p < 0.05$. Standard error bars are shown.

5. RESULTS

5.1. PPARγ-directed ATRA synthesis and signaling in human dendritic cells

5.1.1. ATRA biosynthesis in mouse intestinal DCs

Despite extensive investigation, the components and the exact molecular regulation of ATRA synthesis and signaling pathway are not completely characterized in murine DCs. We hypothesized that RDH10 might be the primary enzyme that initiates retinol oxidation to retinal and the co-expression of RDH10 and RALDH2 determines ATRA production in mucosal DCs. We tested this hypothesis in different *in vivo*- and *in vitro* generated DC subtypes (Figure 7).

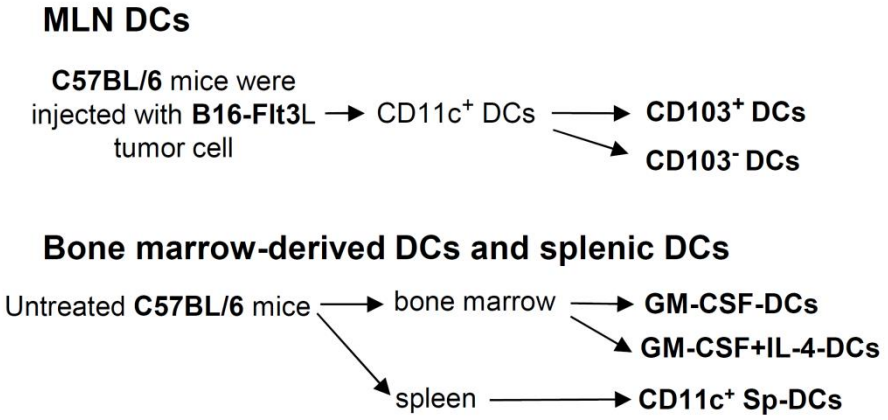

Figure 7: *$CD11c^+$ mesenteric lymph node (MLN)-DCs were obtained from B16-Flt3L tumor cell (B16 melanoma cells engineered to secrete fms-related tyrosine kinase 3 ligand (Flt3L)-injected C57BL/6 mice; $CD103^+$ or $CD103^-$ DC subsets were separated based on CD103 integrin expression. Splenic DCs (Sp-DCs) were isolated by CD11c-magnetic beads. In vitro granulocyte-macrophage colony-stimulating factor (GM-CSF)-DCs and GMCSF+ interleukin 4 (IL-4)-DCs were differentiated from the bone marrow (BM) of C57BL/6 mice (32, 254, 280, 300).*

First we obtained MLN-DCs described in the Materials and Methods. The purity of the sorted subsets was tested by post-sort flow cytometric analysis (Figure 8).

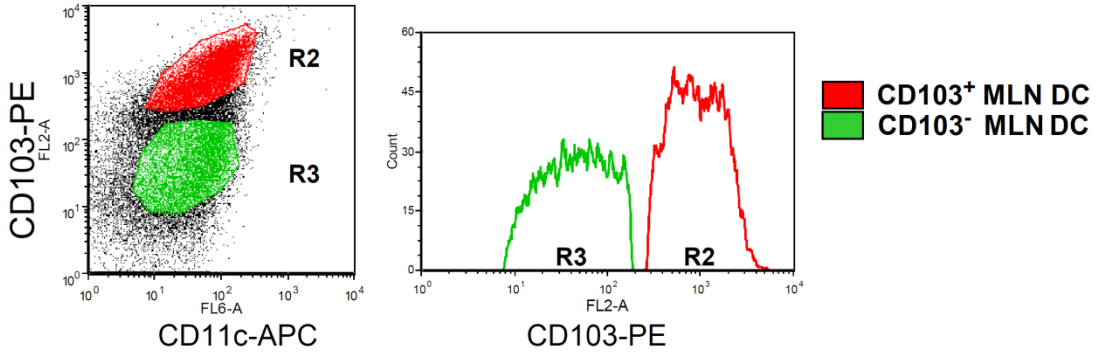

Figure 8: *MLN-DCs were sorted using CD103 mAb on FACSAria. R2: CD103$^+$ MLN DCs, R3: CD103$^-$ MLN-DC population. The histogram represents the post-sorted MLN DC populations according to CD103 expression. The purity of the sorted population was assessed by post-sort flow cytometric analysis.*

We quantificated and compared the expression levels of genes involved in ATRA synthesis in sorted cell populations by RT-qPCR. As expected, *Raldh2* could be detected only in CD103$^+$ DCs. *Rdh10* was expressed in both populations, but at an even higher level in the CD103$^-$ cells (Figure 9).

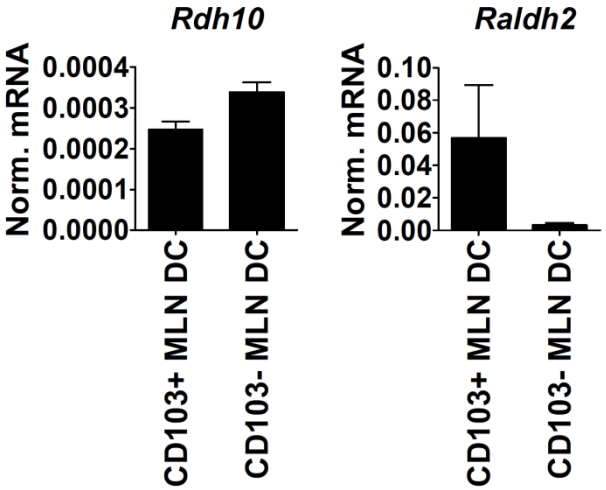

Figure 9: *Real time quantitative PCR (RT-qPCR) analysis of genes involved in all-trans retinoic acid (ATRA) synthesis (retinol dehydrogenase 10 (Rdh10), retinal dehydrogenase (Raldh2), in CD103$^+$ and CD103$^-$ MLN-DCs. Means normalized to Cyclophilin A ± SD.*

Next, we analyzed components of the downstream retinoid signaling pathway, we evaluated the gene expression of *Rar* and *Rxr* isoforms in CD103^{+} MLN DCs (Figure 10).

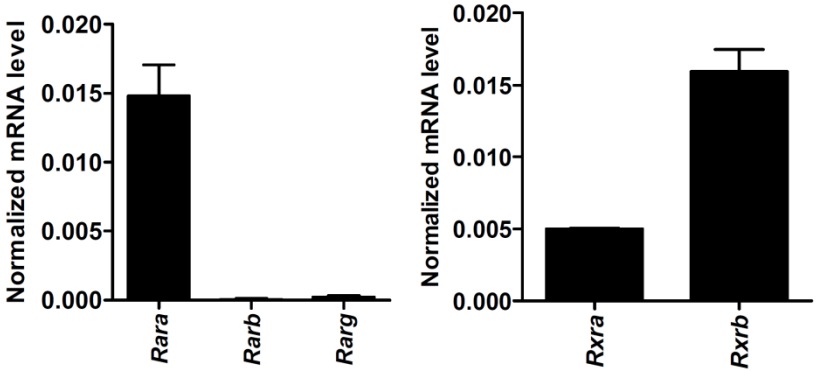

Figure 10: *Normalized mRNA level of retinoic acid receptors (Rara, Rarb, Rarg) and retinoid X receptors (Rxra and Rxrb) were detected by TaqMan low-density array (TLDA) in CD103^{+} MLN-DC population. Means normalized to Cyclophilin A ± SD.*

RAR/RXR heterodimers regulate retinoid target genes such as *Cyp26a1*, which had a similar transcription pattern to the *Raldh2* gene (304). *Cyp26a1* expression is regulated by ATRA through two identified RAREs in the promoter of the gene, suggesting a negative feedback mechanism to control the retinoic acid concentration and active retinoid signaling in cells (305, 306). CD103^{+} and CD103^{-} MLN-DC populations expressed *Tgm2* and *Cd1d1*, two well-established ATRA target genes (239, 307). Unexpectedly, the normalized mRNA levels of the genes did not correlate with either *Raldh2* expression or the ATRA production capacity of the cells (Figure 11).

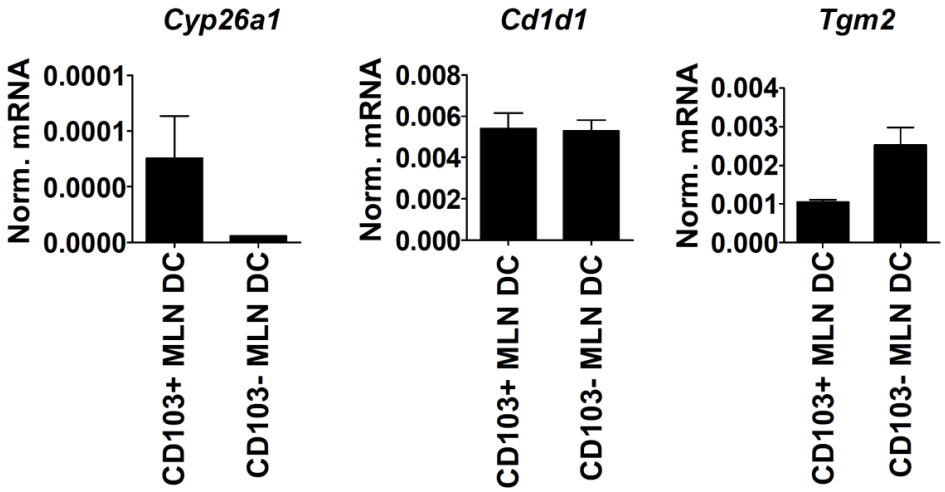

Figure 11: *RT-qPCR analysis of genes involved in ATRA metabolism cytochrome p450 26a1 (Cyp26a1) and retinoid signaling target genes (Cd1d1, transglutaminase 2 (Tgm2)) in CD103^{+} and CD103^{-} MLN-DCs. Means normalized to Cyclophilin A ± SD.*

In search for a more suitable mouse DC model for our mechanistic studies, we characterized *ex vivo* differentiated DCs using TLDA in additional gene expression analyses. We differentiated GM-CSF-DCs or GM-CSF+IL-4-DCs from BM and we used isolated Sp-DCs as a negative control DC population that has no capacity for ATRA generation (251). We validated our BM-DC differentiation- and Sp-DC isolation protocols by analyzing CD11c, F4/80 surface expression on BM-DCs and CD11c on Sp-DCs by flow cytometry (Figure 12).

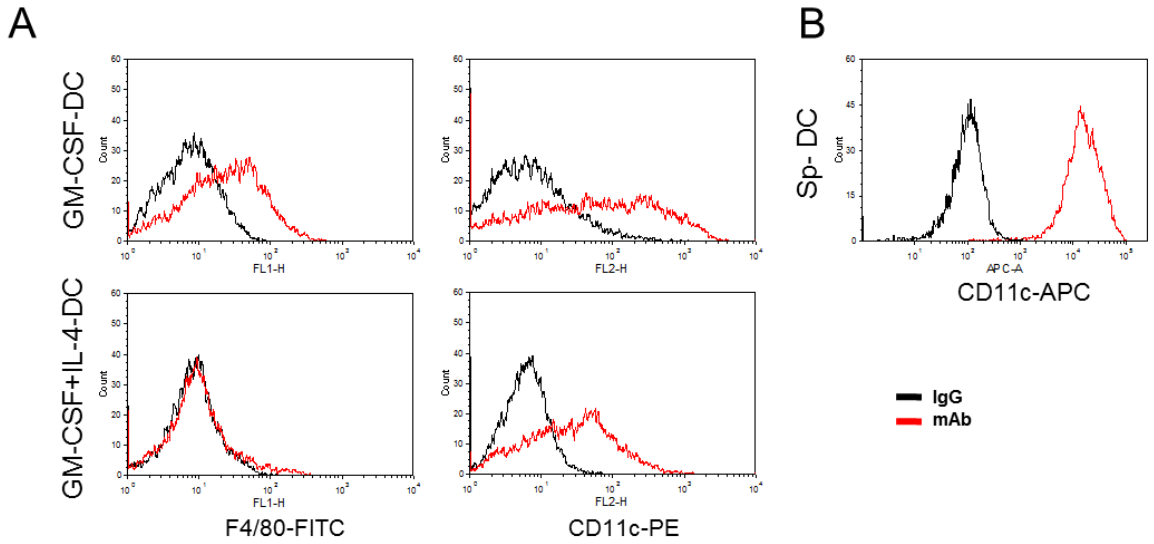

Figure 12: *A, BM cells were differentiated to BM-DCs. Differentiated cells were harvested and stained with mAb-fatty acid binding protein 4 (F4/80) macrophage marker and with mAb-CD11c DC marker. B, Sp-DCs were isolated using CD11c-magnetic beads.*

GM-CSF triggered *Raldh2* expression, the synergistic effect of the two cytokines was confirmed, while *Raldh2* expression in Sp-DCs was barely detectable as it was earlier demonstrated (251). Next we focused on *Rdh10* in *in vivo*- and *ex vivo* generated cells and found that all DCs expressed this gene (Figure 13).

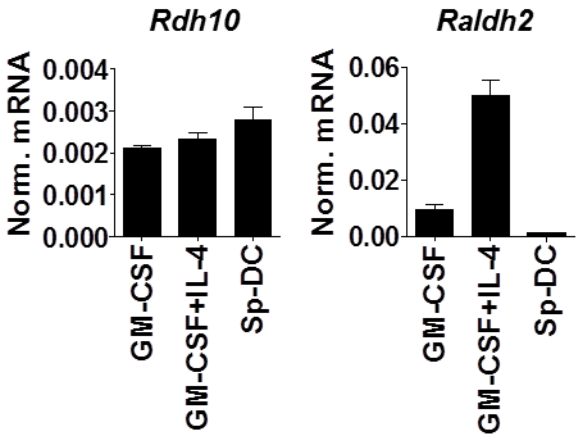

Figure 13: *Comparison of gene expression pattern of genes involved to ATRA synthesis (Rdh10, Raldh2). Means normalized to Cyclophilin A ± SD.*

We compared the gene expression of all *Rar* (*a*, *b*, and *g*) and *Rxr* (*a* or *b*) in mouse DCs (Figure 14).

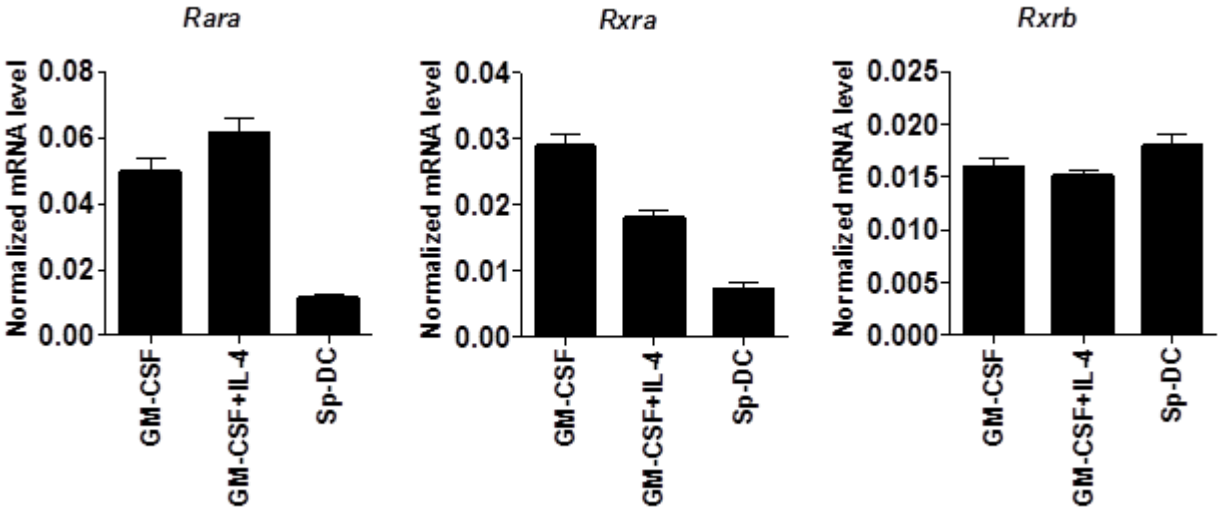

Figure 14: *Gene expression pattern of the mouse Rara, Rxra and Rxrb in GM-CSF-DC, GM-CSF+IL-4-DC and Sp-DCs.*

We also analyzed the gene expression of *Cyp26a1*, *Cd1d1*and *Tgm2* in these DC populations (Figure 15). All DC subsets expressed *Cd1d1*, but it did not show any correlation with retinoid signaling, while *Cyp26a1 and Tgm2* showed a similar gene expression pattern to *Raldh2*, indicating that these genes could be reliable markers of active retinoid signaling.

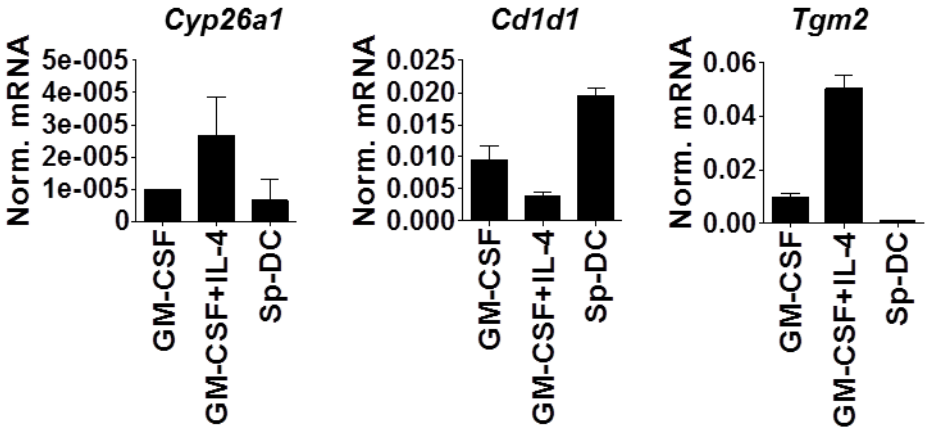

Figure 15: *Comparison of gene expression pattern of retinoid signaling target genes (Cyp26a1) and (Cd1d1, Tgm2) in GM-CSF-DC and GM-CSF+IL-4-DCs and Sp-DCs by TLDA method. Means normalized to Cyclophilin A ± SD.*

Next we assessed the expression of genes involved in retinol uptake and intracellular ATRA transport. Although, we could not quantificated *Stra6* (195, 308) in DC subsets derived from mice (data not shown), we detected the expression of the *Rbpr2* gene in all DC subsets indicating the possibility of retinol uptake through this alternative receptor (196) (Figure 16). Unexpectedly, the transcription of the *Crabp2* gene was not detectable in *in vivo* subsets but quantification of *Crabp2 mRNA* was successful in the case of GM-CSF- or GM-CSF+IL-4 DCs therefore, we used the measured GM-CSF+IL-4 DC *Crabp2* mRNA level, presented in Figure 16, as a technical control of the RT-qPCR assay (labeled with Experiment II/black square; the RT-qPCR results of the $CD103^+$ and $CD103^-$ MLN-DC samples are labeled with Experiment I/white square). We assessed the role of cellular interactions (T cells) using allogenic splenocytes on *Crabp2* and *Rbpr2* gene expression co-culturing with *ex vivo* DCs. In the $CD103^+$ MLN DC/splenocyte co-culture experiment, the expression of both *Crabp2* and *Rbpr2*

was induced in CD103$^+$ DCs, suggesting an enhanced retinol uptake and ATRA delivery to the nucleus as a result of cellular, most likely by T cell interactions (Figure 16).

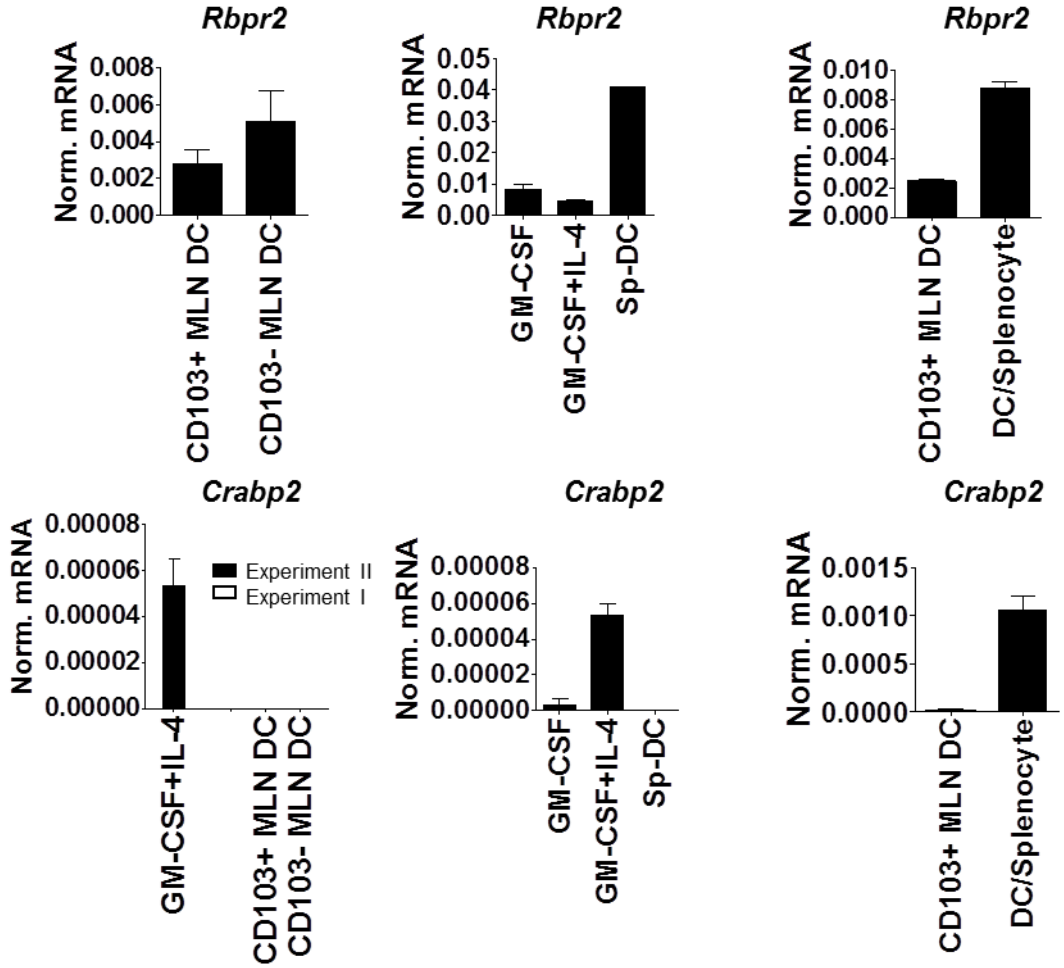

Figure 16: *RT-qPCR analysis of genes involved in retinol uptake (RBP4 receptor-2 (Rbpr2)) and intracellular ATRA transport (cellular retinoic acid binding protein (Crabp2) in CD103$^+$- and CD103$^-$ MLN-DCs, GM-CSF-DC, GMCSF+IL-4-DCs and in Sp-DCs. Gene expression of Rbpr2 and Crabp2 was measured by RT-qPCR in CD103$^+$ MNL-DCs and in CD103$^+$ MNL-DC/Splenocyte co-culture experiment. Means normalized to Cyclophilin A ± SD.*

We confirmed the role of cellular interactions (T cells) on *Crabp2* gene expression in CD103$^+$ MLN- C/CD8a$^+$ T cell co-culture experiment. The expression *Crab2* was induced in CD103$^+$ DCs suggesting a triggered ATRA delivery to the nucleus as a result of cellular interactions (Figure 17).

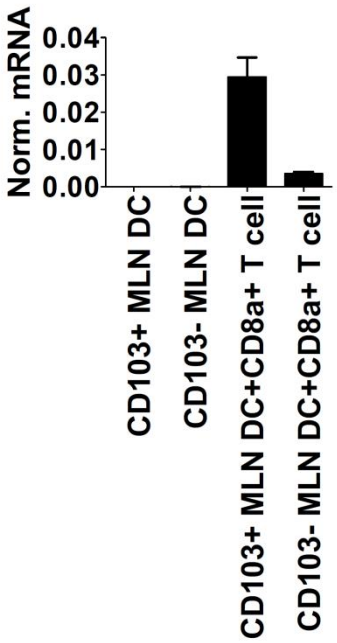

Figure 17: *RT-qPCR analysis of Crabp2 was measured in CD103$^+$ MLN-DCs and in CD103$^-$ MLN-DC/CD8a$^+$ co-culture experiment. Means normalized to Cyclophilin A ± SD.*

Summarizing these data, CD103$^+$ MLN-DCs, and GM-CSF-DCs or GM-CSF+IL-4-DCs have a gene expression signature consistent with active ATRA biosynthesis in line with earlier published data (251). *Cyp26a1* expression with *Raldh2* appears to indicate active retinoid signaling. We found that all DCs express the *Rdh10* gene. Based on these gene expression results, we concluded that ATRA biosynthesis is not a universal feature of DCs, and that, in line with our hypothesis, *Rdh10* expression overlaps with *Raldh2* expression, suggesting that DCs expressing both enzymes are likely to have active ATRA synthesis and signaling.

5.1.2. Characterization of retinoid signaling in human DCs

CD103$^+$ DCs are also present in the human small intestinal MLNs with similar functional properties compared to murine CD103$^+$ MLN-DCs (266). These data suggested that specific DCs with the ability of *de novo* ATRA synthesis can be present in the human body. Despite much effort and previous data (290), the human DC phenotypes are not identical and not easy to match up with the ATRA generating DCs in mice. Therefore we considered using human mo-DCs for our mechanistic characterization of the components of retinoid signaling by

functional assays. To prove that these *ex vivo* cells faithfully replicate the behavior of human *in vivo* DCs, we examined a microarray data set and compared the gene expression pattern of mo-DCs, LCs, dermal DCs from the skin, $CD1c^+$ DCs from the tonsil, $CD1c^+$DCs and pDCs from the blood of healthy donors (169, 175, 301, 302). Our analysis confirmed the notion that mo-DCs expressed common DC markers as *CD83*, *CD1A*, *CD14*, *CD86*, *CD209*, *CD36*, and *ILT7* pDC specific marker such as *in vivo* subsets (Figure 18).

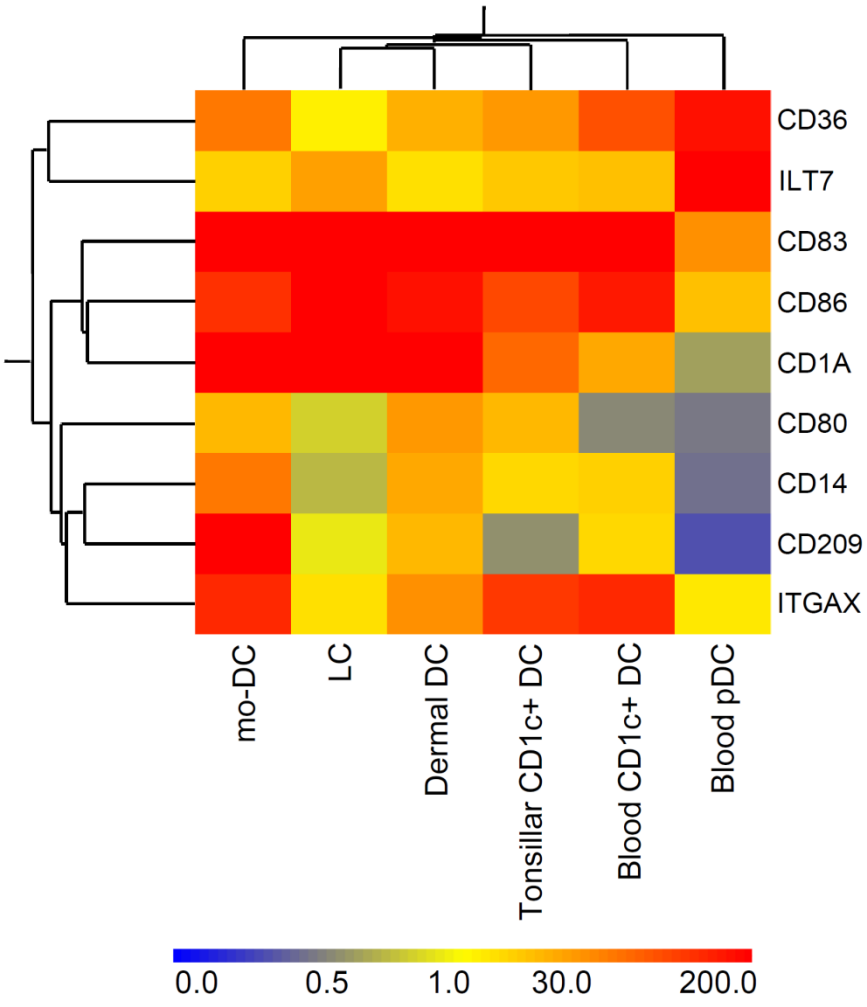

Figure 18: *Heat map analysis shows the gene expression patterns of DC markers in mo-DCs, Langerhans cells (LC), dermal DCs, $CD1c^+$ DCs from the tonsil, $CD1c^+$DCs and pDC from the blood of healthy donors.*

We assessed the surface expression of CD14, CD209, and CD11c on mo-DCS by FACS measurements. Monocytes were $CD14^+/CD11c^+/CD209^-$ while mo-DCs were $CD14^-/CD11c^+/CD209^+$, and thus phenotypically resembled *in vivo* iDCs (Figure 19).

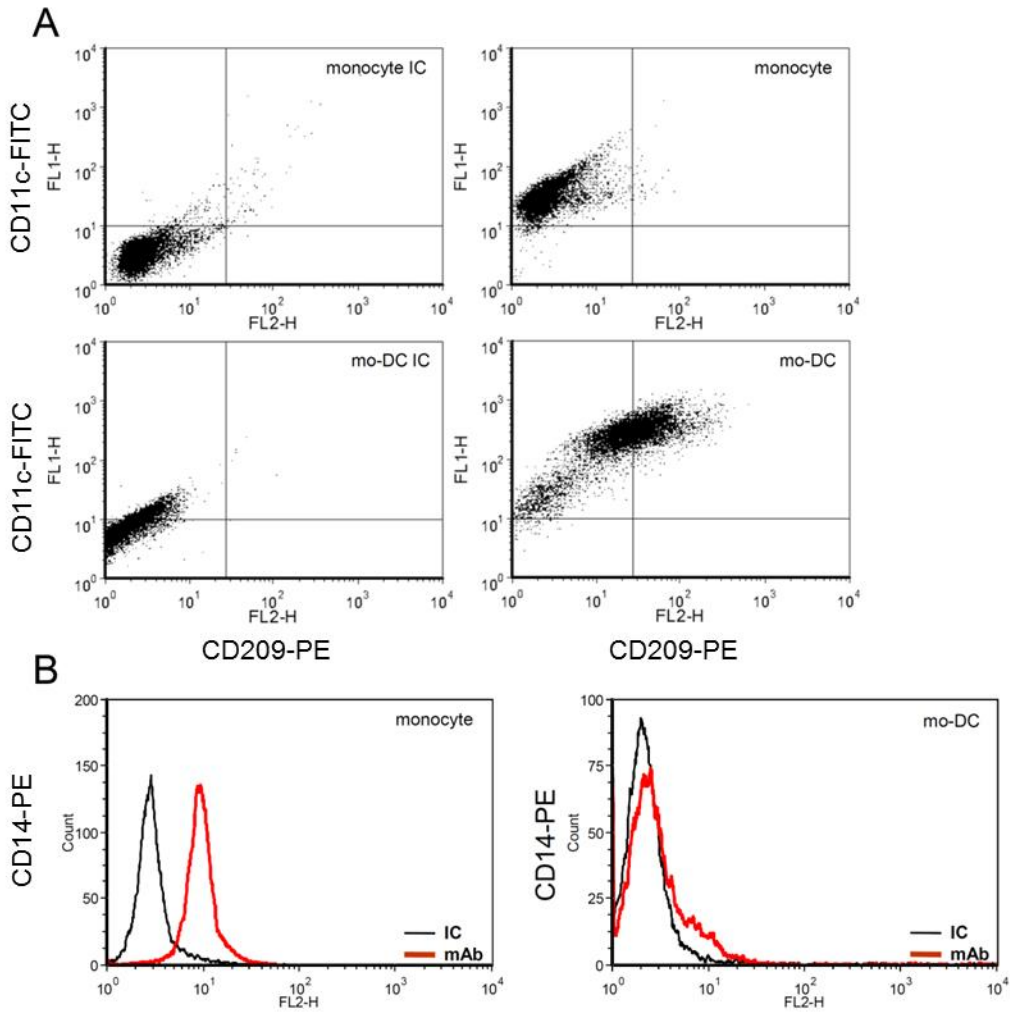

Figure 19: *A, The efficiency of the mo-DC differentiation was analyzed by co-staining of monocytes and mo-DCs with mAb-CD11c and mAb-CD209. B, The cell surface expression of CD14 protein was detected by flow cytometry.*

Next we examined the gene expression profile of a group of selected genes involved specifically in ATRA biosynthesis and signaling (Figure 20). *RDH10*, *RDH11*, and *DHRS9* were expressed in mo-DCs (239). Both *RALDH1* and *RALDH2* were expressed at high levels in mo-DCs, while a moderate level of the transcription of these genes was observed only in dermal DCs, suggesting the possibility of ATRA generation in this *in vivo* DC subtype. *RALDH3* was not expressed in these DC subtypes. Among the genes encoding intracellular ATRA-transporting proteins, *CRABP1* was not expressed, while *CRABP2* was expressed ubiquitously. We also examined the retinoid signaling by analyzing the expression pattern of target genes: tonsillar $CD1c^+$, blood $CD1c^+$ and mo-DCs expressed *CD1D* and *TGM2*.

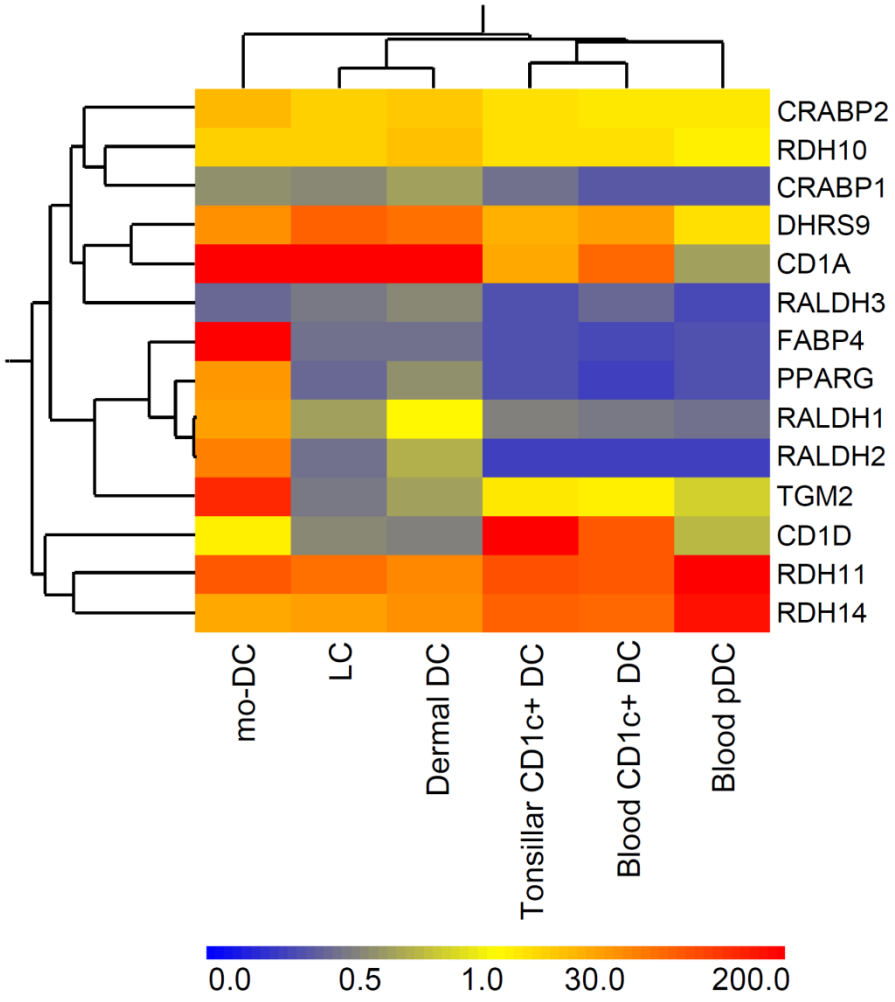

Figure 20: *Heat map representation of genes participating in endogenous production, oxidation, intracellular transport of ATRA, retinoid signaling target genes and PPARγ-mediated pathway, comparison between monocyte-derived dendritic cell (mo-DCs) and in vivo DC subsets.*

Thereafter, we focused on *PPARG* and *FABP4* (a known marker gene of activated PPARγ signaling) (270). Previously we have demonstrated that PPARγ triggered ATRA production by inducing *RDH10* and *RALDH2* gene expression in RSG (synthetic PPARγ ligand)-treated mo-DCs (239). In line with this data, our microarray data demonstrated that the *PPARG* is expressed in mo-DCs. The detectable level of *FABP4* is likely to indicate either the presence of extracellular PPARγ ligand in the serum or the presence of possible endogenous activators inside the cells. Other *in vivo* DC types failed to express *PPARG* or *FABP4*. This systematic

analysis suggested that retinoid signaling is only active in mo-DCs that co-express *RDH10* and *RALDH2*, and in these cells PPARγ signaling is connected to the retinoid signaling pathway.

To validate our microarray data, we quantified the transcriptional changes of the genes contributed to ATRA synthesis during the full differentiation period by RT-qPCR. For this, we cultured monocytes in the presence of DMSO/EtOH for control (C), RSG, RSG and GW9662 (a PPARγ antagonist) or GW9662 alone to assess possible roles of PPARγ in gene expression. We quantified the normalized mRNA level of *RALDH* genes at 6 h, and as indicated at later time points (24, 72, and 120 h) (Figure 21).

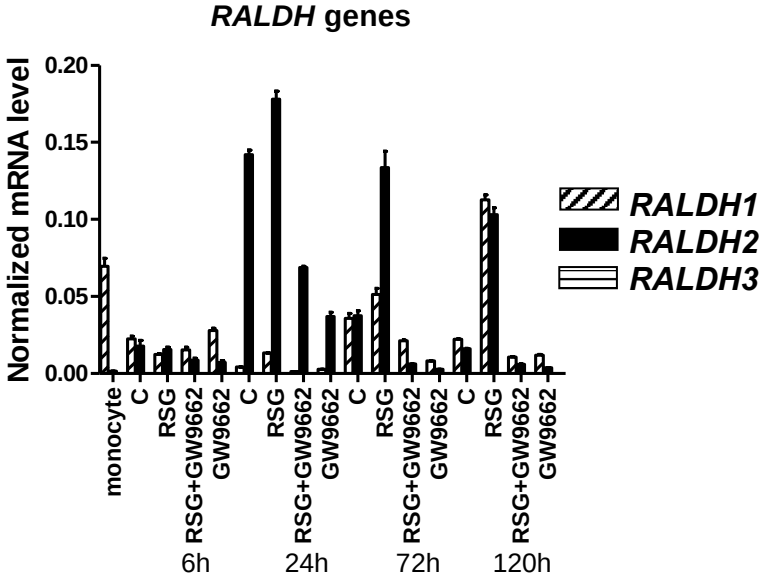

Figure 21: *RT-qPCR analysis of RALDH1, RALDH2 and RALDH3 in human mo-DCs, obtained from monocytes and differentiated in the presence of DMSO/EtOH (C), 2.5 μM (rosiglitazone) RSG or 2.5 μM RSG +100 nM GW9662 and 100 nM GW9662. Means normalized to CYCLOPHILIN A ± SD.*

A high level of *RALDH1* was detected in monocytes that was rapidly down-regulated and was expressed at elevated level again in 120 h samples, indicating that *RALDH1* may be involved in retinal oxidation in fully differentiated cells. In contrast, the human *RALDH2* was barely measurable in monocytes. After 6 h, cells expressed *RALDH2* at comparable levels to *RALDH1*. At all later time points, *RALDH2* was highly up-regulated in the RSG-treated samples and**,** except for day 5, when ligand treatment induced *RALDH2* transcription at similar levels as compared with *RALDH1*, suggesting that *RALDH2* not only has a dominant role in differentiating DCs but also acts as a metabolizing enzyme in differentiated cells. The *RALDH3* isoform was not detectable irrespective of treatments or time points.

As expected, ligand treatment induced the expression of *RDH10* after 6 h, indicating that PPARγ activates this gene probably via direct molecular interaction. The expression of *RDH10* in PPARγ-ligand instructed samples continuously increased during the differentiation period. Interestingly, both *CRABP2* and *TGM2* genes were up-regulated in RSG-treated DCs after 24 h in accordance with earlier results (239); *CD1D* was expressed at a high level in monocytes, but rapidly decreased in cultured cells. Consistent with our previous results, increased *CD1D* transcription was observed at later time points (49) in RSG-treated samples (Figure 22).

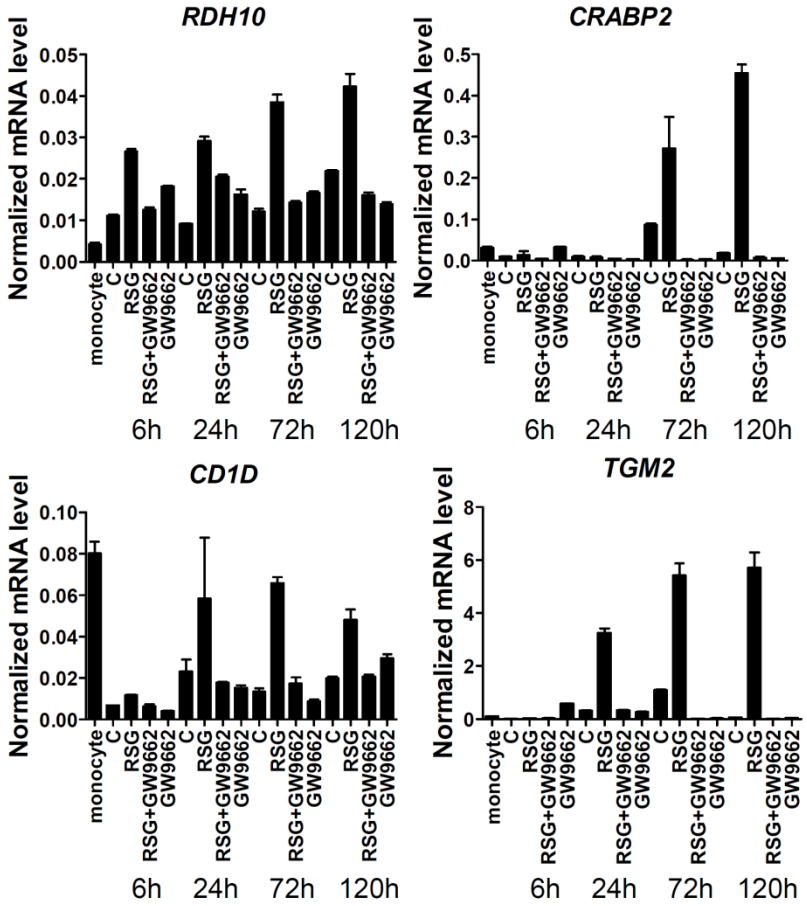

Figure 22: *Kinetics of RDH10, CRABP2, TGM2, and CD1D expressions were determined by RT-qPCR. Monocytes were treated with DMSO/EtOH (C= Control), 2.5 μM RSG or 2.5 μM RSG +100 nM GW9662 or 100 nM GW9662 and harvested at indicated time points (monocyte, 6h, 24h, 72h, and 120h). Means normalized to CYCLOPHILIN A ± SD. One representative donor out of three.*

PPARG was immediately induced in differentiating cells, the highest expression level was detected at 6 h, and the gene was detectable at a somewhat lower level in DCs. We detected a similar expression pattern of *FABP4* compared to *RDH10* (Figure 23).

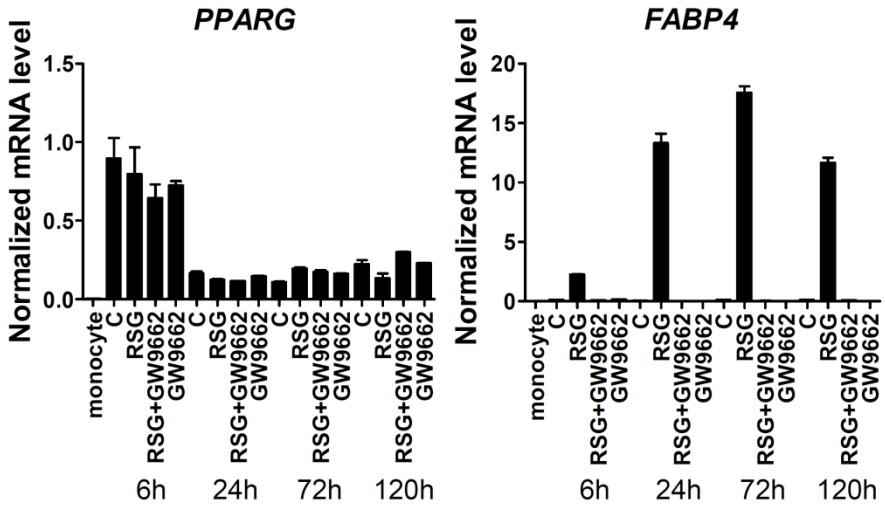

***Figure 23**: Kinetics of peroxisome proliferator-activated receptor γ (PPARG) and fatty acid binding protein 4 (FABP4) expression were determined by RT-qPCR. Monocytes were treated with DMSO/EtOH (C= Control), 2.5 μM RSG or 2.5 μM RSG +100 nM GW9662 or 100 nM GW9662 and harvested at indicated time points (monocyte, 6h, 24h, 72h, and 120h). Means normalized to CYCLOPHILIN A ± SD. One representative donor out of three.*

In summary, ATRA production and signaling is not a universal feature of human DCs and it appears to be tightly regulated. We found evidence that *ex vivo* differentiated mo-DCs expressed all components required for retinol to ATRA conversion and intracellular ATRA transport, suggesting that mo-DCs had the ability for *de novo* ATRA synthesis and signaling. This ATRA producing ability can be induced by the co-ordinate up-regulation of *RDH10*, *RALDH2*, and *CRABP2*.

5.1.3. Transport of ATRA via CRABP2 to the nucleus is PPARγ-regulated

We investigated whether intracellular ATRA delivery could also be regulated by PPARγ. PPARγ activation profoundly induced the transcript levels of *CRABP2* therefore we further characterized its regulation. CRABP2 delivers ATRA to the nucleus, thus enhanced expression of CRABP2 should increase the transcriptional activity of RAR (200, 309). CRABP2 acts as a co-activator molecule, when is present, retinoid signaling is more efficient. Due to the fact that the transcript level of CRABP2 was profoundly induced in RSG-treated samples (Figure 24) we examined if the gene expression changes are manifested at protein level in mo-DCs.

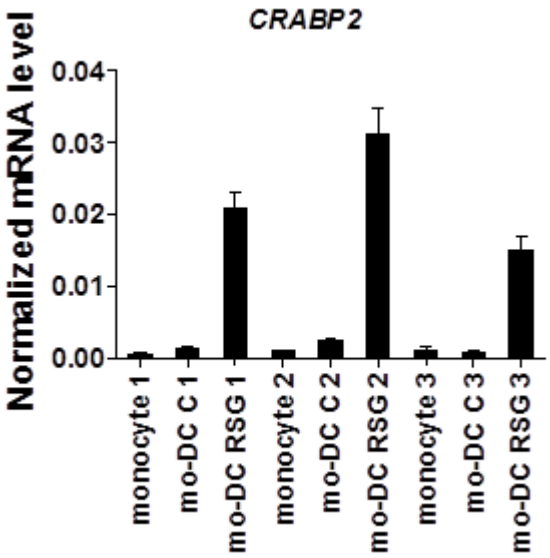

Figure 24: *Expression of human CRABP2 genes was examined by RT-qPCR. mo-DCs were obtained from three healthy donors (1-3) and differentiated with IL-4 and GM-CSF for 5 days. Cells were treated at monocyte state with DMSO/EtOH (C), or 2.5 μM RSG. Means normalized to CYCLOPHILIN A ± SD.*

We found that monocytes did not express CRABP2, while control-treated mo-DCs expressed a detectable level of the protein, which was highly induced in RSG-treated mo-DCs. This appears to be a DC-specific regulation, because monocyte-derived macrophages (Mφs) failed to express any CRABP2 (Figure 25A). We further confirmed the elevated CRABP2 expression at the expression site of the delivery protein within mo-DCs by IHC. We observed elevated CRABP2 protein expression in DCs as compared with monocytes and a strong up-regulation of CRABP2 upon RSG-treatment (Figure 25B).

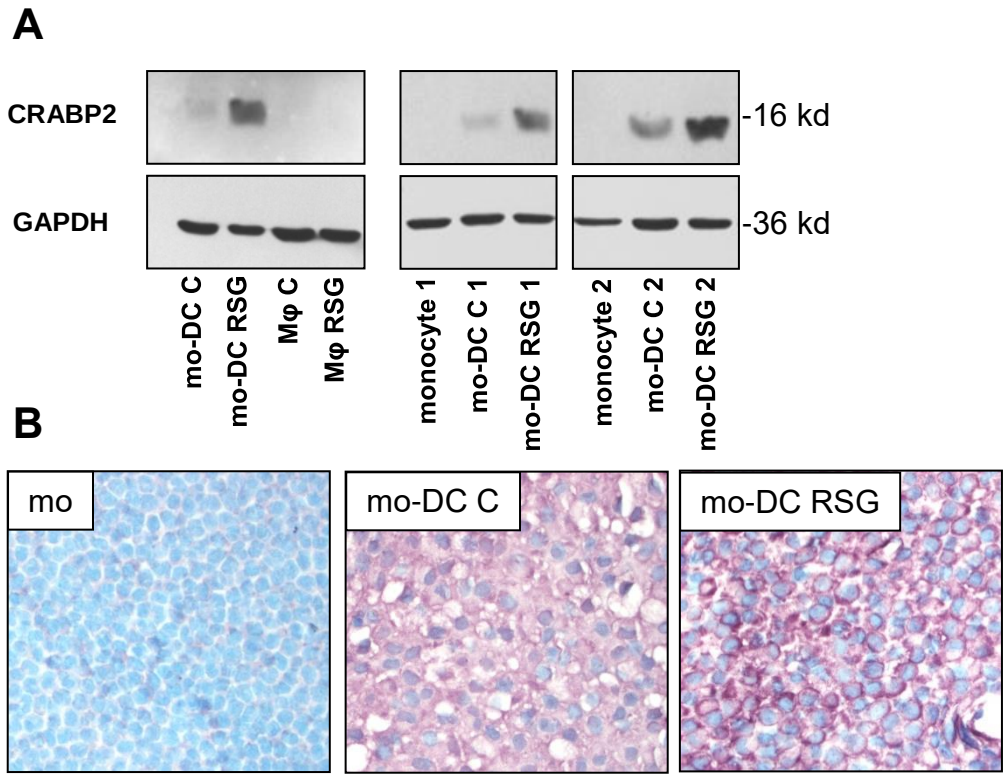

Figure 25: *A, CRABP2 protein level was determined by Western blot. Immune cell specificity was shown as monocyte-derived macrophages (Mφ) failed to express CRABP2. Glyceraldehyde-3-phosphate dehydrogenase (GAPDH) was used as loading control. B, CRABP2 expression was tested by IHC peroxidase-methods, also, in monocytes, control mo-DCs and 2.5 μM RSG-treated mo-DCs respectively. The highest expression level for CRABP2 was observed in differentiated RSG mo-DCs, predominantly located in the cytoplasm. (Immune peroxidase reaction with methyl-green nuclear counterstaining; original magnification: 40x).*

Based on our IHC and Western blot results, we concluded that PPARγ-activated mo-DCs represent a relevant *ex vivo* model system that appears to be suitable to mechanistically dissect the ATRA biosynthesis and signaling pathway composed of RDH10, RALDH2 and CRABP2 proteins that are co-ordinately up-regulated by PPARγ. We postulated that the elevated CRABP2 expression in PPARγ-instructed DCs might contribute to the enhanced ATRA response. We also realized that further investigations are required for providing direct evidence for CRABP2-mediated ATRA delivery to the nucleus in mo-DCs.

5.1.4. PPARγ, RDH10, RALDH2, CRABP2, and the ATRA-regulated TGM2 co-localize in DCs of the human GALT

In order to obtain evidence for the physiological relevance to our findings, we systematically surveyed the expression of the components of ATRA biosynthesis and signaling in human tissues. We tested the expression of PPARγ, RDH10, RALDH2, CRABP2 and TGM2 in resting human GALT with no associated intestinal inflammation using in situ IF staining/DI. We chose GALT (for hematoxylin eosin section see Figure 26B), as this is the most likely place where lipid signaling could contribute to DC differentiation and subtype specification in the gut. As shown in Figure 26A (representing an IF image), we observed that PPARγ could be readily detected in white adipose tissue (WAT; positive control to ensure the specificity of the antibody during DI staining). DI of resting GALT for PPARγ (red) demonstrated that PPARγ was in part co-expressed with Dendritic Cell-Specific Intercellular adhesion molecule-3-Grabbing Non-integrin (DC-SIGN) (green cytoplasmic, arrows) in mucosal lymphoid tissue cells that have cytoplasmic projections in a network pattern indicating DC phenotype (Figure 26C). Interestingly, nuclear PPARγ (red) and the cytoplasmic TGM2 proteins (green) showed co-expression in similar cells of GALT exhibiting cytoplasmic green projection characteristic of DC elements, comparable with the staining pattern as seen for PPARγ-DC-SIGN of image C. Therefore, these cells co-expressing PPARγ/TGM2 should represent the DC population of GALT, similarly to PPARγ/DC-SIGN positive cells (Figure 26D). These results indicate that in resting lymphoid tissues some of the PPARγ-positive DCs express TGM2 simultaneously, suggesting that PPARγ might regulate ATRA-dependent transcription *in vivo* as well.

On the other hand, in the GALT we showed that some PPARγ (red) positive cells co-expressed RDH10 (green cytoplasm) (Figure 26E). Similarly, we observed few PPARγ-expressing DCs with RALDH2 and CRABP2 co-expression, respectively (Figure 26F and G). RDH10, RALDH2, and CRABP2 (green cytoplasmic and/or nucleic) also co-localized with DC-SIGN (red cytoplasmic projections) in some mucosal DCs (Figure 26H–J). Note, that the densities for RDH10-, RALDH2-, and CRABP2-positive cells were roughly the same when Figure 26E–G compared to Figure 26H–J, reflecting non-activated DC conditions in resting GALT. However, the number of PPARγ$^+$ DCs was increased in cases of inflammatory bowel diseases (IBDs) (data not shown).

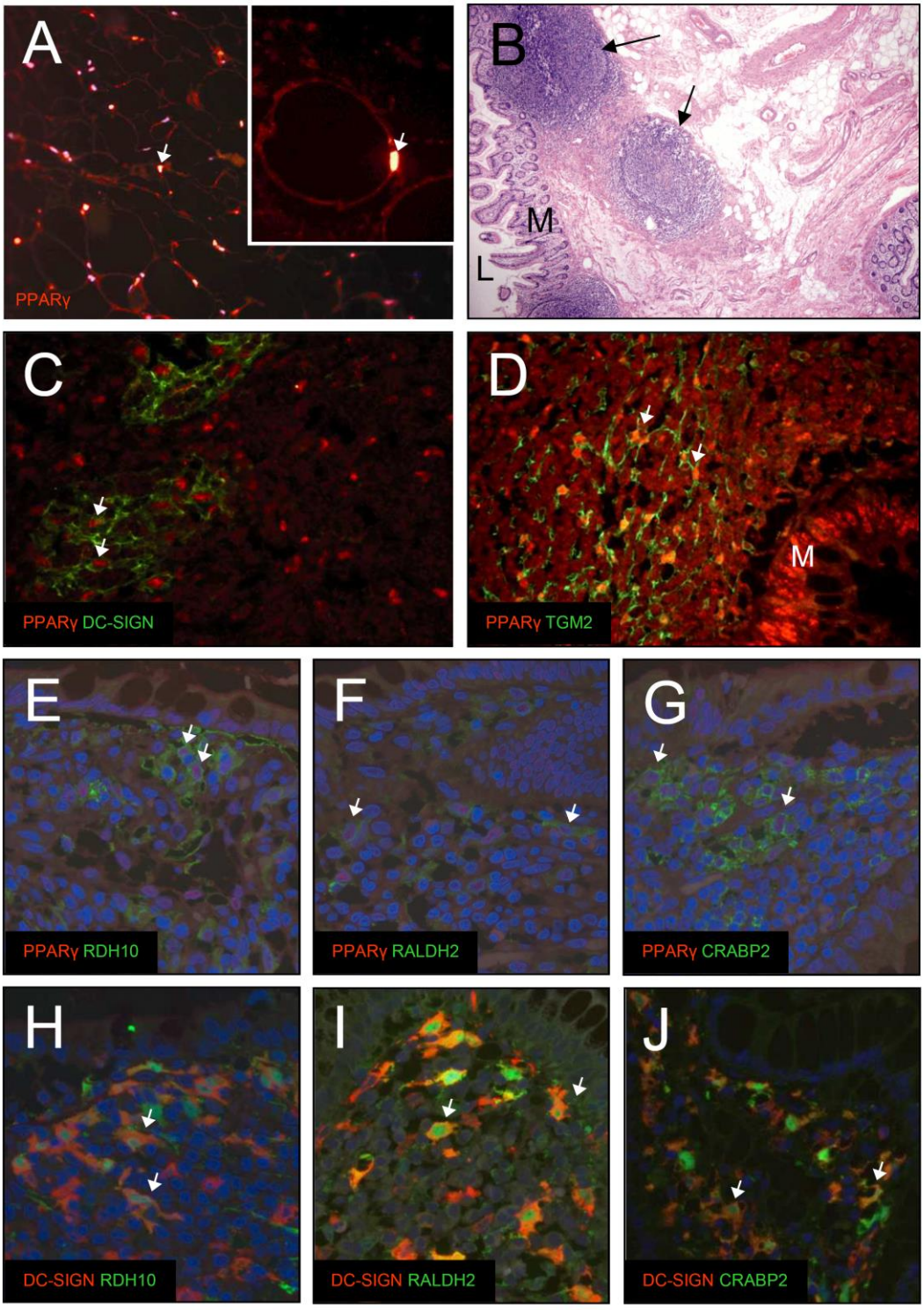

Figure 26: *DI staining analysis of ATRA synthesis and the putative signaling pathways along with PPARγ expression in human gut-associated lymphoid tissue (GALT). A, Positive control for PPARγ immunofluorescent (IF) staining: the nuclei of white adipose tissue (WAT) cells showed characteristic expression [lighting-red fluorescence (arrows) is magnified in the insert]. B, A representative area of hematoxylin eosin-stained human GALT was shown where arrows pointed to the mucosa-associated lymphoid tissue (M, mucosa; L, lumen). C, Using double immunofluorescence (DI, the same tissue*

showed that the PPARγ protein (nuclear red fluorescence) was in part co-expressed with dendritic cell-specific intercellular adhesion molecule-3-grabbing non-integrin (DC-SIGN) (green cytoplasmic, arrows) in mucosal lymphoid tissue cells that had exhibiting cytoplasmic projection in a network pattern indicating DC phenotype. D, The nuclear PPARγ (red) and the cytoplasmic TGM2 proteins (green) showed co-expression in the similar cells of GALT exhibiting cytoplasmic green projection characteristic of DC elements comparable with the staining pattern as seen for the PPARγ-DC-SIGN of image (C). E, Some of the DCs exhibiting PPARγ (red nuclei) also expressed RDH10 (green cytoplasm) in resting GALT. F, Rarely, PPARγ (red nuclei) was also co-labeled with RALDH2 (green cytoplasm) in the same GALT. G, Also scattered cells with PPARγ positivity (red nuclei) showed simultaneous expression with CRABP2 (green cytoplasm, arrows) in the same GALT. H, In many DC-SIGN-positive DCs (red cytoplasm) there was a RDH10 (green nucleic and cytoplasmic) co-expression (arrows). J, DC-SIGN expressing DCs (cells with red cytoplasmic projections) showed co-expression with RALDH2 (arrow) as well (cells with green nuclei or cytoplasm). I., Few DC-SIGN-positive cells (red cytoplasm) showed co-localization with CRABP2 protein (green nuclei and cytoplasm), also (arrow) indicating that CRABP2-positive cells were of DC type within resting GALT. [Except for image (B), all were DI photographs with DAPI nuclear counterstaining. Original magnifications: (A, C, D), 20×; (B), 10×; (E–G), 40×; (H–J), 60×].

These data collectively strongly suggest that the key components of ATRA synthesis and the PPARγ are expressed together in some of the antigen-presenting cells (APCs) of the mucosal lymphoid tissues, consistent with a previous report which demonstrated that murine intestinal DCs expressed RALDH2 (253).

5.1.5. Increased RALDH activity in PPARγ-activated mo-DCs

We wanted to provide functional evidence that retinoic acid biosynthesis take place in mo-DCs. Utilizing a sensitive and quantitative liquid chromatography-mass spectrometry (LC-MS) method, we previously demonstrated that mo-DCs have the ability to produce ATRA in a PPARγ-dependent manner (239). We aimed to further investigate this result and the function of cellular RALDHs using ALDEFLUOR staining assay that is suitable to detect intracellular enzymatic activity of RALDHs. mo-DCs were differentiated in the presence of DMSO/ethanol (C=Control), RSG, or RSG+GW9662. At 120 h, the cells were divided and incubated with fluorescent ALDEFLUOR, a substrate for RALDHs, either in the absence or the presence of DEAB, a specific RALDH inhibitor. RALDH activity was measured by flow cytometry. There were 8% RALDH active cells in control-treated sample (Figure 27). In the presence of RSG, the number of RALDH active cells was increased to approximately 40%. We noted that a much higher enzyme activity was displayed in these treated DCs than even in the positive ones in control DCs. In the RSG and GW9662 co-treated sample, the RALDH activity was similar to vehicle-treated control DCs.

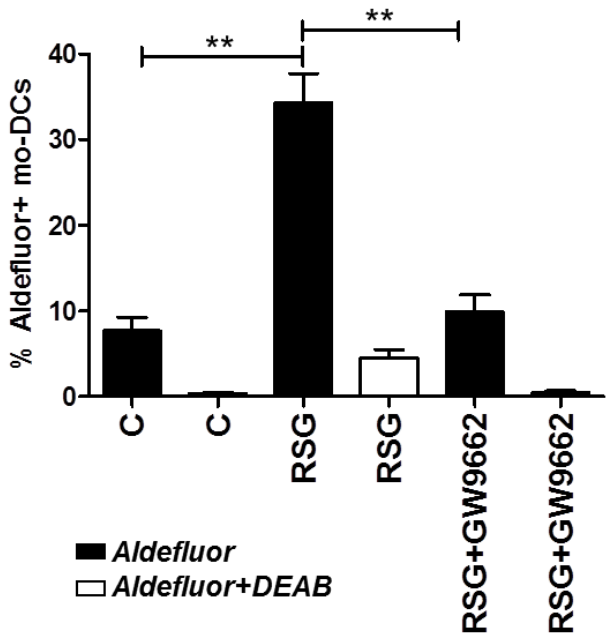

Figure 27: *RALDH activity in PPARγ-activated mo-DCs. RALDH activity was measured by ALDEFLUOR kit. Mo-DCs were differentiated from the monocytes of healthy volunteers. 4-diethyl amino-benzaldehyde (DEAB)-treated DCs served as negative control. The average of RALDH activity of C, RSG, and RSG+GW9662-treated mo-DCs obtained from three individual donors. **C-RSG (P = 0.0021), **RSG-RSG+GW9662 (P =0.0035).*

Next, we examined RALDH activity in mo-DCs electroporated at monocyte stage using specific siRNAs against *RDH10*, *RALDH2*, *CRABP2* and NS-scrambled control siRNA. We treated cells with DMSO/ethanol (C), RSG, and RSG+GW9662. At day five ALDEFLOUR staining was quantified. We measured lower RALDH activity only in the siRALDH2 electroporated sample (Figure 28). These results suggest that RALDHs are active in mo-DCs, and the enhanced ATRA production capacity of mo-DCs is PPARγ dependent. Interestingly, we could detect heterogeneity in this respect in the RSG-mo-DC population, but the generated endogenous ATRA level is at the range of RAR activation.

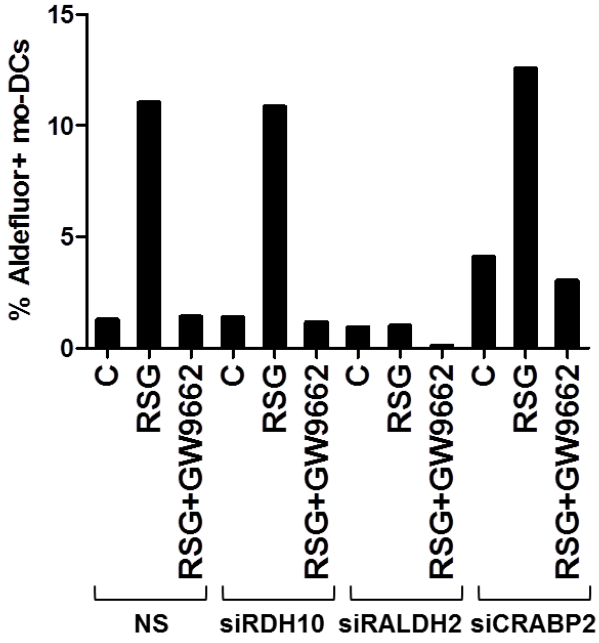

Figure 28: *Quantification of RALDH activity in mo-DCs. Monocytes were electroporated with small interfering RNA (siRNA) against RDH10, RALDH2 and CRABP2. NS: non-silencing control sample electroporated with scrambled control siRNA. C: DMSO/EtOH, RSG and RSG+GW9662 treatments were applied at monocytic stage. RALDH activity was measured by Aldefluor assay Kit in mo-DCs. One representative donor out of three.*

5.1.6. PPARγ activation induces RAR signaling/gene expression via RDH10, RALDH2 and CRABP2

Based on these data, we hypothesized that RDH10, RALDH2, and CRABP2 might be required for PPARγ-regulated ATRA production and gene expression. Despite the murine DC results (290), the model one can test this in is the human mo-DC. PPARγ activation leads to transcriptional activation of several RAR target genes in human mo-DCs (239). Pharmacological analysis revealed that administration of the RALDH inhibitor DEAB reduced gene expression of *CD1D* and *TGM2* upon RSG treatment, suggesting the importance of RALDH2 in PPARγ-enhanced retinoid signaling (239). We have extended our studies by testing to determine whether the oxidizing enzymes and CRABP2 are indeed mechanistically indispensable for retinoid-regulated gene expression induced by PPARγ. To test this hypothesis, we decided to use a siRNA-based approach. Monocytes were electroporated with siRNA against *RDH10*, *RALDH2*, or *CRABP2* and *FABP4* (as a control). RSG was administered as indicated in Figure 29. After 24 or 48 h of RSG treatment, we quantified the

transcript level of *CD1D* and *TGM2* using RT-qPCR. PPARγ-induced *CD1D* expression was down-modulated by all except *FABP4*–specific siRNA at both indicated time points (24 and 48 h). *TGM2* expression changes were similar at 24 h, but only *RDH10*-specific siRNA reduced it significantly at 48 h as compared with non-silencing control electroporated (NS) DCs (Figure 29).

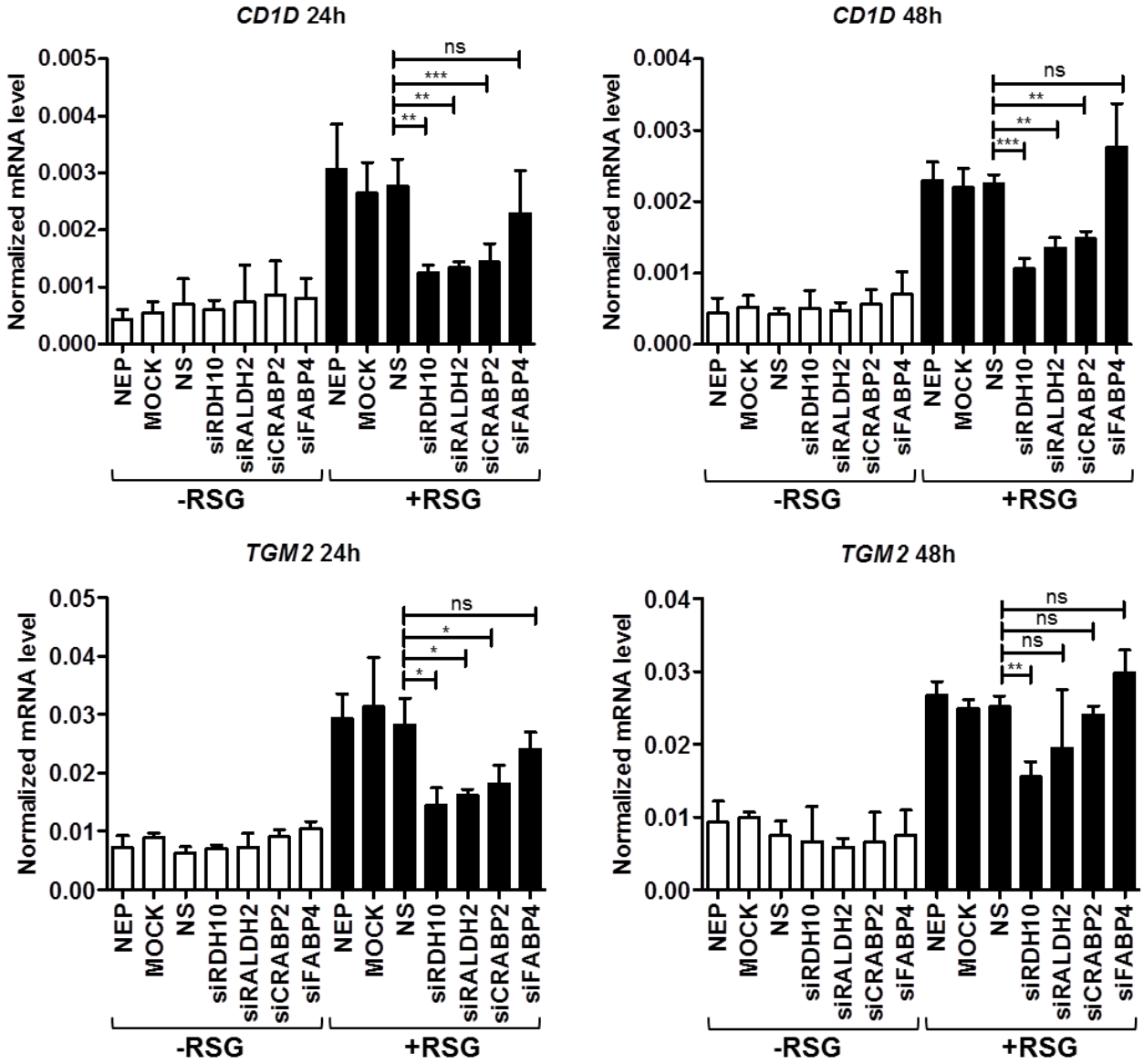

Figure 29: *Expression of RDH10, RALDH2, and CRABP2 was required for PPARγ-induced retinoid signaling and gene expression in mo-DCs. Monocytes were electroporated with siRNA against RDH10, RALDH , CRABP2, and FABP4, NEP: no electroporated control sample, NS: non-silencing control sample electroporated with scrambled control siRNA. Gene expression of CD1D was determined by RT-qPCR. Means normalized to CYCLOPHILIN A ± SD; n = 3; **NS-RDH10 24h (P = 0.0062); **NS-RALDH2 24h (P = 0.0074); *NS-CRABP2 24h (P = 0.0161); NS-FABP4 24h (P = 0.4082); ***NS-RDH10 48h (P = 0.0005); **NS-RALDH2 24h (P = 0.00713); **NS-CRABP2 24h (P = 0.0014); NS-*

*FABP4 24h (P = 0.2188). Gene expression of TGM2 was determined by RT-qPCR. Means normalized to CYCLOPHILIN A ± SD; n = 3;*NS-RDH10 24h (P = 0.0119); *NS-RALDH2 24h (P = 0.0111); *NS-CRABP2 24h (P = 0.0346); NS-FABP4 24h (P = 0.2539); **NS-RDH10 48h (P = 0.0030); NS-RALDH2 24h (P = 0.2974); NS-CRABP2 24h (P = 0.3895); NS-FABP4 24h (P = 0.0854). Cells were treated with DMSO/EtOH (-RSG) or with PPARγ specific ligand (+RSG).*

We measured the gene expression of *RALDH2* in the same experiment. Only siRALDH2 could significantly reduce the normalized mRNA level of *RALDH2* as was expected (Figure 30).

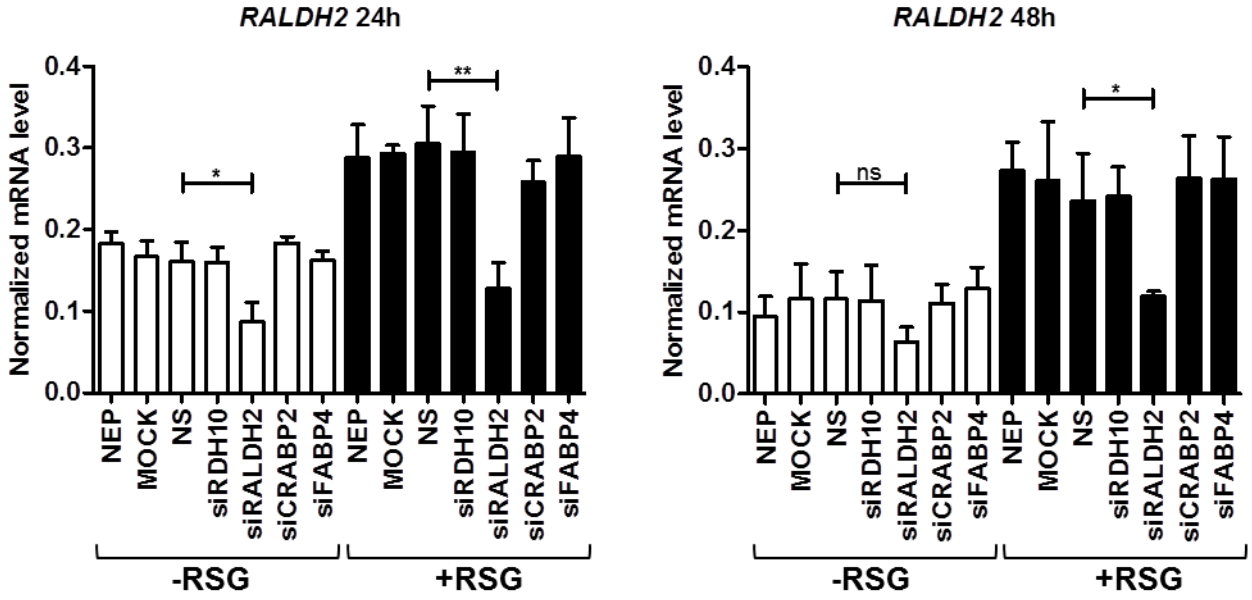

Figure 30: *Quantification of RALDH2 gene expression by RT-qPCR. Monocytes were electroporated with siRNA against RDH10, RALDH2, CRABP2 and FABP4. NEP- no electroporated control samples, NS: non-silencing control sample electroporated with scrambled control siRNA. Gene expression of RALDH2 was determined by RT-qPCR. Means normalized to CYCLOPHILIN A ± SD, n=3; *NS-RALDH2 24h (P= 0.0208 –RSG); **NS-RALDH2 24h (P= 0.0055 +RSG); NS-RALDH2 48h (P= 0.0778 –RSG); *NS-RALDH2 48h (P= 0.0250 +RSG).*

These data suggest that RDH10 is a key component of retinol conversion, and PPARγ-mediated retinal oxidation is catalyzed by RALDH2 in mo-DCs.

In the next set of experiments, we electroporated monocytes with *RDH10*-specific siRNA and treated as described in Figure 31; then we measured CD1d cell surface protein expression by flow cytometry. Transient transfection of siRDH10 reduced CD1d levels on DCs and it was still down-regulated at day 5 post-electroporation (Figure 31).

These results strongly suggested that PPARγ-mediated signaling induced retinol conversion by RDH10 in mo-DCs. The produced retinal was oxidized to ATRA by RALDH2. The

enhanced retinoid signaling was more effective in the presence of the CRABP2 ATRA transporter. In the nucleus, ATRA activates regulated target genes via RAR/RXR heterodimers due to integrated PPARγ-RAR signaling.

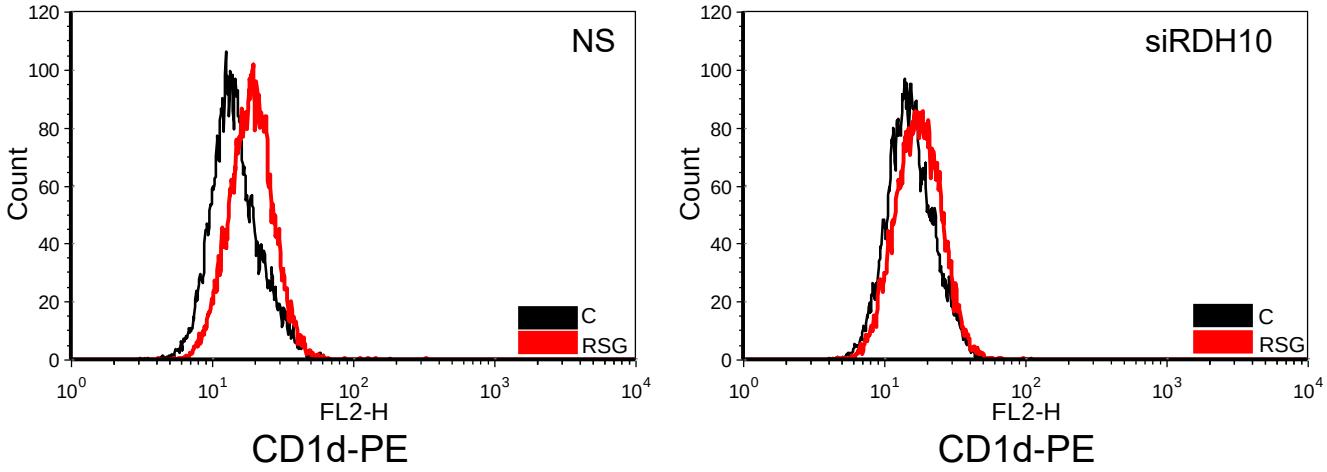

Figure 31: *Expression of CD1d protein on 5 day mo-DCs was measured by FACS analysis. Monocytes were electroporated with scramble control siRNA (NS) and siRNA against RDH10 (siRDH10). mo-DCs were differentiated in the presence of DMSO/EtOH (C=Control) or 2.5 μM RSG (RSG).*

5.1.7. PPARγ-induced iNKT expansion is attenuated by RDH10, RALDH2, or CRABP2 knock down

Next we aimed to assess the functional consequence of RDH10, RALDH2, and CRAB2 in *in vitro* functional assay. The lipid antigen-presentation properties of PPARγ-activated DCs is induced and mediated through the up-regulated cell surface protein expression of CD1d protein (49, 239, 310). Human iNKT cells respond to αGC, a lipid antigen presented exclusively by CD1d molecules. First, we sought to investigate whether RDH10 can influence the PPARγ-mediated iNKT expansion capacity of the APCs. For this, we silenced the *RDH10* gene in monocytes with siRDH10 or with non-silencing control siRNA (NS siRNA). Cells were differentiated to mo-DCs in the presence of DMSO/ethanol for the control-treated sample or RSG for PPARγ activation; cells were pulsed with or without αGC for 48 h and then co-cultured with autologous PBMCs. The iNKT proliferation capacity was monitored by Vα24/Vβ11 double staining. As expected, enhanced iNKT expansion was detected in RSG-treated and NS siRNA-transfected samples, while reduced iNKT cell numbers were detected in RDH10 siRNA-treated cells (Figure 32).

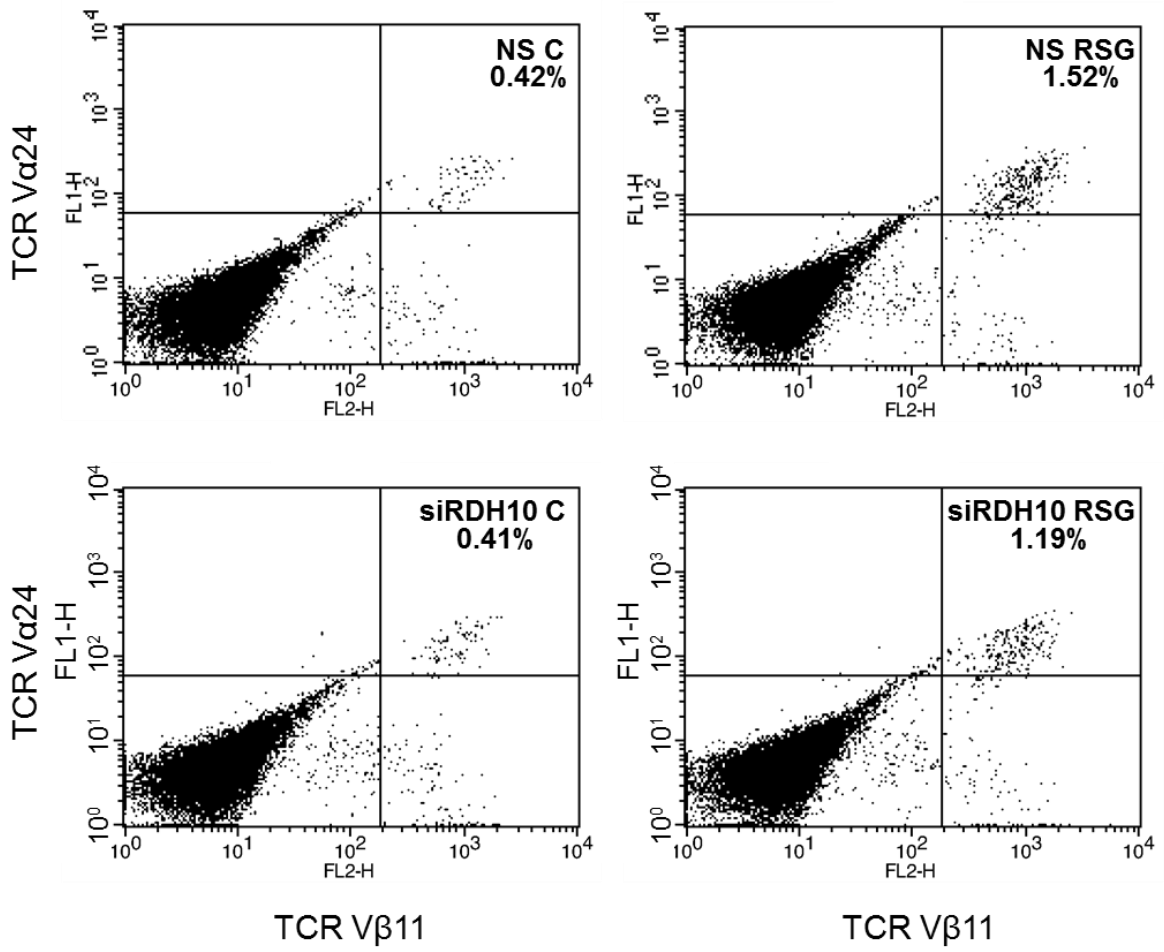

Figure 32: *RDH10 was required for PPARγ-induced iNKT activation in mo-DCs. A, Expansion of invariant natural killer T cell (iNKT) cells was assessed in lipid antigen presentation assay. Monocytes were electroporated with siRNA against RDH10 and scramble control siRNA (NS). Cells were differentiated in the presence of DMSO/EtOH(C=Control) or 2.5 μM RSG (RSG) for 5 days. iNKT differentiation was detected by T cell receptor (TCR Vα24/TCR Vβ11) double staining utilizing FACS analysis.*

During iNKT expansion, the mRNA expression of the invariant Vα24-Jα18 (iNKT) TCRα marker gene correlated with the cell surface expression of TCR Vα24 and TCR Vβ11 (310) on iNKT cells. We validated the RT-qPCR measurements on iNKT cells expanded by αGC-loaded control or RSG-treated mo-DCs (Figure 33A). Therefore, we studied the functional consequence of RDH10, RALDH2, and CRABP2 knock-down on iNKT expansion by measuring Vα24-Jα18 (iNKT) TCRα gene expression as described in Figure 33B. αGC-pulsed mo-DCs have displayed enhanced Vα24-Jα18 (iNKT) TCRα gene expression, further inducible by RSG treatment as compared with control (NS) treated cells. Next, siRNA-treated mo-DCs were loaded with αGC and co-cultured for 5 days. As shown in Figure 33B, siRNA

against *RDH10*, *RALDH2*, and *CRABP2* reduced the normalized *TCR Vα24* mRNA levels in RSG-treated samples as compared with non-silencing control (NS)-treated cells. Our data revealed significantly reduced Vα24-Jα18 (iNKT) TCRα transcription (Figure 33B).

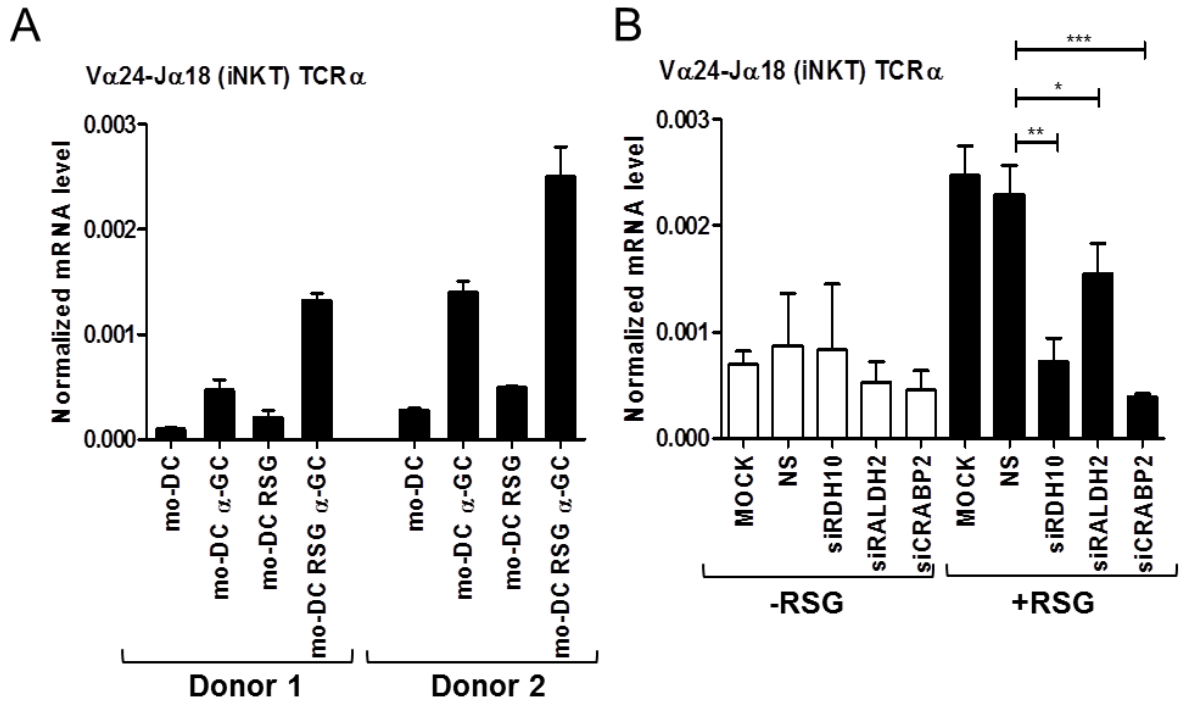

Figure 33: *iNKT expansion was quantified by RT-qPCR. A, mo-DCs/peripheral blood mononuclear cell (PBMC) co-culture experiments. Expression of Vα24-Jβ18 (iNKT) TCR gene was quantified by RT-qPCR. Means normalized to CYCLOPHILIN A ± SD. αGC: α-galactosylceramide. B, Expression of Vα24-Jβ18 (iNKT) TCR gene was quantified by RT-qPCR. Monocytes were electroporated with siRNA against RDH10, RALDH2, and CRABP2. NS: non-silencing control sample electroporated with scrambled control siRNA. Mo-DCs were differentiated in the presence of DMSO/EtOH (-RSG) or 2.5 μM RSG (+RSG) for 5 days, cells were pulsed with αGC. Means normalized to CYCLOPHILIN A ± SD; n = 3; **NS-RDH10 (P = 0.0016); *NS-RALDH2 (P = 0.0315); ***NS-CRABP2 (P = 0.0003).*

Based on these functional results, we could conclude that PPARγ was acutely involved in retinoid signaling via inducing endogenous ATRA production. The primary enzyme for retinol oxidation was RDH10. The RSG-treated cells had the ability to synthesize ATRA because the co-expression of RDH10 and RALDH2 in the cells allowed it. Moreover, retinoid signaling was more effective in the presence of PPARγ-induced CRABP2 protein that transported ATRA to the nucleus.

In the second part of the Result section, we present our recent published data about PPARγ-regulated CatD expression in human mo-DCS. This project was co-ordinated by Dr. Britt Nakken and Dr. Tamás Varga.

5.2. PPARγ-regulated Cathepsin D (CatD) is required for lipid antigen presentation by DCs

5.2.1. PPARγ-regulated CatD expression in human mo-DCs

Our goal was to uncover how PPARγ modulates lipid antigen presentation events in mo-DCs in addition to regulating of the expression of CD1d molecules. We hypothesized, that if PPARγ enhances lipid presentation by regulating a yet unidentified mechanism, then this must be reflected in the gene expression changes upon PPARγ ligand treatment. Therefore, we analyzed our previous microarray data set of differentiating human mo-DCs (169, 239). We compared the gene expression profiles of differentiating DCs at 6 h, 24 h, and 120 h in control- or RSG-treated samples. This analysis revealed PPARγ-mediated regulation of genes, participated in lipid antigen presentation such as endogenous lipid antigen processing (Hexosaminidase B-*HEXB*) (75) and lipid uptake and lysosomal delivery (apolipoprotein E-*APOE*) (86) (Figure 34).

We supposed that a subset of the genes whose expression patterns follows that of known lipid presentation genes, but have previously not been connected to lipid presentation, might also be involved in lipid antigen processing. CatD, L, and S (Figure 34) lysosomal proteinases, were up-regulated in RSG-treated samples. Previously, CatL and S have been connected to lipid antigen presentation in mice (101, 311). However, the role of CatD in lipid antigen presentation has not been published to date. Based on this microarray result *CATD was* up-regulated by PPARγ in mo-DCs (Figure 34).

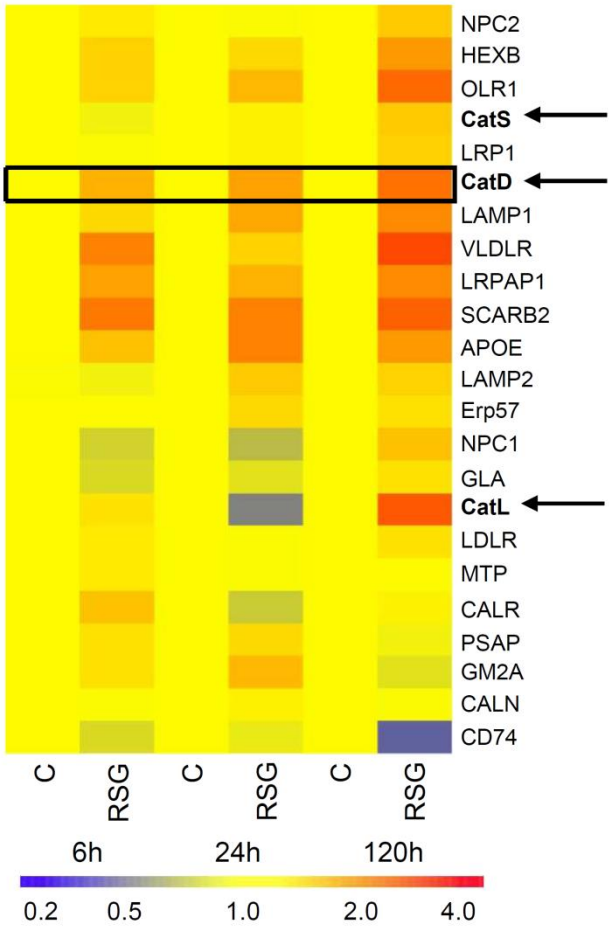

Figure 34: *Heat map representation of genes participating in lipid antigen presentation in mo-DCs in the presence or absence of RSG at the indicated time points.*

We validated the microarray results by RT-qPCR that indicated a robust up-regulation of the *CATD* (6- to 10-fold up-regulation; Figure 35, upper panel) in RSG-treated samples, and *CATD* was the dominant Cats in mo-DCs (Figure 35). These data let us to determine the possibility of PPARγ-regulated CatD as a novel component of the lipid antigen processing machinery to support iNKT cell expansion.

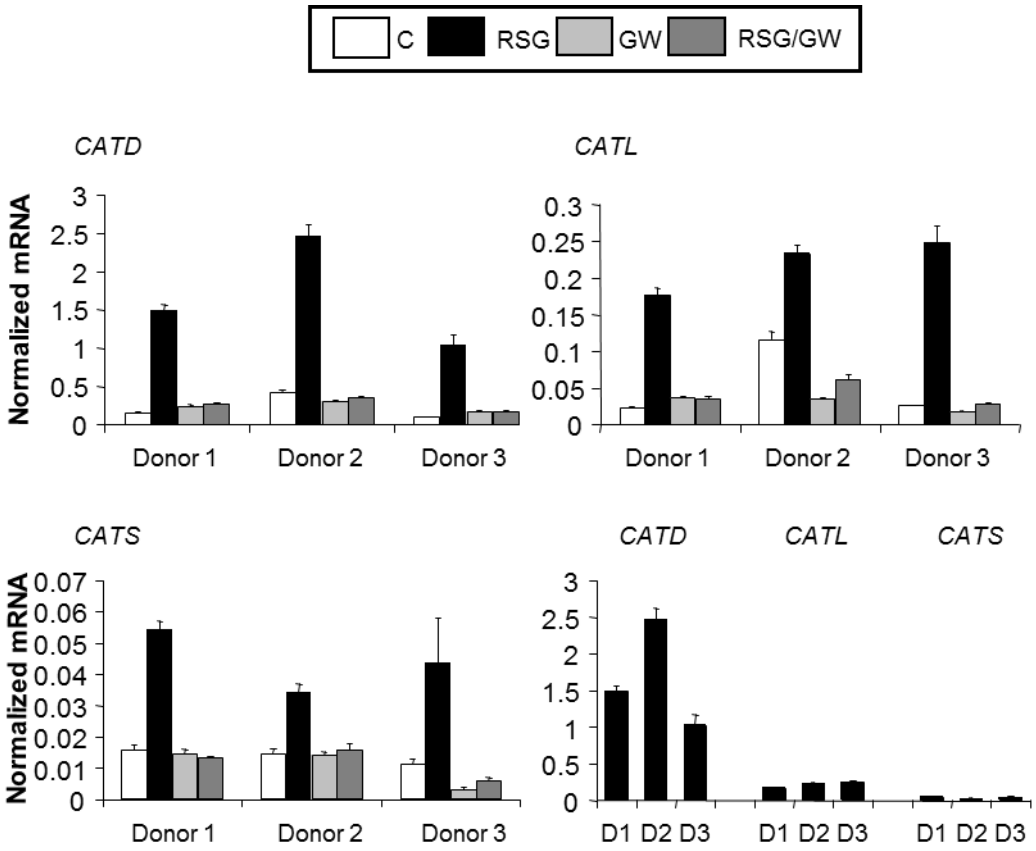

Figure 35: *Expression pattern and regulation of cathepsins (Cats) by PPARγ in mo-DCs were detected by RT-qPCR. Normalized mRNA levels of the cathepsin genes in mo-DCs from three representative donors (1-3) were represented (D= Donor).*

Western blot analysis confirmed PPARγ-mediated up-regulation of CatD at protein level. Furthermore, DI result demonstrated the nuclear localization PPARγ (green) and cytoplasmic localization of CatD (red), consistent with previous reports showing predominant localization of the protein in the lysosomal compartments (312) (Figure 36A and B).

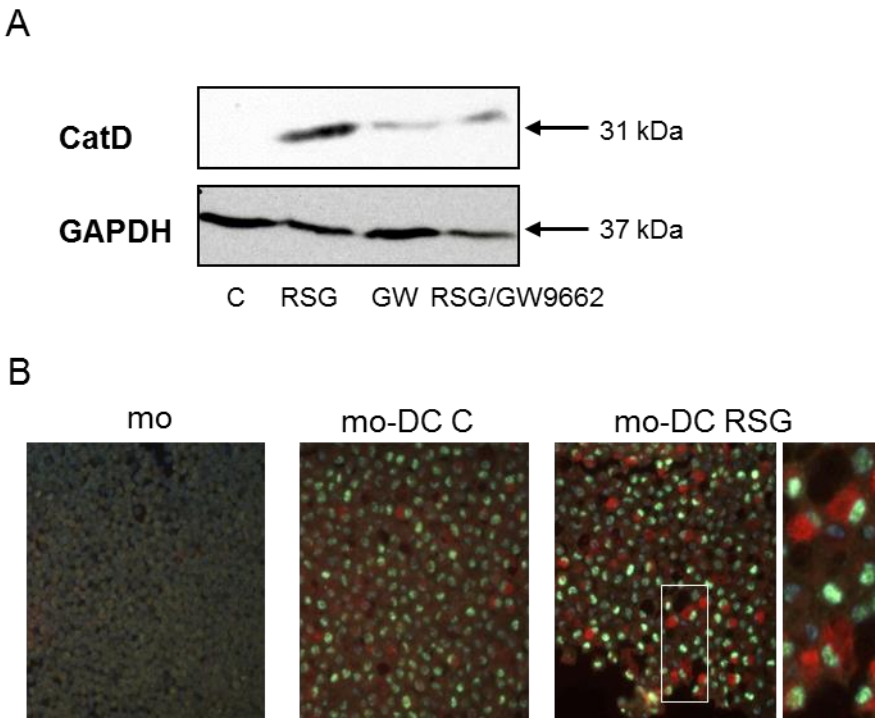

Figure 36: *A, Western blot analysis of CatD protein in mo-DCs treated with DMSO/EtOH (C=Control) and with RSG or RSG+GW9662. B, Immunofluorescence detection of PPARγ (green) and CatD (red) using monocytes (mo), mo-DC and mo-DCs treated with RSG (mo-DC RSG). Nuclei are visualized by DAPI (blue). Original magnification: X40. In case of mo-DC RSG, a panel (labeled with white box) with further magnification (100X) was also demonstrated.*

5.2.2. CatD is dually regulated by PPARγ and RARα

To further confirm the PPARγ dependence of *CATD* expression obtained by pharmacological means, we knocked-down PPARγ in differentiating mo-DCs by electoporation. *PPARG* expression was reduced at an efficiency of approximately 60% (Figure 37) and it has down-regulated the expression of the *FABP4*. The PPARγ-dependent up-regulation of *CATD* was robustly reduced (to 56.8%) by siPPARγ compared to non-silencing control siRNA or mock-transfected samples (Figure 37, lower panel). Based on these results, we concluded that CatD is regulated by PPARγ.

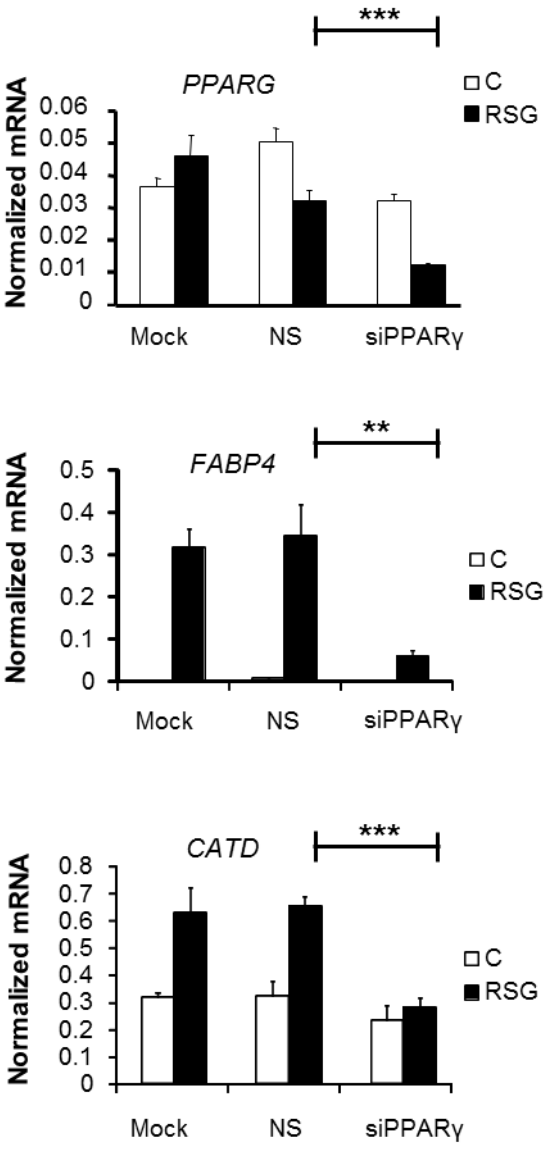

Figure 37: *PPARγ-dependent CATD expression was confirmed by siRNA silencing of PPARγ in mo-DCs. Gene expression levels were measured by RT-qPCR normalized to CYCLOPHILIN A from cells either Mock transfected or electroporated by PPARγ-specific or non-silencing control (NS) siRNAs. Transcript levels of PPARγ, FABP4 and CATD were shown. Means normalized to CYCLOPHILIN A ± SD; n= 3; SD ***NS-PPARG (P = 0.0003); ** NS-FABP4 (P = 0.0028); ***NS- CATD (P= 0.0001).*

According to our previous results, a subset of the PPARγ-mediated genes can be regulated via induced ATRA synthesis and subsequent activation of RXRα (239). To identify the exact molecular components of the signaling events from PPARγ activation to *CATD* up-regulation, we aimed to examine the involvement of retinoid signaling in the regulation of *CATD*. We mapped the signaling pathways required for *CATD* induction by analyzing the expression levels of *FABP4* and *TGM2* that are under control of PPARγ or RARα, respectively. RSG induced

FABP4 expression and *TGM2* was primarily up-regulated upon RAR ligand AM580 treatment confirming proper ligand response. We found that both receptor specific ligands could induce *CATD* (Figure 38).

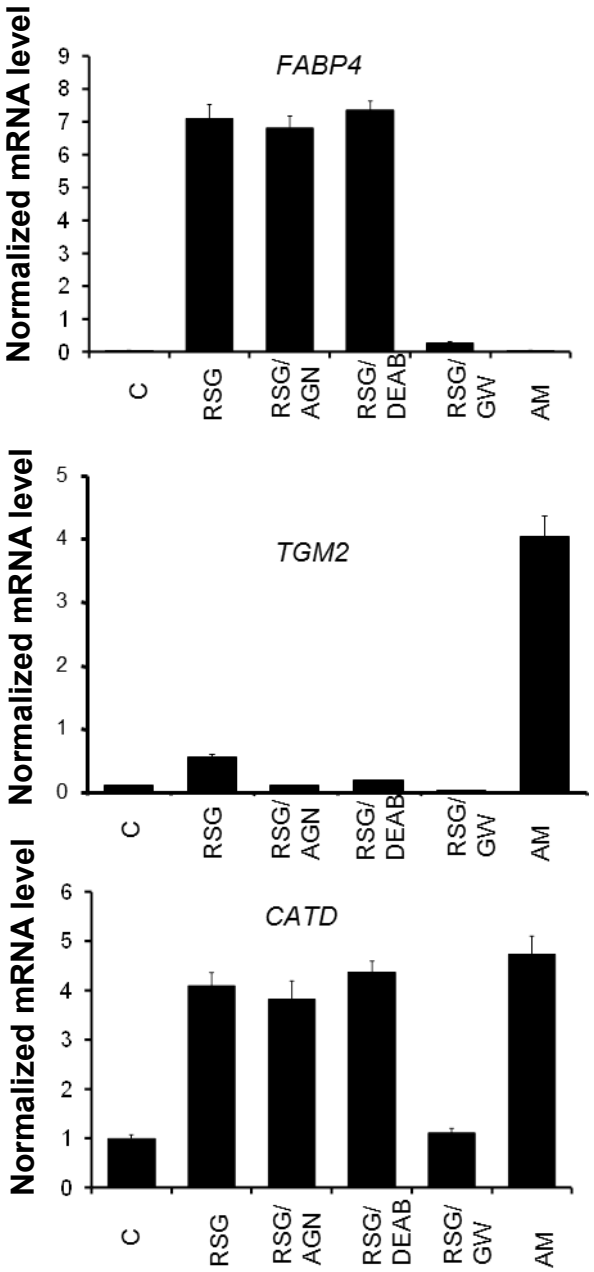

Figure 38: *Gene expression levels of CATD, FABP4 and TGM2 in mo-DCs upon treatment of indicated compounds were quantified by RT-qPCR. Normalized gene expression levels ± SD are shown. DEAB: 4-diethyl amino-benzaldehyde, inhibitor of RALDH; AM580 (AM, RARα agonist); AGN193109 (AGN RARα antagonist); GW (GW9662, PPARγ antagonist).*

The PPARγ-induced *CATD* expression was barely inhibited by the RARα antagonist (AGN193109) or by a treatment with a RALDH inhibitor, DEAB. The separate activation of PPARγ or RARα signaling in mo-DCs effectively induced CD1d cell surface protein expression and led to an enhanced iNKT expansion in T cell co-culture experiments (Figure 39A and B).

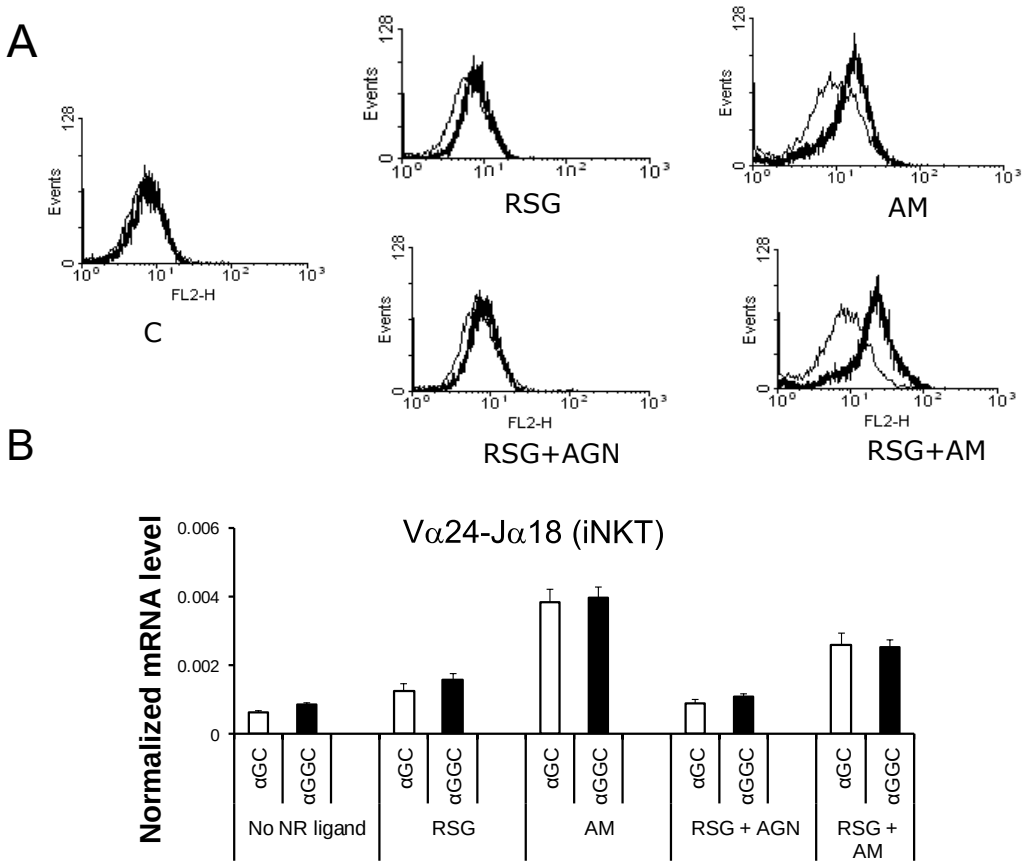

Figure 39: *Effect of nuclear hormone receptor pathways in mo-DCs on CD1d expression and iNKT expansion. Lipid antigen (αGC or galactosyl(1-2) galactosylceramide (αGGC))-loaded DCs were treated with RSG, AM580 (AM), RARα antagonist AGN193109 (AGN) or with the combination of above ligands. A, Cell surface expression of CD1d protein was measured by FACS. B, Nuclear receptor ligand treatment of DCs regulates iNKT expansion. RT-qPCR measurements were shown.*

Interestingly, the co-administration of the two receptor-specific ligands did not result in a synergistic further elevated level of iNKT expansion. This result verified our *in vitro* model that predicted that PPARγ and RARα are components of the same molecular pathway that regulates iNKT expansion. These data suggest that *CATD* is under the control of multiple nuclear receptors in developing DCs and that it is under dual control by both PPARγ and RAR.

We hypothesized also, that the induction of CD1d expression might be not the only mechanism, by which PPARγ signaling can enhance iNKT expansion. The result that silencing of PPARγ in day 3 DCs by siRNA did not alter the CD1d transcript level in DCs (Figure 40), whereas regulation of iNKT activation could still be found under these conditions (Data not shown), suggested that PPARγ signaling pathway in mo-DCs enhanced iNKT expansion by regulating other molecules as well, including CatD. This finding is in line with our previous results that demonstrated that CD1d is an indirect and late target of PPARγ (239).

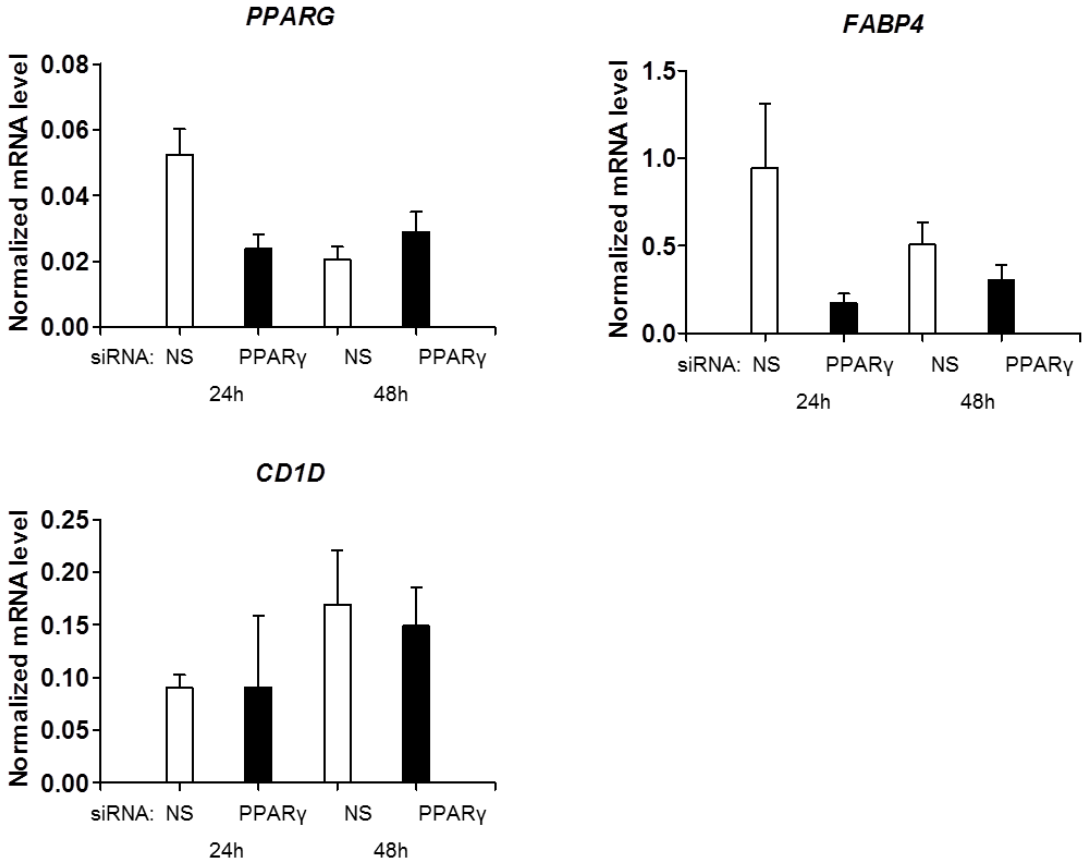

Figure 40: *Gene expression levels of PPARG, FABP4 and the CD1D in mo-DCs upon RSG treatment and from cells either electroporated with PPARγ-specific or non-silencing control (NS) siRNAs. Gene expression levels were measured by RT-qPCR normalized to CYCLOPHILIN A. Normalized gene expression levels ± SD are represented.*

5.2.3. Inhibition of CatD leads to decreased iNKT proliferation in response to lipid antigen through reduced lysosomal events important for lipid antigen presentation in the context of CD1d

To investigate the possible function of CatD in lipid antigen presentation and iNKT cell stimulation, we used pepstatin A, a selective proteolytic activity inhibitor of CatD. RSG treatment of DCs did not result in iNKT expansion in the absence of a lipid antigen. When the precursor form of αGC lipid antigen, αGGC, was also administrated in culture media, PPARγ ligand treated mo-DCs acquired a substantial increase in their ability to induce iNKT expansion (Figure 41 and 42).

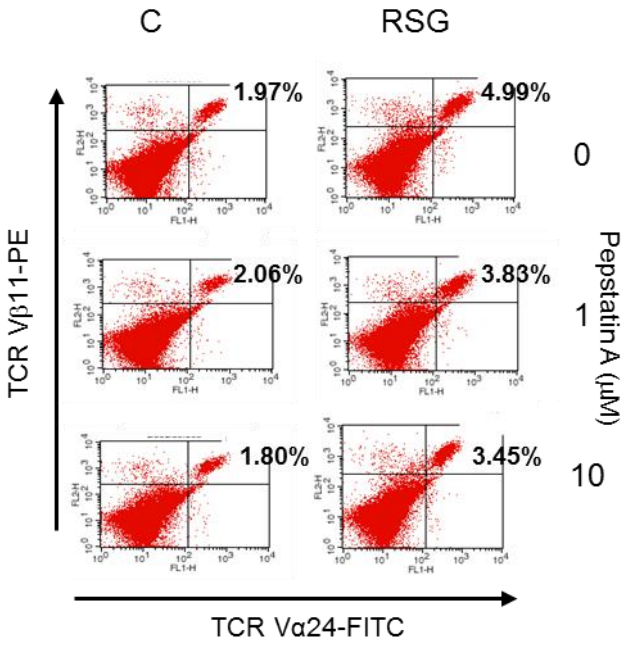

Figure 41: *INKT cell expansion in αGGC-iDC/PBMC co-cultures was measured by two-color flow cytometry (Vα24-FITC/Vβ11-PE) in the presence of the indicated doses of pepstatin A.*

We found that pepstatin A reverted αGGC-induced iNKT cell expansion in a dose-dependent manner in RSG treated mo-DCs (Figure 41). Moreover, we provided evidence of a correlation between iNKT cell density measured by flow cytometry using Vα24/Vβ11 double-staining and RT-qPCR detection of the invariant Vα-chain (Vα24-Jα18) validating the utility of this RT-qPCR approach in quantitation of iNKT cells (Figure 42).

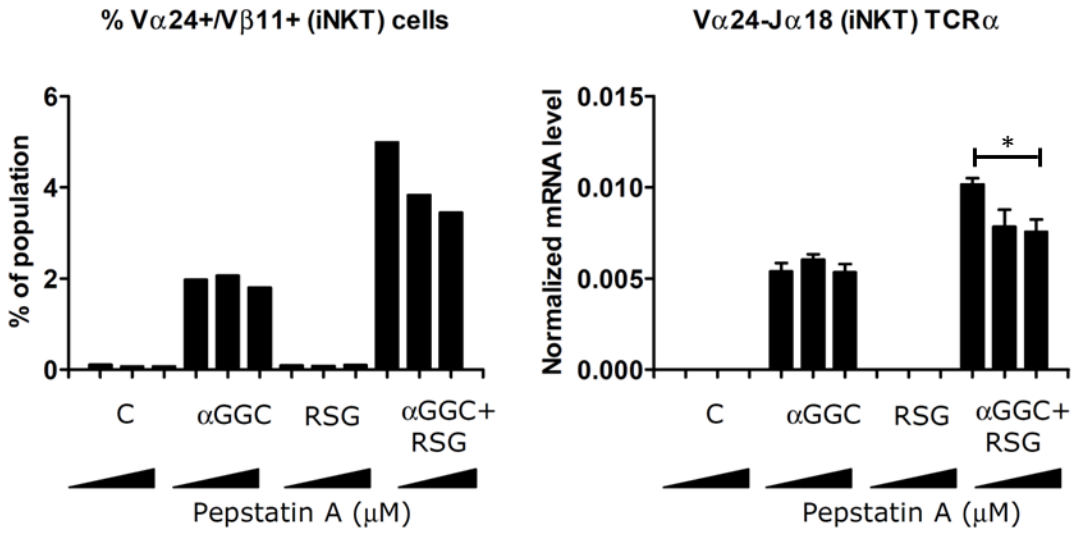

Figure 42: *Correlation of the flow cytometric and RT-qPCR measurements (iNKT TCR α-chain) of the detected iNKT expansion in the same experiments in the presence of αGGC. Applied pepstatin A concentrations: 0-1-10 μM. P=0.0147.*

The endosomal processes involved in lipid antigen presentation to iNKT cells in DCs remains mostly undefined. Due to the fact that CatD is a lysosomal protease and the lysosomal localization of CD1d is required for efficient iNKT cell induction, we though that CatD might be required for a specific lysosomal process through the lipid antigen presentation in the context of CD1d. To investigate this possibility further, we took advantage of two synthetic model lipid antigens, αGC, which can bind to cell surface CD1d (313), and its precursor, αGGC, which is strictly dependent on the uptake and lysosomal transport for its processing to the active form, αGC by α-galactosidase A (89). We found that inhibiting endosomal acidification by bafilomycin in RSG-treated mo-DCs absolutely reduced iNKT expansion in the presence of the precursor lipid αGGC but not in the presence of its mature form (αGC) (Figure 43A). This result indicated that PPARγ could induce an endosomal process included to the effective lipid presentation and enhanced iNKT expansion. Furthermore, we detected that only the αGGC-induced iNKT expansion was sensitive to pepstatin A (Figure 43B), suggesting the function of CatD in the lysosomal lipid antigen processing.

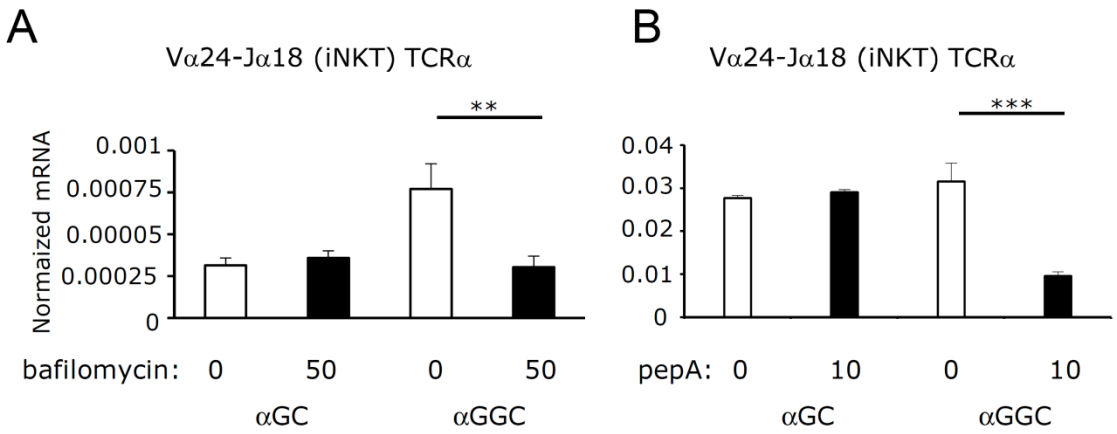

Figure 43: *A, Effect of bafilomycin (0 or 50 nM) on iNKT expansion in RSG-treated DC/PBMC samples; P=0.0017. B, Effect of pepstatin A (pepA) on iNKT expansion. P=0,0009. Mo-DCs were differentiated in the presence of RSG.*

The non-specific inhibition of pepstatin A in the antigen presentation was excluded in MLR reaction. This inhibitor did not affect peptide antigen-mediated conventional T cell proliferation in MLR reactions (*Figure 43*).

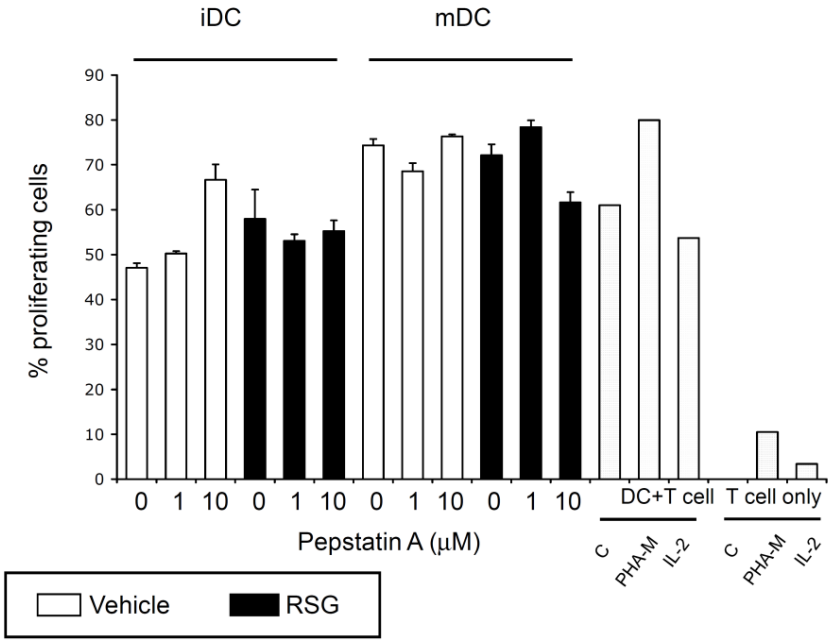

Figure 44: *A, Effect of pepstatin A (0, 1 or 10 μM) on iNKT expansion and in mixed leucocyte reaction (MLR). The proliferation of carboxyfluorescein succinimidyl ester (CFSE)-labeled T cells was determined on day 5 by flow cytometry.*

Therefore CatD constitutes a previous unknown link between lipid metabolism and immunity in DCs.

6. DISCUSSION

6.1. ATRA synthesis in murine DCs

Mucosal DCs orchestrates intestinal homeostasis, in particular, intestinal innate and adaptive immune responses. Several of these DC functions are tightly regulated by ATRA (251, 314). The conversion of retinol to retinal can be catalyzed by ubiquitously expressed ADHs in these DCs, whereas the oxidation of retinal to ATRA is mediated by RALDHs which are restricted to ATRA-producer cells (32, 253, 254, 257, 260, 261). The expression profile of the three isoenzymes of RALDH (RALDH1, RALDH2 and RALDH3) was assessed in murine PP-DCs and MLN-DCs (251, 253). It has subsequently been shown that in agreement with the expression of *Raldh2*, $CD103^+$ DCs are one of the main producers of ATRA (32, 254). Interestingly, DCs located at the proximal small intestine exhibit higher RALDH activity compared to distal small intestinal- or colonic DCs likely due to increased absorption of vitamin A in the proximal part of the intestine (238, 257, 315).

ATRA producing capacity correlates with GALT DC functions. $CD103^+$ DCs migrate towards the MLNs in CCR7-dependent manner and present luminal self- or harmful antigens to naïve T cells (32). 1, DCs isolated form the proximal small intestine stimulated higher levels of immunosuppressive $Foxp3^+$Treg differentiation in conjunction with TGFβ. 2, DCs induced imprinting of gut tropism of effector T cells. ATRA triggered the cell surface expression of gut homing receptors such as CCR9 and α4β7 on T cells. 3, DCs induced also gut tropism and IgA class switching on B cells in an ATRA-dependent manner. 4. Depending on the microenvironment, cytokine milieu and the level of DC-produced ATRA, mucosal DC-primed naïve T cells could differentiate to pro-inflammatory Th17 cells as well, indicating that ATRA required in mice for inflammatory T-cell responses in infection and the complexity of ATRA signaling in intestinal immunity (253, 254, 257, 314, 316).

Importantly, mice fed with VAD diet are almost devoid of $CD4^+$ and $CD8^+$ T cells and mice expressing a dominant-negative form of the RARα, specifically in $CD4^+$ T cells or B cells lacked the $CD4^+$ T cell population or B cells in the small intestinal LP, respectively, highlighting the physiological importance of retinol in intestinal lymphocyte homeostasis (253, 317). Of note, low level of ATRA seemed to be required for the induction of intestinal Th17 cells differentiation. ATRA regulated the balance between Th17 and Treg differentiation as well (318-320). In a mouse model of intestinal inflammation, reduced generation of ATRA as a consequence of reduced Raldh2 expression by $CD103^+$ DCs was linked to lower capacity to

induce Tregs (321). Contrary, the low ATRA concentration synergized with IL-15 to induce Th17 cell differentiation and enhanced gut inflammation (322).

In *in vitro* differentiation models, intestinal-like DCs can be differentiated form a specialized subset of DC precursor (323). These pre-mucosal DCs have been identified in lymphoid organs, in the BM of mice and ATRA expanded the level of this precursor cell type among the total BM progenitors. ATRA treatment resulted in the development of a set of BM-DCs which preferentially expressed CD103 and homed to the intestine (323). Mice fed with a VAD diet had reduced number of the pre-mucosal DC pool in the BM, coupled by the selective reduction of the $CD103^{+}/CD11b^{+}$ DCs in the GALT and of the developmentally related $CD11b^{+}/CD8a^{-}/Esam^{high}$ DCs in the Sp-DC populations (245, 324). After migration to the intestine, specific DC subsets acquired the ability to sense and respond to ATRA which promoted an anti-inflammatory phenotype (245).

Multiple factors and pathways have been investigated to influence the ATRA producing capacity of DCs and ATRA itself was shown to direct the development of DCs that mimicked the transcriptomic profile particularly of *in vivo* intestinal cDC subsets (324). A systematic analysis of different mouse DCs transcriptional profiles for ATRA production and signaling was still remained to be tested. Our goal was to identify and validate additional key regulatory components of ATRA synthesis in mouse DCs. The enzyme required for the retinal production from retinol has not been evaluated in ATRA-producing DCs. RDH10 was found to be indispensable for embryonic retinol metabolism and the intracellular localization of RDH10 and RALDH2 could be correlated (217, 224). We focused on RDH10 which might be the key enzyme that could initiate retinol metabolism in intestinal DCs. We tested this hypothesis by using RT-qPCR and TLDA methods. While transcription of *Rdh10* gene was detectable in all DC subtypes, irrespective of ATRA-production capacity, overlapping expression of *Rdh10* with *Raldh2* suggested that RDH10 could be responsible for the initial retinol oxidation to retinal in ATRA-generating DCs. The role of RDH10 enzymatic activity in these DC subtypes is remained to be investigated.

ATRA sensing in DC is dependent on the expression of retinoid receptors. We assessed the expression of RAR and RXR isoforms in *in vitro* differentiated- or in *in vivo* DCs. In $CD103^{+}$ MLN-DCs ATRA signaling could be mediated via the RARα/RXRβ heterodimer. All other DCs subtypes expressed RARα but the expression level of this retinoid receptor was lower in Sp-DCs compared to ATRA-producing cells. Interestingly, among the analyzed RAR target genes only the expression pattern of the metabolizing *Cyp26a1* gene was correspondence to the active ATRA generation and signaling in these DCs. We failed to detect correlations between

T*gm2* and *Cd1d* genes and ATRA-producing capacity in DCs of different origin, particularly in the most widely characterized intestinal $CD103^+$ cells.

ATRA synthesis itself can be regulated by nuclear receptor-mediated signals. In contrast to human DCs, PPARγ agonist did not significantly induce *Raldh2* expression in Flt3L-generated BM-DCs and purified Sp-DCs in the absence of IL-4 or GM-CSF compared with the effects of IL-4 or IL-13 (251, 257). This apparent disparity between mouse and human data may reflect a species difference but remains to be clarified. These results suggest that caution should be exercised when extrapolating mouse data on the manipulation of ATRA signaling to generate efficient mucosal immune responses in the human intestine.

6.2. ATRA production in human DCs

ATRA synthesis in the human intestinal DC subtypes is less investigated compared to their murine counterparts. Beside the small intestine, ATRA is also contributes to the immune homeostasis in the gastric mucosa that contains high levels of retinol (325). It has been revealed that primary gastric epithelial cells produced ATRA from retinol and triggered ATRA synthesis by the up-regulation of the *RALDH2* in co-cultured monocytes, suggesting that epithelial cells may also trigger DCs to synthetize ATRA in the gastric mucosa as well. However gastric DCs were $CD103^-$, the purified gastric-DCs had similar RALDH activity as $CD103^+$ small intestinal-DCs and expressed ATRA synthesis genes (*RDH10*, *RALDH2*). Moreover the gene expression level of the *RAR*s and ATRA target genes (*CRABP2* and *TGM2*) was also similar or higher in gastric-DCs compared with intestinal-DCs. ATRA synthesis was hindered in *H. pylori*-infected patients that was correlated with up-regulated *RDH10* and reduced expression of *RALDH2*. *RDH10* expression was also decreased in DCs isolated from the H. pylori infected mice, indicating that the infection disrupted gastric ATRA synthesis and ATRA-mediated immune homeostasis in the mucosa (325).

Retinol has crucial function to the establishment of oral tolerance against commensal bacteria and food antigen in the human gut (326-328). Dysregulated ATRA-mediated tolerogenic immune responses and VAD might lead to food allergies, celiac disease and inflammatory bowel diseases (IBD). Mice fed with VAD diet had exacerbated intestinal inflammation in the dextran sodium sulfate (DSS)-induced colitis models (329). Moreover, chronic inflammation was attenuated in a mouse model of ileitis by ATRA supplementation (320). These data suggested that ATRA triggers a tolerogenic and anti-inflammatory DC phenotype in the intestinal tissues.

In contrast to murine gut DCs, ATRA synthesis is not restricted to $CD103^+$ DC subsets in human DCs. Both $CD103^-$/$SIRP\alpha^+$ and $CD103^+$/$SIRP\alpha^+$ DCs had high levels of RALDH activity, whereas $CD103^+$/$SIRP\alpha^-$ DCs had significantly lower RALDH activity (29). ATRA synthesis was also detectable in DCs isolated from the distal part of the human small intestine or the colonic tissues (330). RDHs as RDH10, DHRS9 and RALDH2 was detected in tissue-derived DCs, indicating that human intestinal myeloid DCs acquired the complete enzymatic machinery to generate ATRA from retinol and efficiently induced the intestinal myeloid DCs to enable their ability to trigger α4β7 gut homing receptor on activated naive $CD4^+$ T cells. All DCs expressed CCR7, suggesting that these populations might migrate to organized lymphoid tissue in the gut to activate naïve T cells (330).

GALT is the most likely place where intensive lipid absorption occurs and PPARγ activators can be produced. This supported the hypothesis that PPARγ-regulated signaling pathways can be contributed to intestinal DC immune phenotype probably in ATRA-dependent manner. Our laboratory previously identified that PPARγ-regulated lipid metabolic pathways could be associated with the altered immune response of DCs (49, 169, 239). The activation of the nuclear receptor leaded to a transcriptional program with altered lipid metabolism in mo-DCs via induced expression of genes that are required for endogenous ATRA synthesis. RSG-treated DCs express higher level of *RDH10* and *RALDH1/2* mRNA level, supporting that key enzymes readily could be regulated in these cells in PPARγ-dependent manner. Importantly, the expression of *RDH10* was induced in the early time point (6h) in RSG-treated samples, suggesting that the regulation of this retinol converting enzyme might be under the direct control of the nuclear hormone receptor. The PPARγ-dependent expression of these enzymes was confirmed by IHC in mo-DCs. The functional consequence of the expressed ATRA synthesis genes was the secreted ATRA detected by LC-MS technic. This method supported that PPARγ induced ATRA synthesis in receptor-dependent manner (239). We verified these result by Aldefluor-based FACS analysis which allowed us to detect RALDH activity at cellular level.

By pharmacological activators/inhibitors, we surveyed the components of the PPARγ-mediated ATRA synthesis and signaling in cultured DCs. PPARγ gene expression was immediately induced under these culture conditions and was detectable only in a narrow time frame in differentiating cells at mRNA level. This tightly regulated inducibility and the fact that monocytes lack any PPARγ make these mo-DCs a suitable model for analysis of the PPARγ-dependent transcriptional events (49, 239). The activation of the receptor activated the transcription of RDHs (*RDH10* and *DHRS9*) which initiate retinol to retinal conversion.

Among them we thought that based on the expression pattern, RDH10 could be the primary enzyme in retinol oxidation in differentiating DCs. The second oxidative step is catalyzed mainly by RALDH2 isoform, indirectly regulated by the receptor (239). Thereafter *de novo* produced ATRA is transported to the nucleus by PPARγ-up-regulated CRABP2 carrier molecules to activate RARα receptors.

Our results suggested that transcriptional events in human mo-DCs that up-regulate the *CD1D* gene were co-ordinately mediated by PPARγ and RARα receptors (239). The consequences of the PPARγ-regulated ATRA signaling was the expression of the lipid antigen presenting CD1d molecules on the surface of the mo-DCs and enhanced lipid antigen presentation capacity of the cells (49, 239). To assess direct evidence that the primary enzyme in this *de novo* ATRA synthesis was readily RDH10 and the PPARγ-induced ATRA signaling pathway required RALDH2 and CRAPB2, we used siRNA-based gene silencing technic. These results supported our previous data and also provided an even more detailed analysis of the components of this PPARγ-initiated *de novo* ATRA synthesis transport and lipid antigen presentation by evidences at molecular level.

However in divergence from murine DC results, our data suggested that *de novo* ATRA synthesis under this culture condition is associated with PPARγ-restricted expression of the RDH10 enzyme rather than RALDHs. These data indicated that ATRA production is regulated differently in mice and human and the expression of RDH10 might providing an important control point to ATRA synthesis in humans DCs.

6.3. PPARγ-dependent nuclear ATRA transport in DCs

Retinol binds to CRBPs for transport within the cytoplasm (197). The transcriptional effects of retinol at a molecular level appeared to be mediated principally by its active metabolite, ATRA. When ATRA synthetized it can follow tree potential routs: 1. First is to exit the cells and act on neighboring cells in paracrine manner. 2. The active metabolite has to bind to CRABPs, hydrophobic molecule binding accessory proteins that prevent it from non-specific degradation and ensure the stability and solubility of hydrophobic retinoid in the aqueous cellular environment. ATRA concentration is tightly regulated in the cells by CRABP1, controlling the rate of ATRA metabolism by presenting ATRA to the degrading CYP26 enzyme family. 3. CRABPs transport ATRA not only to degradation but also to nuclear hormone receptors to regulate transcription. ATRA can be trafficking to the nucleus by CRABP2 harboring an ATRA-binding domain or by FABP5 to PPARβ/δ. In the nucleus

ATRA interacts with RARs, initiates gene transcription and regulation of multiple biological pathways with wide ranging functionality (199).

CRABP2 expression was barely or not detectable in the murine DC subtypes by TLDA analysis. Interestingly, $CD103^+$ intestinal DC also lacked the intracellular ATRA transporter. Utilizing DC/T cell co-culture experiments, we found that the T cell/DC interactions could be an intrinsic factor in the mucosal environment for CRABP2 expression in the APCs.

We found in our human mo-DC model that PPARγ activation resulted in CRABP2 expression in cultured DCs. Our data suggested that the intracellular ATRA transporter protein can be under the direct control of the TF. RSG-treated DCs express CRABP2 at protein level. These results indicated that PPARγ receptor activation is also involved in the nuclear delivery of the active metabolite of retinol. The direct evidence for CRABP2-mediated ATRA transport to the nucleus requires further experimentation.

6.4. PPARγ and retinoid signaling in intestinal DCs

ATRA synthetizing DCs was previously identified in the human gut (29, 266). DCs endow RALDH activity after entry into the intestinal mucosa. As intestine is a privileged area for intensive lipid absorption and for PPARγ ligand generation we decided to assess whether PPARγ contributes in the regulation of DC retinoid signaling in the intestinal GALT.

PPARγ contributes to the intestinal phenotype in murine DCs. Activation of the receptor increased the ability of BM-DCs to polarize naive T cells toward Tregs with enhanced expression of the CCR9 gut homing receptor and to trigger T cell-independent IgA secretion by B cells (290, 331).

The functional relevance of PPARγ was assessed in DSS-induced colitis. The association of the receptor to IBD was supported at genetic level by IEC- and macrophages-specific PPARγ deficient mouse strains in which RSG treatment and other PPAR ligands failed to attenuate the severity of colitis (332-334). Similar to these data, more severe DSS-induced intestinal colitis was observed in mice following depletion of $CD11c^+$ DCs (335). DC-specific PPARγ deficient mouse strain was established by the Cre-Lox system (331). BM-DCs from these mice acquired more inflammatory phenotypes with higher expression of co-stimulatory molecules, pro-inflammatory cytokine secretion compared to WT BM-DCs. In contrast to the inflammatory BM-DC phenotype, the number of colonic-DC was unaffected *in vivo* and only a modest trend toward increase colitis severity was observed in DSS-treated DC-specific, PPARγ deficient mice compared with control animals. Intestinal microenvironment of the colon may maintain the tolerogenic mucosal DC functions that compensate the effect of the loss of PPARγ

expression. Activation of intestinal PPARγ reduced the severity of colitis in human and experimental animals, and PPARγ in IECs and macrophages are involved in this protective effect. Thus PPARγ has an anti-inflammatory role in at least three different intestinal cell types: DCs, macrophages and IECs.

In mouse colitis models ATRA production was decreased in $CD103^+$ DCs. Contrary, DCs had enhanced capacity to synthetized ATRA in human colonic DCs, isolated from inflamed colonic tissues of CD patients (330). This elevated generation of ATRA might contribute to disease pathology. DCs were shown to be accumulated in the MLNs wherein they might acquire pro-inflammatory phenotype. Both $CD103^+$ and $CD103^-$ DC subsets expressed enhanced level of *RALDH2* whereas *RALDH1* was not detectable in these APCs. *RDH10* expression was also measured in the sorted DC populations, indicating that human intestinal DCs have capacity for intracellular ATRA production.

Utilizing DI method we characterized the expression a PPARγ and the components of ATRA signaling in human intestinal tissues. We found that GALT-associated immune cells readily express the key components of ATRA production (RDH10, RALDH2) and transport (CRABP2). PPARγ-positive DC-like cells co-expressed the RAR target gene, TGM2, suggesting that these cells possess the complete enzymatic machinery to generate ATRA from retinol, have an active retinoid signaling system and represent a relevant ATRA-producing APCs. The proportion of PPARγ positive DC-like APCs was increased in IBD samples. Our results suggested that the RALDH activity of human intestinal myeloid DCs was indicative of the generation of ATRA that signals via RARα to modulate T cell function in the gut. These data also suggested that PPARγ and ATRA signaling might be connected in intestinal DCs and our *ex vivo* mo-DCs may correspond to these *in vivo* DC-like APCs.

6.5. CatD and lipid antigen presentation in human mo-DCs

CatD has been studied over the last three decades. It is widely accepted that the primary biological function of this aspartic protease is the intracellular protein degradation within the lysosomal compartment. Many lysosomal enzymes, in particular the cysteine protease CatB and L, have been implicated in lipid antigen presentation (97, 101, 311).

Multiple aspects of lipid presentation were linked to these lysosomal proteases such as the cell surface expression of CD1d and processing of lipid antigens. However, the function of nuclear hormone receptors in the regulation of the lipid presentation process was poorly investigated in DCs. We assumed that lipid antigen presentation might be regulated at multiple

steps and must be transcriptionally controlled. Previously we demonstrated that PPARγ and RARα regulated the expression of CD1d. We tested what other steps of lipid presentation can be under the control of PPARγ in mo-DCs. Our results revealed that the expression of CatD in differentiating DCs was regulated by the receptor and its expression was closely matched with that of genes already functionally connected to lipid presentation. We also investigated that CatD was up-regulated by both PPARγ and RARα, but in contrast to CD1d, the two receptors regulate the protease dually and likely indirectly. The inhibition of the CatD protease activity resulted in the blocking of PPARγ-dependent iNKT activation. Pepstatin A/RSG-treated DCs had lower capacity to present αGGC, which requires lysosomal processing before presentation. Moreover bafilomycin treatment further supported the requirement for lysosomal processing of the precursor lipid antigen in the PPARγ-dependent lipid presentation. We also found that PPARγ forced the proteolytic cleavage of the lipid transporter prosaposin in CatD-dependent manner (data not shown). These experiments provided us with mechanistic links between PPARγ, CatD and lipid antigen presentation. This clearly suggests that CatD in lysosomes is required for the processing and loading of the lipid precursor.

As DCs are critical APCs during tumour progression the reduced peptide presentation capacity of these cells might be compensated by the activated lipid presentation capacity during tumour development. Our data in mo-DCs raises the possibility of the existence of a PPARγ–CatD–Saposin–CD1d regulatory axis in the cellular glycolipid metabolism that may be active in the tumor supporting microenvironment.

6.6. Lipid antigen presentation, PPARγ in cancer

Tumor infiltrating DCs acquire dysfunctional immune phenotype supporting by the components of TAS. A fraction of these signals are mediated via activation of nuclear hormone receptors, eliciting either activation or suppression. Although dysregulated nuclear hormone receptors functions have been demonstrated in tumor cells, the role of these TFs in the TAS and immune cells is still elusive. Tumor cells can be relevant sources of nuclear hormone receptor activating ligands. Some neoplastic cancer cells produce LXR-specific ligand. The activation of the receptor by tumor-derived lipid resulted in lower motility of DCs to LNs as a consequence of the down-regulated CCR7 (336).

About the 20 expressed nuclear hormone receptors in DCs, PPARγ is one of the most controversial TF in term of tumor progression. In DC-based vaccination therapy the relevant question is how PPARγ affects DC-controlled immune responses. Transcriptional activation of

this receptor is crucial during DC development, resulting in a specific DC characteristic, suggesting that PPARγ active DCs have a regulatory DC phenotype that would be detrimental during the development or the optimization of *in vivo* DC-based vaccination therapies (49, 169, 239, 284-288, 291).

DCs were demonstrated to elicit effective anti-tumor immune responses by presentation of lipid antigens to reactive iNKTs (119, 337, 338). iNKTs played primarily protective function in various experimental tumor models in mice (83, 115, 339). This anti-tumor immunogenicity was dependent on their rapid pro-inflammatory cytokine secretion as INFγ, leading to the subsequent down-stream activation of innate and adaptive immune cells. The success of preclinical results in tumor bearing animals to regress advanced cancer supported the idea to design clinical trials, which either harness the function of resting iNKTs or increase the frequency of the cells by adoptive transfer of *ex vivo* expanded autologous iNKTs as a vaccine. The unpredicted limited success of these trials could be explained with the much lower frequency of iNKTs in healthy volunteers compared to mice; moreover in patients with advanced cancer iNKTs had even more reduced number/function (340-342). Soluble αGC administration caused anergy or overactivation of iNKTs and only transient iNKT activation was detected in patients (114, 343-345). The αGC-pulsed DC strategy avoided iNKT cell anergy and induced prolonged cytokine responses (346-349).

An alternative approach to exploit this innate anti-tumor system is the adoptive transfer of iNKTs to patients. The number of iNKT cells and the level of INFγ were increased after intravenous administration. Although no partial response was detected, 4 of the 6 treated patients had stable disease (350). To improve the efficacy of the iNKT vaccine therapy, our *ex vivo* DC-model offer many advances for optimization. Although most of the key qualities of DCs, which are critical during DC-vaccination design, are negatively affected by PPARγ, mo-DCs can be differentiated at high number for experimentation. Upon RSG treatment DCs express all molecules which required for potent lipid antigen presentation, therefore these model DCs let us to understand the molecular mechanisms essential for clinical harnessing of this iNKT population. Optimal manipulation of these DCs in anti-tumor trials is critically dependent on our knowledge of iNKT– and DC biology and of the factors that activate and regulate these cells. PPARγ^{+} DCs promote iNKT cell functions through enhanced CD1d thus the receptor could be a potential target for CD1d-restricted iNKT-based cancer therapy.

6.7. Publications citing our articles

Our research article, published in the Journal of Lipid Research, was cited in 11 publications. The relevance or our data was supported by Bimczok at al., suggesting that DCs in the gastric mucosa can synthetize ATRA by RDH10 and RALDH2 (325). These DCs similarly to our RSG-treated mo-DCs express all the components of the retinoid signaling. Gastric DCs acquire retinol metabolizing capacity by epithelial cell-derived ATRA. Interestingly the gastric mucosa contains more retinol than the small intestinal mucosa, isolated from donor-matched samples. Gastric epithelial cells convert retinol to retinal by the same metabolizing enzyme. DCs and epithelial cells have co-ordinate expression of the retinoid signaling pathway components at significantly higher level compared to small intestinal APCs, indicating a similar capacity to generate and secret ATRA to responding cells as T cells. These data provide clear physiological evidence that DCs in the gastric mucosa contribute to homeostasis by regulating the local immune responses.

Our data, published in the Journal of Immunologywas cited in 15 publications. The scientific relevance of our results in the context of lipid antigen presentation in DCs was emphasized in excellent reviews (143, 184, 351). Our *in vitro* mo-DC data can be also supported by the research article of Bene et. al. (352). In their *in vitro* mo-DC model ATRA administration resulted in the differentiation of $CD1d^{+}CD1a^{-}CD103^{+}$ DCs that express PPARγ. These APCs phenotypically resemble our RSG-treated DCs. Their results confirmed that human mo-DCs can be differentiated to mucosal-like DCs that express CD103. Mucosal microbe modified the DC phenotype and immune regulatory function in strain- and ATRA-dependent manner. Their results provided functional evidence that DCs plasticity is critical to their adaptation to the complex intestinal microenvironment under the control of a nuclear hormone receptor.

Although we utilized synthetic PPARγ agonist in our experiments, to support physiological functions of these results it require a competent microenvironment in which endogenous or natural ligands can activates the receptor. The potent endogenous/natural ligends remains poorly investigated. Some reports suggested that PPARγ bind natural ligands as prostaglandin PGJ_2, arachidonic acid metabolites, polyunsaturated fatty acids (PUFAs) or conjugated linoleic acid (CLA) (353). These ligands modify DC immune phenotype by altered

cytokine profile, maturation and migration properties and subsequent Th cell response (354, 355). These natural ligands are frequently present in the intestines as nutritional supplements of the diet. This supports the hypothesis that PPARγ ligands in the GALT alter intestinal DC function and this may have potential therapeutic effects in inflammatory disorders

7. SUMMARY

DC network represent a complex APC family of a number of specific subpopulations. From the first stage of their differentiation, all developmental and differentiation status of DCs are TF-regulated. DCs have to adapt to various environmental cues during homing peripheral tissues or in the course of their shuttle to LNs. As professional APCs, the main function of DCs is the continuous grading of all potent molecules into the state of harmful or self-antigens to sustain effective immune protection (2). In this regard, DCs acquire the capacity to process a huge amount of surrounding information, which triggers specific signaling pathways in the cells. The functional flexibility of DCs is frequently accompanied by TF-mediated transcription. DCs express nuclear hormone receptors that translate intra/extracellular signals to the level of gene expression, required for appropriate immune phenotype of the cells (169).The precise transcription network, which regulates DC immune specificities has to be characterized. Therefore we analyzed the functions of PPARγ and RARα in DCs.

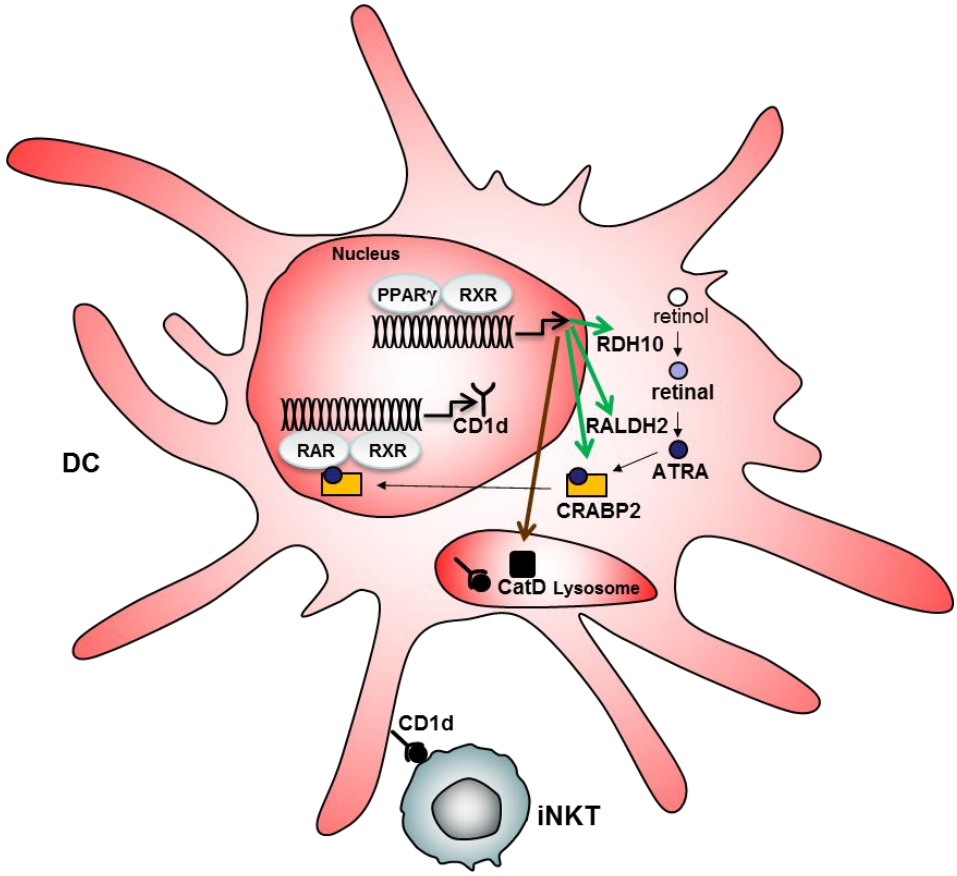

Figure 45: *CD1d-mediated lipid antigen presentation is regulated by PPARγ.*

PPARγ activation turns on the endogenous ATRA production in DC by up-regulated retinol/retinal oxidizing enzyme genes, namely RDH10 and RALDH2. ATRA is transported to

nucleus by the PPARγ-induced CRABP2 transporters, activates RARα, leading to co-ordinated transcriptional regulation of genes, required for lipid antigen presentation, such as CD1d antigen presenting molecules. Lipid antigen-loaded DCs activate CD1d-restricted iNKT cells.

We provided evidence that other step of the lipid presentation could be under the control of the two receptors. We identified CatD as a novel target of the PPARγ and linked this lysosomal protease at molecular- and functional level to DC-based lipid presentation to harness iNKT functions (Figure 45.)

Based on preclinical results, DC-activated iNKTs triggered regression/stabilization of advanced tumors. A set of anti-cancer strategies focused on inducing extended iNKT number and activity in patients. The main challenge of these trials was triggering clinically relevant responses in patients without side-effects. These therapies were generally well tolerated and in some patients, forced prolonged survival. For optimization of these iNKT-based trials we have to understand all step of lipid antigen presentation in DCs and its functional consequences on iNKT immunity. Our *ex vivo* DC/iNKT model allows us to monitor these regulator steps at molecular levels. Collectively our results points out the potential benefit to consider PPARγ as a potential target for CD1d-restricted iNKT-based cancer therapy.

8. MAGYAR NYELVŰ ÖSSZEFOGLALÓ

Az általunk vizsgált dendritikus sejtek a veleszületett immunitás antigén bemutató sejtjei. A szervezet szöveteibe vándorolva, az eltérő szöveti környezet hatására, szöveti altípusokká fejlődnek és szövetre jellemző immunválaszt váltanak ki. A dendritikus sejtek funkcióit befolyásoló molekuláris mechanizmusokat az elmúlt évtizedekben számos kutatócsoport vizsgálta. Munkacsoportunk a dendritikus sejtekben jelenlévő magreceptor család tagjainak szerepét vizsgálja a sejtek funkciójára. A receptor család tagjai lipid érzékelőként működnek. Szerepük a sejt környezetéből érkező, illetve a sejten belül termelődött/aktiválódott lipidek hatásának közvetítése a génkifejeződésre. A lipidek által aktivált magreceptorok olyan koordinált génkifejeződési mintázat változást eredményeznek, melyek megváltozott funkcióval rendelkező dendritikus sejtek kialakuláshoz vezethetnek. Munkánk során a magreceptor család két tagjának, a PPARγ és RARα receptorok szerepét vizsgáltuk a humán monocita-eredetű dendritikus sejtek érése során. A PPARγ aktivációja csökkenti a sejtek mozgékonyságát és peptid antigén bemutató képességét. Emellett a receptor fokozza a retinolt oxidáló enzimek (RDH10 és RALDH) kifejeződését a sejtekben, ami a RARα-t aktiváló csupa transz retinsav (all-*trans* retinoic acid (ATRA)) termelődéséhez vezet. A receptor továbbá fokozza az ATRA sejtmagba szállításáért felelős (CRABP2) fehérje szintjét. Az ATRA a sejtmagban fizikailag kötődik és aktiválja a RARα receptort, ami beindítja a lipid antigén bemutató CD1d molekula génjének átíródását. A CD1d sejtfelszíni megjelenésével, a dendritikus sejt az αGC lipid antigént bemutatva a lipiddel specifikusan aktiválható természetes invariáns ölősejtek (iNKT) osztódásához és aktivációjához vezet. A két magreceptor a lipid antigén bemutatás további lépéseit is szabályozza a CD1d sejtfelszíni szintjének befolyásolásától függetlenül. Mindkét receptor fokozza a lizoszómális katepszin D proteáz szintjét a sejtekben. Az aktív proteáz elhasítva a szapozin (Sap) enzimek előalakját (prosaposin), hozzájárulhat a lipid antigének feldolgozásához, valamint a lipid antigének CD1d molekula ligand kötő zsebében történő bekötődéséhez és cserélődéséhez. Így a két magreceptor koordináltan és egymástól függetlenül egy olyan megváltozott funkciójú vagy alternatív dendritikus sejttípus kialakulásához vezet, amely a peptidek bemutatása helyett, elsősorban a fokozott mennyiségű CD1d molekulái segítségével, a lipid antigének bemutatására specializálódott.

Egereken végzett kutatások kimutatták, hogy a dendritikus sejtek által aktivált iNKT sejtek számos daganat modell esetében a daganatok visszafejlődését vagy stabilizálódását eredményezték. A humán kísérletek részben alátámasztották ezeket az eredményeket, de a klinikai tesztek nem vezettek hosszantartó vagy releváns eredményekhez. A lipid antigénnel

kezelt dendritikus sejt alapú terápiák a betegek számára jól tolerálhatóak. Annak érdekében, hogy a közeljövőben klinikailag hatékony daganat ellenes terápiát tudjunk kidolgozni, elengedhetetlen a lipid antigén bemutatás egyes lépéseinek megismerése. Az általunk használt dendritikus sejt modell lehetőséget biztosít ezen lépések molekuláris szinten történő karakterizálására és adataink felhasználhatóak egy dendritikus sejt/iNKT sejt-alapú daganat elleni terápia kidolgozása során.

9. LIST OF KEYWORDS

Dendritic cell, peroxisome proliferator-activated receptor γ, retinoic acid receptor, all-*trans* retinoic acid, retinol dehydrogenase, CD1d, lipid antigen presentation, α-galactosylceramide, invariant natural killer T cell, Cathespsin D

10. TÁRGYSZAVAK

Dendritikus sejt, peroxiszóma proliferátor-aktivált receptor gamma, retinsav receptor, csupa transz retinsav, retinol dehidrogenáz, CD1d, lipid antigén bemutatás, alfa-galaktozilceramid, invariáns természetes ölő T sejt, katepszin D

11. ACKNOWLEDGEMENTS

I would like to express my heartfelt gratitude to my Ph.D. supervisor, **Prof. Dr. László Nagy** for his continuous support, patience, encouragement of my study and research. His guidance helped me in all the time of research and writing of this thesis.

I would like to thank **Prof. Emeritus Dr. László Fésüs** and **Prof. Dr. József Tőzsér,** the former and recent heads of the Department of Biochemistry and Molecular Biology for the opportunity to work in the department.

I am also indebted to **Dr. Britt Nakken**, **Dr. István Szatmári** and **Dr. Tamás Varga** my collaborators for their contribution to my scientific publications. My gratitude is also extended to **Dr. Árpád Lányi** for his help in preparing my manuscript.

I would like to thank our collaborators **Prof. Dr. Balázs Dezső** for performing the IHC analysis and **Dr. Zoltán Pós** for the mouse co-culture experiment.

I also thank to **Ibolya Fürtös** and **Edit Hathy** for outstanding technical help, to **Dr. Lajos Széles**, **Dr. Szilárd Póliska**, **Márta Béladi**, **Attila Pap**, **Péter Brázda**, other members of the **NLAB** and **Dr. Bálint László Bálint** for their support and other members of the Department for any technical helps.

Lastly, I would like to thank my family for all their love, encouragement and unwavering support throughout the years.

Adrienn Gyöngyösi

12. REFERENCES

1. Jarrossay D, Napolitani G, Colonna M, Sallusto F, Lanzavecchia A. 2001. Specialization and complementarity in microbial molecule recognition by human myeloid and plasmacytoid dendritic cells. *Eur J Immunol* 31: 3388-93
2. Banchereau J, Steinman RM. 1998. Dendritic cells and the control of immunity. *Nature* 392: 245-52
3. Steinman RM, Cohn ZA. 1973. Identification of a novel cell type in peripheral lymphoid organs of mice. I. Morphology, quantitation, tissue distribution. *J Exp Med* 137: 1142-62
4. Serbina NV, Salazar-Mather TP, Biron CA, Kuziel WA, Pamer EG. 2003. TNF/iNOS-producing dendritic cells mediate innate immune defense against bacterial infection. *Immunity* 19: 59-70
5. Steinman RM, Banchereau J. 2007. Taking dendritic cells into medicine. *Nature* 449: 419-26
6. Savina A, Amigorena S. 2007. Phagocytosis and antigen presentation in dendritic cells. *Immunol Rev* 219: 143-56
7. Norbury CC. 2006. Drinking a lot is good for dendritic cells. *Immunology* 117: 443-51
8. Cools N, Ponsaerts P, Van Tendeloo VF, Berneman ZN. 2007. Balancing between immunity and tolerance: an interplay between dendritic cells, regulatory T cells, and effector T cells. *J Leukoc Biol* 82: 1365-74
9. Watts C. 1997. Capture and processing of exogenous antigens for presentation on MHC molecules. *Annu Rev Immunol* 15: 821-50
10. Brigl M, Brenner MB. 2004. CD1: antigen presentation and T cell function. *Annu Rev Immunol* 22: 817-90
11. Wykes M, Pombo A, Jenkins C, MacPherson GG. 1998. Dendritic cells interact directly with naive B lymphocytes to transfer antigen and initiate class switching in a primary T-dependent response. *J Immunol* 161: 1313-9
12. Pallmer K, Oxenius A. 2016. Recognition and Regulation of T Cells by NK Cells. *Front Immunol* 7: 251
13. Shortman K, Naik SH. 2007. Steady-state and inflammatory dendritic-cell development. *Nat Rev Immunol* 7: 19-30
14. Gilliet M, Cao W, Liu YJ. 2008. Plasmacytoid dendritic cells: sensing nucleic acids in viral infection and autoimmune diseases. *Nat Rev Immunol* 8: 594-606
15. Zhang H, Gregorio JD, Iwahori T, Zhang X, Choi O, Tolentino LL, Prestwood T, Carmi Y, Engleman EG. 2017. A distinct subset of plasmacytoid dendritic cells induces activation and differentiation of B and T lymphocytes. *Proc Natl Acad Sci U S A* 114: 1988-93
16. Merad M, Sathe P, Helft J, Miller J, Mortha A. 2013. The dendritic cell lineage: ontogeny and function of dendritic cells and their subsets in the steady state and the inflamed setting. *Annu Rev Immunol* 31: 563-604
17. Kondo M, Wagers AJ, Manz MG, Prohaska SS, Scherer DC, Beilhack GF, Shizuru JA, Weissman IL. 2003. Biology of hematopoietic stem cells and progenitors: implications for clinical application. In *Annu Rev Immunol*, pp. 759-806
18. Fogg DK, Sibon C, Miled C, Jung S, Aucouturier P, Littman DR, Cumano A, Geissmann F. 2006. A clonogenic bone marrow progenitor specific for macrophages and dendritic cells. *Science* 311: 83-7
19. Liu K, Victora GD, Schwickert TA, Guermonprez P, Meredith MM, Yao K, Chu FF, Randolph GJ, Rudensky AY, Nussenzweig M. 2009. In vivo analysis of dendritic cell development and homeostasis. *Science* 324: 392-7
20. Onai N, Obata-Onai A, Schmid MA, Ohteki T, Jarrossay D, Manz MG. 2007. Identification of clonogenic common Flt3+M-CSFR+ plasmacytoid and conventional dendritic cell progenitors in mouse bone marrow. *Nat Immunol* 8: 1207-16

21. Randolph GJ, Ochando J, Partida-Sanchez S. 2008. Migration of dendritic cell subsets and their precursors. *Annu Rev Immunol* 26: 293-316
22. Bogunovic M, Ginhoux F, Helft J, Shang L, Hashimoto D, Greter M, Liu K, Jakubzick C, Ingersoll MA, Leboeuf M, Stanley ER, Nussenzweig M, Lira SA, Randolph GJ, Merad M. 2009. Origin of the lamina propria dendritic cell network. *Immunity* 31: 513-25
23. Sallusto F, Lanzavecchia A. 1994. Efficient presentation of soluble antigen by cultured human dendritic cells is maintained by granulocyte/macrophage colony-stimulating factor plus interleukin 4 and downregulated by tumor necrosis factor alpha. *J Exp Med* 179: 1109-18
24. Dudziak D, Kamphorst AO, Heidkamp GF, Buchholz VR, Trumpfheller C, Yamazaki S, Cheong C, Liu K, Lee HW, Park CG, Steinman RM, Nussenzweig MC. 2007. Differential antigen processing by dendritic cell subsets in vivo. *Science* 315: 107-11
25. Langlet C, Tamoutounour S, Henri S, Luche H, Ardouin L, Gregoire C, Malissen B, Guilliams M. 2012. CD64 expression distinguishes monocyte-derived and conventional dendritic cells and reveals their distinct role during intramuscular immunization. *J Immunol* 188: 1751-60
26. Niess JH. 2010. What are CX3CR1+ mononuclear cells in the intestinal mucosa? *Gut Microbes* 1: 396-400
27. Varol C, Vallon-Eberhard A, Elinav E, Aychek T, Shapira Y, Luche H, Fehling HJ, Hardt WD, Shakhar G, Jung S. 2009. Intestinal lamina propria dendritic cell subsets have different origin and functions. *Immunity* 31: 502-12
28. Li HS, Yang CY, Nallaparaju KC, Zhang H, Liu YJ, Goldrath AW, Watowich SS. 2012. The signal transducers STAT5 and STAT3 control expression of Id2 and E2-2 during dendritic cell development. *Blood* 120: 4363-73
29. Watchmaker PB, Lahl K, Lee M, Baumjohann D, Morton J, Kim SJ, Zeng R, Dent A, Ansel KM, Diamond B, Hadeiba H, Butcher EC. 2014. Comparative transcriptional and functional profiling defines conserved programs of intestinal DC differentiation in humans and mice. *Nat Immunol* 15: 98-108
30. Li J, Park J, Foss D, Goldschneider I. 2009. Thymus-homing peripheral dendritic cells constitute two of the three major subsets of dendritic cells in the steady-state thymus. *J Exp Med* 206: 607-22
31. Vremec D, Pooley J, Hochrein H, Wu L, Shortman K. 2000. CD4 and CD8 expression by dendritic cell subtypes in mouse thymus and spleen. *J Immunol* 164: 2978-86
32. Johansson-Lindbom B, Svensson M, Pabst O, Palmqvist C, Marquez G, Forster R, Agace WW. 2005. Functional specialization of gut CD103+ dendritic cells in the regulation of tissue-selective T cell homing. *J Exp Med* 202: 1063-73
33. Iwasaki A, Kelsall BL. 2001. Unique functions of CD11b+, CD8 alpha+, and double-negative Peyer's patch dendritic cells. *J Immunol* 166: 4884-90
34. Sallusto F, Cella M, Danieli C, Lanzavecchia A. 1995. Dendritic cells use macropinocytosis and the mannose receptor to concentrate macromolecules in the major histocompatibility complex class II compartment: downregulation by cytokines and bacterial products. *J Exp Med* 182: 389-400
35. Sallusto F, Schaerli P, Loetscher P, Schaniel C, Lenig D, Mackay CR, Qin S, Lanzavecchia A. 1998. Rapid and coordinated switch in chemokine receptor expression during dendritic cell maturation. *Eur J Immunol* 28: 2760-9
36. MartIn-Fontecha A, Sebastiani S, Hopken UE, Uguccioni M, Lipp M, Lanzavecchia A, Sallusto F. 2003. Regulation of dendritic cell migration to the draining lymph node: impact on T lymphocyte traffic and priming. *J Exp Med* 198: 615-21
37. Alvarez D, Vollmann EH, von Andrian UH. 2008. Mechanisms and consequences of dendritic cell migration. *Immunity* 29: 325-42

38. **Cerovic V, Houston SA, Scott CL, Aumeunier A, Yrlid U, Mowat AM, Milling SW. 2013. Intestinal CD103(-) dendritic cells migrate in lymph and prime effector T cells. *Mucosal Immunol* 6: 104-13**

39. **Gunzer M, Schafer A, Borgmann S, Grabbe S, Zanker KS, Brocker EB, Kampgen E, Friedl P. 2000. Antigen presentation in extracellular matrix: interactions of T cells with dendritic cells are dynamic, short lived, and sequential. *Immunity* 13: 323-32**

40. **Rothoeft T, Balkow S, Krummen M, Beissert S, Varga G, Loser K, Oberbanscheidt P, van den Boom F, Grabbe S. 2006. Structure and duration of contact between dendritic cells and T cells are controlled by T cell activation state. *Eur J Immunol* 36: 3105-17**

41. **Jenkins MK. 1994. The ups and downs of T cell costimulation. *Immunity* 1: 443-6**

42. **Elgueta R, Benson MJ, de Vries VC, Wasiuk A, Guo Y, Noelle RJ. 2009. Molecular mechanism and function of CD40/CD40L engagement in the immune system. *Immunol Rev* 229: 152-72**

43. **Zhu J, Paul WE. 2008. CD4 T cells: fates, functions, and faults. *Blood* 112: 1557-69**

44. **Kurachi M, Barnitz RA, Yosef N, Odorizzi PM, DiIorio MA, Lemieux ME, Yates K, Godec J, Klatt MG, Regev A, Wherry EJ, Haining WN. 2014. The transcription factor BATF operates as an essential differentiation checkpoint in early effector CD8+ T cells. *Nat Immunol* 15: 373-83**

45. **Zhang N, Bevan MJ. 2011. CD8(+) T cells: foot soldiers of the immune system. *Immunity* 35: 161-8**

46. **Park SH, Roark JH, Bendelac A. 1998. Tissue-specific recognition of mouse CD1 molecules. *J Immunol* 160: 3128-34**

47. **Rossjohn J, Pellicci DG, Patel O, Gapin L, Godfrey DI. 2012. Recognition of CD1d-restricted antigens by natural killer T cells. *Nat Rev Immunol* 12: 845-57**

48. **Adams EJ. 2014. Lipid presentation by human CD1 molecules and the diverse T cell populations that respond to them. *Curr Opin Immunol* 26: 1-6**

49. **Szatmari I, Gogolak P, Im JS, Dezso B, Rajnavolgyi E, Nagy L. 2004. Activation of PPARgamma specifies a dendritic cell subtype capable of enhanced induction of iNKT cell expansion. *Immunity* 21: 95-106**

50. **Duperrier K, Eljaafari A, Dezutter-Dambuyant C, Bardin C, Jacquet C, Yoneda K, Schmitt D, Gebuhrer L, Rigal D. 2000. Distinct subsets of dendritic cells resembling dermal DCs can be generated in vitro from monocytes, in the presence of different serum supplements. *J Immunol Methods* 238: 119-31**

51. **Kang SJ, Cresswell P. 2002. Calnexin, calreticulin, and ERp57 cooperate in disulfide bond formation in human CD1d heavy chain. *J Biol Chem* 277: 44838-44**

52. **Brozovic S, Nagaishi T, Yoshida M, Betz S, Salas A, Chen D, Kaser A, Glickman J, Kuo T, Little A, Morrison J, Corazza N, Kim JY, Colgan SP, Young SG, Exley M, Blumberg RS. 2004. CD1d function is regulated by microsomal triglyceride transfer protein. *Nat Med* 10: 535-9**

53. **Dougan SK, Salas A, Rava P, Agyemang A, Kaser A, Morrison J, Khurana A, Kronenberg M, Johnson C, Exley M, Hussain MM, Blumberg RS. 2005. Microsomal triglyceride transfer protein lipidation and control of CD1d on antigen-presenting cells. *J Exp Med* 202: 529-39**

54. **De Libero G, Mori L. 2006. How T lymphocytes recognize lipid antigens. *FEBS Lett* 580: 5580-7**

55. **Sugita M, Peters PJ, Brenner MB. 2000. Pathways for lipid antigen presentation by CD1 molecules: nowhere for intracellular pathogens to hide. *Traffic* 1: 295-300**

56. **Spada FM, Borriello F, Sugita M, Watts GF, Koezuka Y, Porcelli SA. 2000. Low expression level but potent antigen presenting function of CD1d on monocyte lineage cells. *Eur J Immunol* 30: 3468-77**

57. **Gerlini G, Hefti HP, Kleinhans M, Nickoloff BJ, Burg G, Nestle FO. 2001. Cd1d is expressed on dermal dendritic cells and monocyte-derived dendritic cells. *J Invest Dermatol* 117: 576-82**

58. Brasel K, De Smedt T, Smith JL, Maliszewski CR. 2000. Generation of murine dendritic cells from flt3-ligand-supplemented bone marrow cultures. *Blood* 96: 3029-39
59. Krajina T, Leithauser F, Moller P, Trobonjaca Z, Reimann J. 2003. Colonic lamina propria dendritic cells in mice with CD4+ T cell-induced colitis. *Eur J Immunol* 33: 1073-83
60. Liu J, Shaji D, Cho S, Du W, Gervay-Hague J, Brutkiewicz RR. 2010. A threonine-based targeting signal in the human CD1d cytoplasmic tail controls its functional expression. *J Immunol* 184: 4973-81
61. Gelin C, Sloma I, Charron D, Mooney N. 2009. Regulation of MHC II and CD1 antigen presentation: from ubiquity to security. *J Leukoc Biol* 85: 215-24
62. Chiu YH, Park SH, Benlagha K, Forestier C, Jayawardena-Wolf J, Savage PB, Teyton L, Bendelac A. 2002. Multiple defects in antigen presentation and T cell development by mice expressing cytoplasmic tail-truncated CD1d. *Nat Immunol* 3: 55-60
63. Kang SJ, Cresswell P. 2002. Regulation of intracellular trafficking of human CD1d by association with MHC class II molecules. *EMBO J* 21: 1650-60
64. Elewaut D, Lawton AP, Nagarajan NA, Maverakis E, Khurana A, Honing S, Benedict CA, Sercarz E, Bakke O, Kronenberg M, Prigozy TI. 2003. The adaptor protein AP-3 is required for CD1d-mediated antigen presentation of glycosphingolipids and development of Valpha14i NKT cells. *J Exp Med* 198: 1133-46
65. Roberts TJ, Sriram V, Spence PM, Gui M, Hayakawa K, Bacik I, Bennink JR, Yewdell JW, Brutkiewicz RR. 2002. Recycling CD1d1 molecules present endogenous antigens processed in an endocytic compartment to NKT cells. *J Immunol* 168: 5409-14
66. Sugita M, Cao X, Watts GF, Rogers RA, Bonifacino JS, Brenner MB. 2002. Failure of trafficking and antigen presentation by CD1 in AP-3-deficient cells. *Immunity* 16: 697-706
67. Exley M, Garcia J, Balk SP, Porcelli S. 1997. Requirements for CD1d recognition by human invariant Valpha24+ CD4-CD8- T cells. *J Exp Med* 186: 109-20
68. Spada FM, Koezuka Y, Porcelli SA. 1998. CD1d-restricted recognition of synthetic glycolipid antigens by human natural killer T cells. *J Exp Med* 188: 1529-34
69. Chen X, Wang X, Keaton JM, Reddington F, Illarionov PA, Besra GS, Gumperz JE. 2007. Distinct endosomal trafficking requirements for presentation of autoantigens and exogenous lipids by human CD1d molecules. *J Immunol* 178: 6181-90
70. Cao X, Sugita M, Van Der Wel N, Lai J, Rogers RA, Peters PJ, Brenner MB. 2002. CD1 molecules efficiently present antigen in immature dendritic cells and traffic independently of MHC class II during dendritic cell maturation. *J Immunol* 169: 4770-7
71. Gumperz JE. 2006. The ins and outs of CD1 molecules: bringing lipids under immunological surveillance. *Traffic* 7: 2-13
72. Angenieux C, Fraisier V, Maitre B, Racine V, van der Wel N, Fricker D, Proamer F, Sachse M, Cazenave JP, Peters P, Goud B, Hanau D, Sibarita JB, Salamero J, de la Salle H. 2005. The cellular pathway of CD1e in immature and maturing dendritic cells. *Traffic* 6: 286-302
73. Bendelac A, Savage PB, Teyton L. 2007. The biology of NKT cells. *Annu Rev Immunol* 25: 297-336
74. McEwen-Smith RM, Salio M, Cerundolo V. 2015. CD1d-dependent endogenous and exogenous lipid antigen presentation. *Curr Opin Immunol* 34: 116-25
75. Zhou D, Mattner J, Cantu C, 3rd, Schrantz N, Yin N, Gao Y, Sagiv Y, Hudspeth K, Wu YP, Yamashita T, Teneberg S, Wang D, Proia RL, Levery SB, Savage PB, Teyton L, Bendelac A. 2004. Lysosomal glycosphingolipid recognition by NKT cells. *Science* 306: 1786-9
76. Porubsky S, Speak AO, Luckow B, Cerundolo V, Platt FM, Grone HJ. 2007. Normal development and function of invariant natural killer T cells in mice with isoglobotrihexosylceramide (iGb3) deficiency. *Proc Natl Acad Sci U S A* 104: 5977-82
77. Christiansen D, Milland J, Mouhtouris E, Vaughan H, Pellicci DG, McConville MJ, Godfrey DI, Sandrin MS. 2008. Humans lack iGb3 due to the absence of functional iGb3-synthase: implications for NKT cell development and transplantation. *PLoS Biol* 6: e172

78. Speak AO, Cerundolo V, Platt FM. 2008. CD1d presentation of glycolipids. *Immunol Cell Biol* 86: 588-97
79. Kain L, Webb B, Anderson BL, Deng S, Holt M, Costanzo A, Zhao M, Self K, Teyton A, Everett C, Kronenberg M, Zajonc DM, Bendelac A, Savage PB, Teyton L. 2014. The identification of the endogenous ligands of natural killer T cells reveals the presence of mammalian alpha-linked glycosylceramides. *Immunity* 41: 543-54
80. Halder RC, Aguilera C, Maricic I, Kumar V. 2007. Type II NKT cell-mediated anergy induction in type I NKT cells prevents inflammatory liver disease. *J Clin Invest* 117: 2302-12
81. Brossay L, Chioda M, Burdin N, Koezuka Y, Casorati G, Dellabona P, Kronenberg M. 1998. CD1d-mediated recognition of an alpha-galactosylceramide by natural killer T cells is highly conserved through mammalian evolution. *J Exp Med* 188: 1521-8
82. Koch M, Stronge VS, Shepherd D, Gadola SD, Mathew B, Ritter G, Fersht AR, Besra GS, Schmidt RR, Jones EY, Cerundolo V. 2005. The crystal structure of human CD1d with and without alpha-galactosylceramide. *Nat Immunol* 6: 819-26
83. Kawano T, Cui J, Koezuka Y, Toura I, Kaneko Y, Motoki K, Ueno H, Nakagawa R, Sato H, Kondo E, Koseki H, Taniguchi M. 1997. CD1d-restricted and TCR-mediated activation of valpha14 NKT cells by glycosylceramides. *Science* 278: 1626-9
84. Fujii S, Shimizu K, Hemmi H, Fukui M, Bonito AJ, Chen G, Franck RW, Tsuji M, Steinman RM. 2006. Glycolipid alpha-C-galactosylceramide is a distinct inducer of dendritic cell function during innate and adaptive immune responses of mice. *Proc Natl Acad Sci U S A* 103: 11252-7
85. Oki S, Tomi C, Yamamura T, Miyake S. 2005. Preferential T(h)2 polarization by OCH is supported by incompetent NKT cell induction of CD40L and following production of inflammatory cytokines by bystander cells in vivo. *Int Immunol* 17: 1619-29
86. van den Elzen P, Garg S, Leon L, Brigl M, Leadbetter EA, Gumperz JE, Dascher CC, Cheng TY, Sacks FM, Illarionov PA, Besra GS, Kent SC, Moody DB, Brenner MB. 2005. Apolipoprotein-mediated pathways of lipid antigen presentation. *Nature* 437: 906-10
87. Freigang S, Zadorozhny V, McKinney MK, Krebs P, Herro R, Pawlak J, Kain L, Schrantz N, Masuda K, Liu Y, Savage PB, Bendelac A, Cravatt BF, Teyton L. 2010. Fatty acid amide hydrolase shapes NKT cell responses by influencing the serum transport of lipid antigen in mice. *J Clin Invest* 120: 1873-84
88. Freigang S, Landais E, Zadorozhny V, Kain L, Yoshida K, Liu Y, Deng S, Palinski W, Savage PB, Bendelac A, Teyton L. 2012. Scavenger receptors target glycolipids for natural killer T cell activation. *J Clin Invest* 122: 3943-54
89. Prigozy TI, Naidenko O, Qasba P, Elewaut D, Brossay L, Khurana A, Natori T, Koezuka Y, Kulkarni A, Kronenberg M. 2001. Glycolipid antigen processing for presentation by CD1d molecules. *Science* 291: 664-7
90. Zhou D, Cantu C, 3rd, Sagiv Y, Schrantz N, Kulkarni AB, Qi X, Mahuran DJ, Morales CR, Grabowski GA, Benlagha K, Savage P, Bendelac A, Teyton L. 2004. Editing of CD1d-bound lipid antigens by endosomal lipid transfer proteins. *Science* 303: 523-7
91. Kang SJ, Cresswell P. 2004. Saposins facilitate CD1d-restricted presentation of an exogenous lipid antigen to T cells. *Nat Immunol* 5: 175-81
92. Hiraiwa M, Martin BM, Kishimoto Y, Conner GE, Tsuji S, O'Brien JS. 1997. Lysosomal proteolysis of prosaposin, the precursor of saposins (sphingolipid activator proteins): its mechanism and inhibition by ganglioside. *Arch Biochem Biophys* 341: 17-24
93. Darmoise A, Maschmeyer P, Winau F. 2010. The immunological functions of saposins. *Adv Immunol* 105: 25-62
94. Yuan W, Qi X, Tsang P, Kang SJ, Illarionov PA, Besra GS, Gumperz J, Cresswell P. 2007. Saposin B is the dominant saposin that facilitates lipid binding to human CD1d molecules. *Proc Natl Acad Sci U S A* 104: 5551-6

95. Bai L, Sagiv Y, Liu Y, Freigang S, Yu KO, Teyton L, Porcelli SA, Savage PB, Bendelac A. 2009. Lysosomal recycling terminates CD1d-mediated presentation of short and polyunsaturated variants of the NKT cell lipid antigen alphaGalCer. *Proc Natl Acad Sci U S A* 106: 10254-9
96. Turk V, Stoka V, Vasiljeva O, Renko M, Sun T, Turk B, Turk D. 2012. Cysteine cathepsins: from structure, function and regulation to new frontiers. *Biochim Biophys Acta* 1824: 68-88
97. Honey K, Benlagha K, Beers C, Forbush K, Teyton L, Kleijmeer MJ, Rudensky AY, Bendelac A. 2002. Thymocyte expression of cathepsin L is essential for NKT cell development. *Nat Immunol* 3: 1069-74
98. Kopitar-Jerala N. 2012. The role of cysteine proteinases and their inhibitors in the host-pathogen cross talk. *Curr Protein Pept Sci* 13: 767-75
99. van der Wel NN, Sugita M, Fluitsma DM, Cao X, Schreibelt G, Brenner MB, Peters PJ. 2003. CD1 and major histocompatibility complex II molecules follow a different course during dendritic cell maturation. *Mol Biol Cell* 14: 3378-88
100. McCurley N, Mellman I. 2010. Monocyte-derived dendritic cells exhibit increased levels of lysosomal proteolysis as compared to other human dendritic cell populations. *PLoS One* 5: e11949
101. Riese RJ, Shi GP, Villadangos J, Stetson D, Driessen C, Lennon-Dumenil AM, Chu CL, Naumov Y, Behar SM, Ploegh H, Locksley R, Chapman HA. 2001. Regulation of CD1 function and NK1.1(+) T cell selection and maturation by cathepsin S. *Immunity* 15: 909-19
102. Kakehashi H, Nishioku T, Tsukuba T, Kadowaki T, Nakamura S, Yamamoto K. 2007. Differential regulation of the nature and functions of dendritic cells and macrophages by cathepsin E. *J Immunol* 179: 5728-37
103. Heinrich M, Wickel M, Schneider-Brachert W, Sandberg C, Gahr J, Schwandner R, Weber T, Saftig P, Peters C, Brunner J, Kronke M, Schutze S. 1999. Cathepsin D targeted by acid sphingomyelinase-derived ceramide. *EMBO J* 18: 5252-63
104. Godfrey DI, Kronenberg M. 2004. Going both ways: immune regulation via CD1d-dependent NKT cells. *J Clin Invest* 114: 1379-88
105. Georgiev H, Ravens I, Benarafa C, Forster R, Bernhardt G. 2016. Distinct gene expression patterns correlate with developmental and functional traits of iNKT subsets. *Nat Commun* 7: 13116
106. Brigl M, Tatituri RV, Watts GF, Bhowruth V, Leadbetter EA, Barton N, Cohen NR, Hsu FF, Besra GS, Brenner MB. 2011. Innate and cytokine-driven signals, rather than microbial antigens, dominate in natural killer T cell activation during microbial infection. *J Exp Med* 208: 1163-77
107. Matsuda JL, Gapin L, Baron JL, Sidobre S, Stetson DB, Mohrs M, Locksley RM, Kronenberg M. 2003. Mouse V alpha 14i natural killer T cells are resistant to cytokine polarization in vivo. *Proc Natl Acad Sci U S A* 100: 8395-400
108. Stetson DB, Mohrs M, Reinhardt RL, Baron JL, Wang ZE, Gapin L, Kronenberg M, Locksley RM. 2003. Constitutive cytokine mRNAs mark natural killer (NK) and NK T cells poised for rapid effector function. *J Exp Med* 198: 1069-76
109. Bendelac A, Rivera MN, Park SH, Roark JH. 1997. Mouse CD1-specific NK1 T cells: development, specificity, and function. *Annu Rev Immunol* 15: 535-62
110. Sandberg JK, Bhardwaj N, Nixon DF. 2003. Dominant effector memory characteristics, capacity for dynamic adaptive expansion, and sex bias in the innate Valpha24 NKT cell compartment. *Eur J Immunol* 33: 588-96
111. McEwen-Smith RM, Salio M, Cerundolo V. 2015. The regulatory role of invariant NKT cells in tumor immunity. *Cancer Immunol Res* 3: 425-35

112. **Crowe NY, Coquet JM, Berzins SP, Kyparissoudis K, Keating R, Pellicci DG, Hayakawa Y, Godfrey DI, Smyth MJ. 2005. Differential antitumor immunity mediated by NKT cell subsets in vivo. *J Exp Med* 202: 1279-88**

113. **Crowe NY, Smyth MJ, Godfrey DI. 2002. A critical role for natural killer T cells in immunosurveillance of methylcholanthrene-induced sarcomas. *J Exp Med* 196: 119-27**

114. **Crowe NY, Uldrich AP, Kyparissoudis K, Hammond KJ, Hayakawa Y, Sidobre S, Keating R, Kronenberg M, Smyth MJ, Godfrey DI. 2003. Glycolipid antigen drives rapid expansion and sustained cytokine production by NK T cells. *J Immunol* 171: 4020-7**

115. **Kawano T, Cui J, Koezuka Y, Toura I, Kaneko Y, Sato H, Kondo E, Harada M, Koseki H, Nakayama T, Tanaka Y, Taniguchi M. 1998. Natural killer-like nonspecific tumor cell lysis mediated by specific ligand-activated Valpha14 NKT cells. *Proc Natl Acad Sci U S A* 95: 5690-3**

116. **Fujii S, Liu K, Smith C, Bonito AJ, Steinman RM. 2004. The linkage of innate to adaptive immunity via maturing dendritic cells in vivo requires CD40 ligation in addition to antigen presentation and CD80/86 costimulation. *J Exp Med* 199: 1607-18**

117. **Hayakawa Y, Takeda K, Yagita H, Kakuta S, Iwakura Y, Van Kaer L, Saiki I, Okumura K. 2001. Critical contribution of IFN-gamma and NK cells, but not perforin-mediated cytotoxicity, to anti-metastatic effect of alpha-galactosylceramide. *Eur J Immunol* 31: 1720-7**

118. **Nakagawa R, Nagafune I, Tazunoki Y, Ehara H, Tomura H, Iijima R, Motoki K, Kamishohara M, Seki S. 2001. Mechanisms of the antimetastatic effect in the liver and of the hepatocyte injury induced by alpha-galactosylceramide in mice. *J Immunol* 166: 6578-84**

119. **Smyth MJ, Wallace ME, Nutt SL, Yagita H, Godfrey DI, Hayakawa Y. 2005. Sequential activation of NKT cells and NK cells provides effective innate immunotherapy of cancer. *J Exp Med* 201: 1973-85**

120. **Fujii S, Shimizu K, Smith C, Bonifaz L, Steinman RM. 2003. Activation of natural killer T cells by alpha-galactosylceramide rapidly induces the full maturation of dendritic cells in vivo and thereby acts as an adjuvant for combined CD4 and CD8 T cell immunity to a coadministered protein. *J Exp Med* 198: 267-79**

121. **Semmling V, Lukacs-Kornek V, Thaiss CA, Quast T, Hochheiser K, Panzer U, Rossjohn J, Perlmutter P, Cao J, Godfrey DI, Savage PB, Knolle PA, Kolanus W, Forster I, Kurts C. 2010. Alternative cross-priming through CCL17-CCR4-mediated attraction of CTLs toward NKT cell-licensed DCs. *Nat Immunol* 11: 313-20**

122. **Taraban VY, Martin S, Attfield KE, Glennie MJ, Elliott T, Elewaut D, Van Calenbergh S, Linclau B, Al-Shamkhani A. 2008. Invariant NKT cells promote CD8+ cytotoxic T cell responses by inducing CD70 expression on dendritic cells. *J Immunol* 180: 4615-20**

123. **Ko HJ, Lee JM, Kim YJ, Kim YS, Lee KA, Kang CY. 2009. Immunosuppressive myeloid-derived suppressor cells can be converted into immunogenic APCs with the help of activated NKT cells: an alternative cell-based antitumor vaccine. *J Immunol* 182: 1818-28**

124. **Song L, Asgharzadeh S, Salo J, Engell K, Wu HW, Sposto R, Ara T, Silverman AM, DeClerck YA, Seeger RC, Metelitsa LS. 2009. Valpha24-invariant NKT cells mediate antitumor activity via killing of tumor-associated macrophages. *J Clin Invest* 119: 1524-36**

125. **Marrero I, Ware R, Kumar V. 2015. Type II NKT Cells in Inflammation, Autoimmunity, Microbial Immunity, and Cancer. *Front Immunol* 6: 316**

126. **Blomqvist M, Rhost S, Teneberg S, Lofbom L, Osterbye T, Brigl M, Mansson JE, Cardell SL. 2009. Multiple tissue-specific isoforms of sulfatide activate CD1d-restricted type II NKT cells. *Eur J Immunol* 39: 1726-35**

127. **Dhodapkar MV, Kumar V. 2017. Type II NKT Cells and Their Emerging Role in Health and Disease. *J Immunol* 198: 1015-21**

128. **Chen YH, Chiu NM, Mandal M, Wang N, Wang CR. 1997. Impaired NK1+ T cell development and early IL-4 production in CD1-deficient mice. *Immunity* 6: 459-67**

129. **Cui J, Shin T, Kawano T, Sato H, Kondo E, Toura I, Kaneko Y, Koseki H, Kanno M, Taniguchi M. 1997. Requirement for Valpha14 NKT cells in IL-12-mediated rejection of tumors. *Science* 278: 1623-6**

130. **Park JM, Terabe M, van den Broeke LT, Donaldson DD, Berzofsky JA. 2005. Unmasking immunosurveillance against a syngeneic colon cancer by elimination of CD4+ NKT regulatory cells and IL-13. *Int J Cancer* 114: 80-7**

131. **Terabe M, Berzofsky JA. 2004. Immunoregulatory T cells in tumor immunity. *Curr Opin Immunol* 16: 157-62**

132. **Terabe M, Matsui S, Noben-Trauth N, Chen H, Watson C, Donaldson DD, Carbone DP, Paul WE, Berzofsky JA. 2000. NKT cell-mediated repression of tumor immunosurveillance by IL-13 and the IL-4R-STAT6 pathway. *Nat Immunol* 1: 515-20**

133. **Ambrosino E, Terabe M, Halder RC, Peng J, Takaku S, Miyake S, Yamamura T, Kumar V, Berzofsky JA. 2007. Cross-regulation between type I and type II NKT cells in regulating tumor immunity: a new immunoregulatory axis. *J Immunol* 179: 5126-36**

134. **Terabe M, Matsui S, Park JM, Mamura M, Noben-Trauth N, Donaldson DD, Chen W, Wahl SM, Ledbetter S, Pratt B, Letterio JJ, Paul WE, Berzofsky JA. 2003. Transforming growth factor-beta production and myeloid cells are an effector mechanism through which CD1d-restricted T cells block cytotoxic T lymphocyte-mediated tumor immunosurveillance: abrogation prevents tumor recurrence. *J Exp Med* 198: 1741-52**

135. **Chawla A, Boisvert WA, Lee CH, Laffitte BA, Barak Y, Joseph SB, Liao D, Nagy L, Edwards PA, Curtiss LK, Evans RM, Tontonoz P. 2001. A PPAR gamma-LXR-ABCA1 pathway in macrophages is involved in cholesterol efflux and atherogenesis. *Mol Cell* 7: 161-71**

136. **Evans RM. 1988. The steroid and thyroid hormone receptor superfamily. *Science* 240: 889-95**

137. **Kastner P, Mark M, Chambon P. 1995. Nonsteroid nuclear receptors: what are genetic studies telling us about their role in real life? *Cell* 83: 859-69**

138. **Mangelsdorf DJ, Evans RM. 1995. The RXR heterodimers and orphan receptors. *Cell* 83: 841-50**

139. **Zhang Z, Burch PE, Cooney AJ, Lanz RB, Pereira FA, Wu J, Gibbs RA, Weinstock G, Wheeler DA. 2004. Genomic analysis of the nuclear receptor family: new insights into structure, regulation, and evolution from the rat genome. *Genome Res* 14: 580-90**

140. **Shulman AI, Mangelsdorf DJ. 2005. Retinoid x receptor heterodimers in the metabolic syndrome. *N Engl J Med* 353: 604-15**

141. **Laudet V. 1997. Evolution of the nuclear receptor superfamily: early diversification from an ancestral orphan receptor. *J Mol Endocrinol* 19: 207-26**

142. **Mangelsdorf DJ, Thummel C, Beato M, Herrlich P, Schutz G, Umesono K, Blumberg B, Kastner P, Mark M, Chambon P, Evans RM. 1995. The nuclear receptor superfamily: the second decade. *Cell* 83: 835-9**

143. **Kiss M, Czimmerer Z, Nagy L. 2013. The role of lipid-activated nuclear receptors in shaping macrophage and dendritic cell function: From physiology to pathology. *J Allergy Clin Immunol* 132: 264-86**

144. **Lavery DN, McEwan IJ. 2005. Structure and function of steroid receptor AF1 transactivation domains: induction of active conformations. *Biochem J* 391: 449-64**

145. **Katzenellenbogen JA, Katzenellenbogen BS. 1996. Nuclear hormone receptors: ligand-activated regulators of transcription and diverse cell responses. *Chem Biol* 3: 529-36**

146. **Hard T, Kellenbach E, Boelens R, Maler BA, Dahlman K, Freedman LP, Carlstedt-Duke J, Yamamoto KR, Gustafsson JA, Kaptein R. 1990. Solution structure of the glucocorticoid receptor DNA-binding domain. *Science* 249: 157-60**

147. **Umesono K, Evans RM. 1989. Determinants of target gene specificity for steroid/thyroid hormone receptors. *Cell* 57: 1139-46**

148. Lee MS, Kliewer SA, Provencal J, Wright PE, Evans RM. 1993. Structure of the retinoid X receptor alpha DNA binding domain: a helix required for homodimeric DNA binding. *Science* 260: 1117-21

149. Zechel C, Shen XQ, Chambon P, Gronemeyer H. 1994. Dimerization interfaces formed between the DNA binding domains determine the cooperative binding of RXR/RAR and RXR/TR heterodimers to DR5 and DR4 elements. *EMBO J* 13: 1414-24

150. Zechel C, Shen XQ, Chen JY, Chen ZP, Chambon P, Gronemeyer H. 1994. The dimerization interfaces formed between the DNA binding domains of RXR, RAR and TR determine the binding specificity and polarity of the full-length receptors to direct repeats. *EMBO J* 13: 1425-33

151. Li Y, Lambert MH, Xu HE. 2003. Activation of nuclear receptors: a perspective from structural genomics. *Structure* 11: 741-6

152. Rastinejad F, Huang P, Chandra V, Khorasanizadeh S. 2013. Understanding nuclear receptor form and function using structural biology. *J Mol Endocrinol* 51: T1-T21

153. Bledsoe RK, Montana VG, Stanley TB, Delves CJ, Apolito CJ, McKee DD, Consler TG, Parks DJ, Stewart EL, Willson TM, Lambert MH, Moore JT, Pearce KH, Xu HE. 2002. Crystal structure of the glucocorticoid receptor ligand binding domain reveals a novel mode of receptor dimerization and coactivator recognition. *Cell* 110: 93-105

154. Xu HE, Lambert MH, Montana VG, Parks DJ, Blanchard SG, Brown PJ, Sternbach DD, Lehmann JM, Wisely GB, Willson TM, Kliewer SA, Milburn MV. 1999. Molecular recognition of fatty acids by peroxisome proliferator-activated receptors. *Mol Cell* 3: 397-403

155. Glass CK. 1994. Differential recognition of target genes by nuclear receptor monomers, dimers, and heterodimers. *Endocr Rev* 15: 391-407

156. Rastinejad F. 2001. Retinoid X receptor and its partners in the nuclear receptor family. *Curr Opin Struct Biol* 11: 33-8

157. Umesono K, Murakami KK, Thompson CC, Evans RM. 1991. Direct repeats as selective response elements for the thyroid hormone, retinoic acid, and vitamin D3 receptors. *Cell* 65: 1255-66

158. Garruti G, Wang HH, Bonfrate L, de Bari O, Wang DQ, Portincasa P. 2012. A pleiotropic role for the orphan nuclear receptor small heterodimer partner in lipid homeostasis and metabolic pathways. *J Lipids* 2012: 304292

159. Smith DF, Toft DO. 1993. Steroid receptors and their associated proteins. *Mol Endocrinol* 7: 4-11

160. Chen JD, Evans RM. 1995. A transcriptional co-repressor that interacts with nuclear hormone receptors. *Nature* 377: 454-7

161. Park EJ, Schroen DJ, Yang M, Li H, Li L, Chen JD. 1999. SMRTe, a silencing mediator for retinoid and thyroid hormone receptors-extended isoform that is more related to the nuclear receptor corepressor. *Proc Natl Acad Sci U S A* 96: 3519-24

162. Ordentlich P, Downes M, Xie W, Genin A, Spinner NB, Evans RM. 1999. Unique forms of human and mouse nuclear receptor corepressor SMRT. *Proc Natl Acad Sci U S A* 96: 2639-44

163. Hartman HB, Yu J, Alenghat T, Ishizuka T, Lazar MA. 2005. The histone-binding code of nuclear receptor co-repressors matches the substrate specificity of histone deacetylase 3. *EMBO Rep* 6: 445-51

164. Chen D, Huang SM, Stallcup MR. 2000. Synergistic, p160 coactivator-dependent enhancement of estrogen receptor function by CARM1 and p300. *J Biol Chem* 275: 40810-6

165. Vo N, Goodman RH. 2001. CREB-binding protein and p300 in transcriptional regulation. *J Biol Chem* 276: 13505-8

166. Pascual G, Fong AL, Ogawa S, Gamliel A, Li AC, Perissi V, Rose DW, Willson TM, Rosenfeld MG, Glass CK. 2005. A SUMOylation-dependent pathway mediates transrepression of inflammatory response genes by PPAR-gamma. *Nature* 437: 759-63

167. Sonoda J, Pei L, Evans RM. 2008. Nuclear receptors: decoding metabolic disease. *FEBS Lett* 582: 2-9

168. Le Naour F, Hohenkirk L, Grolleau A, Misek DE, Lescure P, Geiger JD, Hanash S, Beretta L. 2001. Profiling changes in gene expression during differentiation and maturation of monocyte-derived dendritic cells using both oligonucleotide microarrays and proteomics. *J Biol Chem* 276: 17920-31

169. Szatmari I, Torocsik D, Agostini M, Nagy T, Gurnell M, Barta E, Chatterjee K, Nagy L. 2007. PPARgamma regulates the function of human dendritic cells primarily by altering lipid metabolism. *Blood* 110: 3271-80

170. Chawla A, Repa JJ, Evans RM, Mangelsdorf DJ. 2001. Nuclear receptors and lipid physiology: opening the X-files. *Science* 294: 1866-70

171. Germain P, Chambon P, Eichele G, Evans RM, Lazar MA, Leid M, De Lera AR, Lotan R, Mangelsdorf DJ, Gronemeyer H. 2006. International Union of Pharmacology. LXIII. Retinoid X receptors. *Pharmacol Rev* 58: 760-72

172. Kurokawa R, DiRenzo J, Boehm M, Sugarman J, Gloss B, Rosenfeld MG, Heyman RA, Glass CK. 1994. Regulation of retinoid signalling by receptor polarity and allosteric control of ligand binding. *Nature* 371: 528-31

173. Schulman IG, Li C, Schwabe JW, Evans RM. 1997. The phantom ligand effect: allosteric control of transcription by the retinoid X receptor. *Genes Dev* 11: 299-308

174. Kurakula K, Koenis DS, van Tiel CM, de Vries CJ. 2014. NR4A nuclear receptors are orphans but not lonesome. *Biochim Biophys Acta* 1843: 2543-55

175. Szeles L, Poliska S, Nagy G, Szatmari I, Szanto A, Pap A, Lindstedt M, Santegoets SJ, Ruhl R, Dezso B, Nagy L. Research resource: transcriptome profiling of genes regulated by RXR and its permissive and nonpermissive partners in differentiating monocyte-derived dendritic cells. *Mol Endocrinol* 24: 2218-31

176. Travis GH, Golczak M, Moise AR, Palczewski K. 2007. Diseases caused by defects in the visual cycle: retinoids as potential therapeutic agents. *Annu Rev Pharmacol Toxicol* 47: 469-512

177. Mark M, Ghyselinck NB, Chambon P. 2006. Function of retinoid nuclear receptors: lessons from genetic and pharmacological dissections of the retinoic acid signaling pathway during mouse embryogenesis. *Annu Rev Pharmacol Toxicol* 46: 451-80

178. Stephensen CB. 2001. Vitamin A, infection, and immune function. *Annu Rev Nutr* 21: 167-92

179. Clagett-Dame M, DeLuca HF. 2002. The role of vitamin A in mammalian reproduction and embryonic development. *Annu Rev Nutr* 22: 347-81

180. Love JM, Gudas LJ. 1994. Vitamin A, differentiation and cancer. *Curr Opin Cell Biol* 6: 825-31

181. De Luca LM. 1991. Retinoids and their receptors in differentiation, embryogenesis, and neoplasia. *FASEB J* 5: 2924-33

182. Duong V, Rochette-Egly C. 2011. The molecular physiology of nuclear retinoic acid receptors. From health to disease. *Biochim Biophys Acta* 1812: 1023-31

183. Bastien J, Rochette-Egly C. 2004. Nuclear retinoid receptors and the transcription of retinoid-target genes. *Gene* 328: 1-16

184. Nagy L, Szanto A, Szatmari I, Szeles L. 2012. Nuclear hormone receptors enable macrophages and dendritic cells to sense their lipid environment and shape their immune response. *Physiol Rev* 92: 739-89

185. Mukherjee R, Davies PJ, Crombie DL, Bischoff ED, Cesario RM, Jow L, Hamann LG, Boehm MF, Mondon CE, Nadzan AM, Paterniti JR, Jr., Heyman RA. 1997. Sensitization of diabetic and obese mice to insulin by retinoid X receptor agonists. *Nature* 386: 407-10

186. Harrison EH. 2005. Mechanisms of digestion and absorption of dietary vitamin A. *Annu Rev Nutr* 25: 87-103
187. Fraser PD, Bramley PM. 2004. The biosynthesis and nutritional uses of carotenoids. *Prog Lipid Res* 43: 228-65
188. Rigtrup KM, Kakkad B, Ong DE. 1994. Purification and partial characterization of a retinyl ester hydrolase from the brush border of rat small intestine mucosa: probable identity with brush border phospholipase B. *Biochemistry* 33: 2661-6
189. van Bennekum AM, Fisher EA, Blaner WS, Harrison EH. 2000. Hydrolysis of retinyl esters by pancreatic triglyceride lipase. *Biochemistry* 39: 4900-6
190. Dew SE, Ong DE. 1994. Specificity of the retinol transporter of the rat small intestine brush border. *Biochemistry* 33: 12340-5
191. Harrison EH, Hussain MM. 2001. Mechanisms involved in the intestinal digestion and absorption of dietary vitamin A. *J Nutr* 131: 1405-8
192. Blomhoff R, Helgerud P, Rasmussen M, Berg T, Norum KR. 1982. In vivo uptake of chylomicron [3H]retinyl ester by rat liver: evidence for retinol transfer from parenchymal to nonparenchymal cells. *Proc Natl Acad Sci U S A* 79: 7326-30
193. Blomhoff R, Blomhoff HK. 2006. Overview of retinoid metabolism and function. *J Neurobiol* 66: 606-30
194. Newcomer ME, Ong DE. 2000. Plasma retinol binding protein: structure and function of the prototypic lipocalin. *Biochim Biophys Acta* 1482: 57-64
195. Sun H, Kawaguchi R. 2011. The membrane receptor for plasma retinol-binding protein, a new type of cell-surface receptor. *Int Rev Cell Mol Biol* 288: 1-41
196. Alapatt P, Guo F, Komanetsky SM, Wang S, Cai J, Sargsyan A, Rodriguez Diaz E, Bacon BT, Aryal P, Graham TE. 2013. Liver retinol transporter and receptor for serum retinol-binding protein (RBP4). *J Biol Chem* 288: 1250-65
197. Napoli JL. 2016. Functions of Intracellular Retinoid Binding-Proteins. *Subcell Biochem* 81: 21-76
198. Duester G. 2000. Families of retinoid dehydrogenases regulating vitamin A function: production of visual pigment and retinoic acid. *Eur J Biochem* 267: 4315-24
199. Napoli JL. 2017. Cellular retinoid binding-proteins, CRBP, CRABP, FABP5: Effects on retinoid metabolism, function and related diseases. *Pharmacol Ther* 173: 19-33
200. Delva L, Bastie JN, Rochette-Egly C, Kraiba R, Balitrand N, Despouy G, Chambon P, Chomienne C. 1999. Physical and functional interactions between cellular retinoic acid binding protein II and the retinoic acid-dependent nuclear complex. *Mol Cell Biol* 19: 7158-67
201. Sessler RJ, Noy N. 2005. A ligand-activated nuclear localization signal in cellular retinoic acid binding protein-II. *Mol Cell* 18: 343-53
202. Maden M. 1994. Distribution of Cellular Retinoic Acid-Binding Protein-I and Protein-Ii in the Chick-Embryo and Their Relationship to Teratogenesis. *Teratology* 50: 294-301
203. Ruberte E, Friederich V, Morriss-Kay G, Chambon P. 1992. Differential distribution patterns of CRABP I and CRABP II transcripts during mouse embryogenesis. *Development* 115: 973-87
204. Collins CA, Watt FM. 2008. Dynamic regulation of retinoic acid-binding proteins in developing, adult and neoplastic skin reveals roles for beta-catenin and Notch signalling. *Dev Biol* 324: 55-67
205. Wardlaw SA, Bucco RA, Zheng WL, Ong DE. 1997. Variable expression of cellular retinol- and cellular retinoic acid-binding proteins in the rat uterus and ovary during the estrous cycle. *Biol Reprod* 56: 125-32
206. Zheng WL, Bucco RA, Schmitt MC, Wardlaw SA, Ong DE. 1996. Localization of cellular retinoic acid-binding protein (CRABP) II and CRABP in developing rat testis. *Endocrinology* 137: 5028-35

207. **Zheng WL, Ong DE. 1998. Spatial and temporal patterns of expression of cellular retinol-binding protein and cellular retinoic acid-binding proteins in rat uterus during early pregnancy. *Biol Reprod* 58: 963-70**

208. **Yamamoto M, Drager UC, Ong DE, McCaffery P. 1998. Retinoid-binding proteins in the cerebellum and choroid plexus and their relationship to regionalized retinoic acid synthesis and degradation. *Eur J Biochem* 257: 344-50**

209. **Sakai Y, Meno C, Fujii H, Nishino J, Shiratori H, Saijoh Y, Rossant J, Hamada H. 2001. The retinoic acid-inactivating enzyme CYP26 is essential for establishing an uneven distribution of retinoic acid along the anterio-posterior axis within the mouse embryo. *Genes Dev* 15: 213-25**

210. **Yashiro K, Zhao X, Uehara M, Yamashita K, Nishijima M, Nishino J, Saijoh Y, Sakai Y, Hamada H. 2004. Regulation of retinoic acid distribution is required for proximodistal patterning and outgrowth of the developing mouse limb. *Dev Cell* 6: 411-22**

211. **Uehara M, Yashiro K, Mamiya S, Nishino J, Chambon P, Dolle P, Sakai Y. 2007. CYP26A1 and CYP26C1 cooperatively regulate anterior-posterior patterning of the developing brain and the production of migratory cranial neural crest cells in the mouse. *Dev Biol* 302: 399-411**

212. **Abu-Abed S, Dolle P, Metzger D, Beckett B, Chambon P, Petkovich M. 2001. The retinoic acid-metabolizing enzyme, CYP26A1, is essential for normal hindbrain patterning, vertebral identity, and development of posterior structures. *Genes Dev* 15: 226-40**

213. **Zhang Y, Zolfaghari R, Ross AC. 2010. Multiple retinoic acid response elements cooperate to enhance the inducibility of CYP26A1 gene expression in liver. *Gene* 464: 32-43**

214. **Schug TT, Berry DC, Shaw NS, Travis SN, Noy N. 2007. Opposing effects of retinoic acid on cell growth result from alternate activation of two different nuclear receptors. *Cell* 129: 723-33**

215. **Molotkov A, Deltour L, Foglio MH, Cuenca AE, Duester G. 2002. Distinct retinoid metabolic functions for alcohol dehydrogenase genes Adh1 and Adh4 in protection against vitamin A toxicity or deficiency revealed in double null mutant mice. *J Biol Chem* 277: 13804-11**

216. **Molotkov A, Fan X, Deltour L, Foglio MH, Martras S, Farres J, Pares X, Duester G. 2002. Stimulation of retinoic acid production and growth by ubiquitously expressed alcohol dehydrogenase Adh3. *Proc Natl Acad Sci U S A* 99: 5337-42**

217. **Sandell LL, Sanderson BW, Moiseyev G, Johnson T, Mushegian A, Young K, Rey JP, Ma JX, Staehling-Hampton K, Trainor PA. 2007. RDH10 is essential for synthesis of embryonic retinoic acid and is required for limb, craniofacial, and organ development. *Genes Dev* 21: 1113-24**

218. **Zhang M, Hu P, Krois CR, Kane MA, Napoli JL. 2007. Altered vitamin A homeostasis and increased size and adiposity in the rdh1-null mouse. *FASEB J* 21: 2886-96**

219. **Feng L, Hernandez RE, Waxman JS, Yelon D, Moens CB. 2010. Dhrs3a regulates retinoic acid biosynthesis through a feedback inhibition mechanism. *Developmental Biology* 338: 1-14**

220. **Boerman MH, Napoli JL. 1996. Cellular retinol-binding protein-supported retinoic acid synthesis. Relative roles of microsomes and cytosol. *J Biol Chem* 271: 5610-6**

221. **Niederreither K, Vermot J, Messaddeq N, Schuhbaur B, Chambon P, Dolle P. 2001. Embryonic retinoic acid synthesis is essential for heart morphogenesis in the mouse. *Development* 128: 1019-31**

222. **Wu BX, Chen Y, Fan J, Rohrer B, Crouch RK, Ma JX. 2002. Cloning and characterization of a novel all-trans retinol short-chain dehydrogenase/reductase from the RPE. *Invest Ophthalmol Vis Sci* 43: 3365-72**

223. **Wu BX, Moiseyev G, Chen Y, Rohrer B, Crouch RK, Ma JX. 2004. Identification of RDH10, an All-trans Retinol Dehydrogenase, in Retinal Muller Cells. *Invest Ophthalmol Vis Sci* 45: 3857-62**

224. **Cammas L, Romand R, Fraulob V, Mura C, Dolle P. 2007. Expression of the murine retinol dehydrogenase 10 (Rdh10) gene correlates with many sites of retinoid signalling during embryogenesis and organ differentiation. *Dev Dyn* 236: 2899-908**

225. **Rossant J, Zirngibl R, Cado D, Shago M, Giguere V. 1991. Expression of a retinoic acid response element-hsplacZ transgene defines specific domains of transcriptional activity during mouse embryogenesis. *Genes Dev* 5: 1333-44**

226. **Kumar S, Sandell LL, Trainor PA, Koentgen F, Duester G. 2012. Alcohol and aldehyde dehydrogenases: retinoid metabolic effects in mouse knockout models. *Biochim Biophys Acta* 1821: 198-205**

227. **Niederreither K, Vermot J, Fraulob V, Chambon P, Dolle P. 2002. Retinaldehyde dehydrogenase 2 (RALDH2)- independent patterns of retinoic acid synthesis in the mouse embryo. *Proc Natl Acad Sci U S A* 99: 16111-6**

228. **Mic FA, Haselbeck RJ, Cuenca AE, Duester G. 2002. Novel retinoic acid generating activities in the neural tube and heart identified by conditional rescue of Raldh2 null mutant mice. *Development* 129: 2271-82**

229. **Niederreither K, Subbarayan V, Dolle P, Chambon P. 1999. Embryonic retinoic acid synthesis is essential for early mouse post-implantation development. *Nat Genet* 21: 444-8**

230. **Kastner P, Chan S. 2001. Function of RARalpha during the maturation of neutrophils. *Oncogene* 20: 7178-85**

231. **Buck J, Derguini F, Levi E, Nakanishi K, Hammerling U. 1991. Intracellular signaling by 14-hydroxy-4,14-retro-retinol. *Science* 254: 1654-6**

232. **Buck J, Myc A, Garbe A, Cathomas G. 1991. Differences in the action and metabolism between retinol and retinoic acid in B lymphocytes. *J Cell Biol* 115: 851-9**

233. **Garbe A, Buck J, Hammerling U. 1992. Retinoids are important cofactors in T cell activation. *J Exp Med* 176: 109-17**

234. **Yang Y, Vacchio MS, Ashwell JD. 1993. 9-cis-retinoic acid inhibits activation-driven T-cell apoptosis: implications for retinoid X receptor involvement in thymocyte development. *Proc Natl Acad Sci U S A* 90: 6170-4**

235. **Zapata-Gonzalez F, Rueda F, Petriz J, Domingo P, Villarroya F, de Madariaga A, Domingo JC. 2007. 9-cis-Retinoic acid (9cRA), a retinoid X receptor (RXR) ligand, exerts immunosuppressive effects on dendritic cells by RXR-dependent activation: inhibition of peroxisome proliferator-activated receptor gamma blocks some of the 9cRA activities, and precludes them to mature phenotype development. *J Immunol* 178: 6130-9**

236. **Geissmann F, Revy P, Brousse N, Lepelletier Y, Folli C, Durandy A, Chambon P, Dy M. 2003. Retinoids regulate survival and antigen presentation by immature dendritic cells. *J Exp Med* 198: 623-34**

237. **Beijer MR, Molenaar R, Goverse G, Mebius RE, Kraal G, den Haan JM. 2013. A crucial role for retinoic acid in the development of Notch-dependent murine splenic CD8- CD4- and CD4+ dendritic cells. *Eur J Immunol* 43: 1608-16**

238. **Jaensson-Gyllenback E, Kotarsky K, Zapata F, Persson EK, Gundersen TE, Blomhoff R, Agace WW. 2011. Bile retinoids imprint intestinal CD103+ dendritic cells with the ability to generate gut-tropic T cells. *Mucosal Immunol* 4: 438-47**

239. **Szatmari I, Pap A, Ruhl R, Ma JX, Illarionov PA, Besra GS, Rajnavolgyi E, Dezso B, Nagy L. 2006. PPARgamma controls CD1d expression by turning on retinoic acid synthesis in developing human dendritic cells. *J Exp Med* 203: 2351-62**

240. **Hengesbach LM, Hoag KA. 2004. Physiological concentrations of retinoic acid favor myeloid dendritic cell development over granulocyte development in cultures of bone marrow cells from mice. *J Nutr* 134: 2653-9**

241. **Mohty M, Morbelli S, Isnardon D, Sainty D, Arnoulet C, Gaugler B, Olive D. 2003. All-trans retinoic acid skews monocyte differentiation into interleukin-12-secreting dendritic-like cells. *Br J Haematol* 122: 829-36**

242. **Darmanin S, Chen J, Zhao S, Cui H, Shirkoohi R, Kubo N, Kuge Y, Tamaki N, Nakagawa K, Hamada J, Moriuchi T, Kobayashi M. 2007. All-trans retinoic acid enhances murine dendritic cell migration to draining lymph nodes via the balance of matrix metalloproteinases and their inhibitors. *J Immunol* 179: 4616-25**

243. **Meunier L, Bohjanen K, Voorhees JJ, Cooper KD. 1994. Retinoic acid upregulates human Langerhans cell antigen presentation and surface expression of HLA-DR and CD11c, a beta 2 integrin critically involved in T-cell activation. *J Invest Dermatol* 103: 775-9**

244. **Haftek M, Faure M, Schmitt D, Thivolet J. 1983. Langerhans cells in skin from patients with psoriasis: quantitative and qualitative study of T6 and HLA-DR antigen-expressing cells and changes with aromatic retinoid administration. *J Invest Dermatol* 81: 10-4**

245. **Klebanoff CA, Spencer SP, Torabi-Parizi P, Grainger JR, Roychoudhuri R, Ji Y, Sukumar M, Muranski P, Scott CD, Hall JA, Ferreyra GA, Leonardi AJ, Borman ZA, Wang J, Palmer DC, Wilhelm C, Cai R, Sun J, Napoli JL, Danner RL, Gattinoni L, Belkaid Y, Restifo NP. 2013. Retinoic acid controls the homeostasis of pre-cDC-derived splenic and intestinal dendritic cells. *J Exp Med* 210: 1961-76**

246. **Bedford PA, Knight SC. 1989. The effect of retinoids on dendritic cell function. *Clin Exp Immunol* 75: 481-6**

247. **Tao Y, Yang Y, Wang W. 2006. Effect of all-trans-retinoic acid on the differentiation, maturation and functions of dendritic cells derived from cord blood monocytes. *FEMS Immunol Med Microbiol* 47: 444-50**

248. **Jin CJ, Hong CY, Takei M, Chung SY, Park JS, Pham TN, Choi SJ, Nam JH, Chung IJ, Kim HJ, Lee JJ. 2010. All-trans retinoic acid inhibits the differentiation, maturation, and function of human monocyte-derived dendritic cells. *Leuk Res* 34: 513-20**

249. **Manicassamy S, Ravindran R, Deng J, Oluoch H, Denning TL, Kasturi SP, Rosenthal KM, Evavold BD, Pulendran B. 2009. Toll-like receptor 2-dependent induction of vitamin A-metabolizing enzymes in dendritic cells promotes T regulatory responses and inhibits autoimmunity. *Nat Med* 15: 401-9**

250. **Villablanca EJ, Zhou D, Valentinis B, Negro A, Raccosta L, Mauri L, Prinetti A, Sonnino S, Bordignon C, Traversari C, Russo V. 2008. Selected natural and synthetic retinoids impair CCR7- and CXCR4-dependent cell migration in vitro and in vivo. *J Leukoc Biol* 84: 871-9**

251. **Yokota A, Takeuchi H, Maeda N, Ohoka Y, Kato C, Song SY, Iwata M. 2009. GM-CSF and IL-4 synergistically trigger dendritic cells to acquire retinoic acid-producing capacity. *Int Immunol* 21: 361-77**

252. **Stock A, Booth S, Cerundolo V. 2011. Prostaglandin E2 suppresses the differentiation of retinoic acid-producing dendritic cells in mice and humans. *J Exp Med* 208: 761-73**

253. **Iwata M, Hirakiyama A, Eshima Y, Kagechika H, Kato C, Song SY. 2004. Retinoic acid imprints gut-homing specificity on T cells. *Immunity* 21: 527-38**

254. **Coombes JL, Siddiqui KR, Arancibia-Carcamo CV, Hall J, Sun CM, Belkaid Y, Powrie F. 2007. A functionally specialized population of mucosal CD103+ DCs induces Foxp3+ regulatory T cells via a TGF-beta and retinoic acid-dependent mechanism. *J Exp Med* 204: 1757-64**

255. **Edelson BT, Kc W, Juang R, Kohyama M, Benoit LA, Klekotka PA, Moon C, Albring JC, Ise W, Michael DG, Bhattacharya D, Stappenbeck TS, Holtzman MJ, Sung SS, Murphy TL, Hildner K, Murphy KM. 2010. Peripheral CD103+ dendritic cells form a unified subset developmentally related to CD8alpha+ conventional dendritic cells. *J Exp Med* 207: 823-36**

256. **Molenaar R, Knippenberg M, Goverse G, Olivier BJ, de Vos AF, O'Toole T, Mebius RE. 2011. Expression of retinaldehyde dehydrogenase enzymes in mucosal dendritic cells and gut-draining lymph node stromal cells is controlled by dietary vitamin A. *J Immunol* 186: 1934-42**

257. **Villablanca EJ, Wang S, de Calisto J, Gomes DC, Kane MA, Napoli JL, Blaner WS, Kagechika H, Blomhoff R, Rosemblatt M, Bono MR, von Andrian UH, Mora JR. 2011. MyD88 and**

retinoic acid signaling pathways interact to modulate gastrointestinal activities of dendritic cells. *Gastroenterology* 141: 176-85

258. Frota-Ruchon A, Marcinkiewicz M, Bhat PV. 2000. Localization of retinal dehydrogenase type 1 in the stomach and intestine. *Cell Tissue Res* 302: 397-400

259. Hammerschmidt SI, Ahrendt M, Bode U, Wahl B, Kremmer E, Forster R, Pabst O. 2008. Stromal mesenteric lymph node cells are essential for the generation of gut-homing T cells in vivo. *J Exp Med* 205: 2483-90

260. Iliev ID, Mileti E, Matteoli G, Chieppa M, Rescigno M. 2009. Intestinal epithelial cells promote colitis-protective regulatory T-cell differentiation through dendritic cell conditioning. *Mucosal Immunol* 2: 340-50

261. Feng T, Cong Y, Qin H, Benveniste EN, Elson CO. 2010. Generation of mucosal dendritic cells from bone marrow reveals a critical role of retinoic acid. *J Immunol* 185: 5915-25

262. Guilliams M, Crozat K, Henri S, Tamoutounour S, Grenot P, Devilard E, de Bovis B, Alexopoulou L, Dalod M, Malissen B. 2010. Skin-draining lymph nodes contain dermis-derived CD103(-) dendritic cells that constitutively produce retinoic acid and induce Foxp3(+) regulatory T cells. *Blood* 115: 1958-68

263. Wang S, Villablanca EJ, De Calisto J, Gomes DC, Nguyen DD, Mizoguchi E, Kagan JC, Reinecker HC, Hacohen N, Nagler C, Xavier RJ, Rossi-Bergmann B, Chen YB, Blomhoff R, Snapper SB, Mora JR. 2011. MyD88-dependent TLR1/2 signals educate dendritic cells with gut-specific imprinting properties. *J Immunol* 187: 141-50

264. Manicassamy S, Reizis B, Ravindran R, Nakaya H, Salazar-Gonzalez RM, Wang YC, Pulendran B. 2010. Activation of beta-catenin in dendritic cells regulates immunity versus tolerance in the intestine. *Science* 329: 849-53

265. Wang X, Sperkova Z, Napoli JL. 2001. Analysis of mouse retinal dehydrogenase type 2 promoter and expression. *Genomics* 74: 245-50

266. Jaensson E, Uronen-Hansson H, Pabst O, Eksteen B, Tian J, Coombes JL, Berg PL, Davidsson T, Powrie F, Johansson-Lindbom B, Agace WW. 2008. Small intestinal CD103+ dendritic cells display unique functional properties that are conserved between mice and humans. *J Exp Med* 205: 2139-49

267. Kamada N, Hisamatsu T, Honda H, Kobayashi T, Chinen H, Kitazume MT, Takayama T, Okamoto S, Koganei K, Sugita A, Kanai T, Hibi T. 2009. Human CD14+ macrophages in intestinal lamina propria exhibit potent antigen-presenting ability. *J Immunol* 183: 1724-31

268. Braissant O, Foufelle F, Scotto C, Dauca M, Wahli W. 1996. Differential expression of peroxisome proliferator-activated receptors (PPARs): tissue distribution of PPAR-alpha, -beta, and -gamma in the adult rat. *Endocrinology* 137: 354-66

269. Desvergne B, Michalik L, Wahli W. 2006. Transcriptional regulation of metabolism. *Physiol Rev* 86: 465-514

270. Tontonoz P, Hu E, Graves RA, Budavari AI, Spiegelman BM. 1994. mPPAR gamma 2: tissue-specific regulator of an adipocyte enhancer. *Genes Dev* 8: 1224-34

271. Huang JT, Welch JS, Ricote M, Binder CJ, Willson TM, Kelly C, Witztum JL, Funk CD, Conrad D, Glass CK. 1999. Interleukin-4-dependent production of PPAR-gamma ligands in macrophages by 12/15-lipoxygenase. *Nature* 400: 378-82

272. Vidal-Puig AJ, Considine RV, Jimenez-Linan M, Werman A, Pories WJ, Caro JF, Flier JS. 1997. Peroxisome proliferator-activated receptor gene expression in human tissues. Effects of obesity, weight loss, and regulation by insulin and glucocorticoids. *J Clin Invest* 99: 2416-22

273. Lefterova MI, Haakonsson AK, Lazar MA, Mandrup S. 2014. PPARgamma and the global map of adipogenesis and beyond. *Trends Endocrinol Metab* 25: 293-302

274. Barak Y, Nelson MC, Ong ES, Jones YZ, Ruiz-Lozano P, Chien KR, Koder A, Evans RM. 1999. PPAR gamma is required for placental, cardiac, and adipose tissue development. *Mol Cell* 4: 585-95

275. Heikkinen S, Auwerx J, Argmann CA. 2007. PPARgamma in human and mouse physiology. *Biochim Biophys Acta* 1771: 999-1013
276. Kliewer SA, Umesono K, Noonan DJ, Heyman RA, Evans RM. 1992. Convergence of 9-cis retinoic acid and peroxisome proliferator signalling pathways through heterodimer formation of their receptors. *Nature* 358: 771-4
277. Nagy L, Tontonoz P, Alvarez JG, Chen H, Evans RM. 1998. Oxidized LDL regulates macrophage gene expression through ligand activation of PPARgamma. *Cell* 93: 229-40
278. Forman BM, Tontonoz P, Chen J, Brun RP, Spiegelman BM, Evans RM. 1995. 15-Deoxy-delta 12, 14-prostaglandin J2 is a ligand for the adipocyte determination factor PPAR gamma. *Cell* 83: 803-12
279. Goldberg RB, Kendall DM, Deeg MA, Buse JB, Zagar AJ, Pinaire JA, Tan MH, Khan MA, Perez AT, Jacober SJ, Investigators GS. 2005. A comparison of lipid and glycemic effects of pioglitazone and rosiglitazone in patients with type 2 diabetes and dyslipidemia. *Diabetes Care* 28: 1547-54
280. Szanto A, Benko S, Szatmari I, Balint BL, Furtos I, Ruhl R, Molnar S, Csiba L, Garuti R, Calandra S, Larsson H, Diczfalusy U, Nagy L. 2004. Transcriptional regulation of human CYP27 integrates retinoid, peroxisome proliferator-activated receptor, and liver X receptor signaling in macrophages. *Mol Cell Biol* 24: 8154-66
281. Zelcer N, Hong C, Boyadjian R, Tontonoz P. 2009. LXR regulates cholesterol uptake through Idol-dependent ubiquitination of the LDL receptor. *Science* 325: 100-4
282. Ricote M, Li AC, Willson TM, Kelly CJ, Glass CK. 1998. The peroxisome proliferator-activated receptor-gamma is a negative regulator of macrophage activation. *Nature* 391: 79-82
283. Szatmari I, Nagy L. 2008. Nuclear receptor signalling in dendritic cells connects lipids, the genome and immune function. *EMBO J* 27: 2353-62
284. Faveeuw C, Fougeray S, Angeli V, Fontaine J, Chinetti G, Gosset P, Delerive P, Maliszewski C, Capron M, Staels B, Moser M, Trottein F. 2000. Peroxisome proliferator-activated receptor gamma activators inhibit interleukin-12 production in murine dendritic cells. *FEBS Lett* 486: 261-6
285. Gosset P, Charbonnier AS, Delerive P, Fontaine J, Staels B, Pestel J, Tonnel AB, Trottein F. 2001. Peroxisome proliferator-activated receptor gamma activators affect the maturation of human monocyte-derived dendritic cells. *Eur J Immunol* 31: 2857-65
286. Nencioni A, Grunebach F, Zobywlaski A, Denzlinger C, Brugger W, Brossart P. 2002. Dendritic cell immunogenicity is regulated by peroxisome proliferator-activated receptor gamma. *J Immunol* 169: 1228-35
287. Appel S, Mirakaj V, Bringmann A, Weck MM, Grunebach F, Brossart P. 2005. PPAR-gamma agonists inhibit toll-like receptor-mediated activation of dendritic cells via the MAP kinase and NF-kappaB pathways. *Blood* 106: 3888-94
288. Angeli V, Hammad H, Staels B, Capron M, Lambrecht BN, Trottein F. 2003. Peroxisome proliferator-activated receptor gamma inhibits the migration of dendritic cells: consequences for the immune response. *J Immunol* 170: 5295-301
289. Gogolak P, Rethi B, Szatmari I, Lanyi A, Dezso B, Nagy L, Rajnavolgyi E. 2007. Differentiation of CD1a- and CD1a+ monocyte-derived dendritic cells is biased by lipid environment and PPARgamma. *Blood* 109: 643-52
290. Housley WJ, O'Conor CA, Nichols F, Puddington L, Lingenheld EG, Zhu L, Clark RB. 2009. PPARgamma regulates retinoic acid-mediated DC induction of Tregs. *J Leukoc Biol* 86: 293-301
291. Hammad H, de Heer HJ, Soullie T, Angeli V, Trottein F, Hoogsteden HC, Lambrecht BN. 2004. Activation of peroxisome proliferator-activated receptor-gamma in dendritic cells inhibits the development of eosinophilic airway inflammation in a mouse model of asthma. *Am J Pathol* 164: 263-71

292. Jung K, Tanaka A, Fujita H, Matsuda A, Oida K, Karasawa K, Okamoto N, Ohmori K, Jee Y, Shin T, Matsuda H. 2011. Peroxisome proliferator-activated receptor gamma-mediated suppression of dendritic cell function prevents the onset of atopic dermatitis in NC/Tnd mice. *J Allergy Clin Immunol* 127: 420-9 e1-6

293. Aldridge JR, Jr., Moseley CE, Boltz DA, Negovetich NJ, Reynolds C, Franks J, Brown SA, Doherty PC, Webster RG, Thomas PG. 2009. TNF/iNOS-producing dendritic cells are the necessary evil of lethal influenza virus infection. *Proc Natl Acad Sci U S A* 106: 5306-11

294. Albert ML, Pearce SF, Francisco LM, Sauter B, Roy P, Silverstein RL, Bhardwaj N. 1998. Immature dendritic cells phagocytose apoptotic cells via alphavbeta5 and CD36, and cross-present antigens to cytotoxic T lymphocytes. *J Exp Med* 188: 1359-68

295. Belz GT, Vremec D, Febbraio M, Corcoran L, Shortman K, Carbone FR, Heath WR. 2002. CD36 is differentially expressed by CD8+ splenic dendritic cells but is not required for cross-presentation in vivo. *J Immunol* 168: 6066-70

296. Szatmari I, Vamosi G, Brazda P, Balint BL, Benko S, Szeles L, Jeney V, Ozvegy-Laczka C, Szanto A, Barta E, Balla J, Sarkadi B, Nagy L. 2006. Peroxisome proliferator-activated receptor gamma-regulated ABCG2 expression confers cytoprotection to human dendritic cells. *J Biol Chem* 281: 23812-23

297. Ardavin C, Martinez del Hoyo G, Martin P, Anjuere F, Arias CF, Marin AR, Ruiz S, Parrillas V, Hernandez H. 2001. Origin and differentiation of dendritic cells. *Trends Immunol* 22: 691-700

298. Leslie DS, Dascher CC, Cembrola K, Townes MA, Hava DL, Hugendubler LC, Mueller E, Fox L, Roura-Mir C, Moody DB, Vincent MS, Gumperz JE, Illarionov PA, Besra GS, Reynolds CG, Brenner MB. 2008. Serum lipids regulate dendritic cell CD1 expression and function. *Immunology* 125: 289-301

299. Szanto A, Balint BL, Nagy ZS, Barta E, Dezso B, Pap A, Szeles L, Poliska S, Oros M, Evans RM, Barak Y, Schwabe J, Nagy L. 2010. STAT6 transcription factor is a facilitator of the nuclear receptor PPARgamma-regulated gene expression in macrophages and dendritic cells. *Immunity* 33: 699-712

300. Mach N, Gillessen S, Wilson SB, Sheehan C, Mihm M, Dranoff G. 2000. Differences in dendritic cells stimulated in vivo by tumors engineered to secrete granulocyte-macrophage colony-stimulating factor or Flt3-ligand. *Cancer Res* 60: 3239-46

301. Lindstedt M, Lundberg K, Borrebaeck CA. 2005. Gene family clustering identifies functionally associated subsets of human in vivo blood and tonsillar dendritic cells. *J Immunol* 175: 4839-46

302. Santegoets SJ, Gibbs S, Kroeze K, van de Ven R, Scheper RJ, Borrebaeck CA, de Gruijl TD, Lindstedt M. 2008. Transcriptional profiling of human skin-resident Langerhans cells and CD1a+ dermal dendritic cells: differential activation states suggest distinct functions. *J Leukoc Biol* 84: 143-51

303. Schaft N, Dorrie J, Thumann P, Beck VE, Muller I, Schultz ES, Kampgen E, Dieckmann D, Schuler G. 2005. Generation of an optimized polyvalent monocyte-derived dendritic cell vaccine by transfecting defined RNAs after rather than before maturation. *J Immunol* 174: 3087-97

304. White JA, Guo YD, Baetz K, Beckett-Jones B, Bonasoro J, Hsu KE, Dilworth FJ, Jones G, Petkovich M. 1996. Identification of the retinoic acid-inducible all-trans-retinoic acid 4-hydroxylase. *J Biol Chem* 271: 29922-7

305. Loudig O, Maclean GA, Dore NL, Luu L, Petkovich M. 2005. Transcriptional co-operativity between distant retinoic acid response elements in regulation of Cyp26A1 inducibility. *Biochem J* 392: 241-8

306. Ray WJ, Bain G, Yao M, Gottlieb DI. 1997. CYP26, a novel mammalian cytochrome P450, is induced by retinoic acid and defines a new family. *J Biol Chem* 272: 18702-8

307. Chiocca EA, Davies PJ, Stein JP. 1988. The molecular basis of retinoic acid action. Transcriptional regulation of tissue transglutaminase gene expression in macrophages. *J Biol Chem* 263: 11584-9
308. Kawaguchi R, Yu J, Honda J, Hu J, Whitelegge J, Ping P, Wiita P, Bok D, Sun H. 2007. A membrane receptor for retinol binding protein mediates cellular uptake of vitamin A. *Science* 315: 820-5
309. Dong D, Ruuska SE, Levinthal DJ, Noy N. 1999. Distinct roles for cellular retinoic acid-binding proteins I and II in regulating signaling by retinoic acid. *J Biol Chem* 274: 23695-8
310. Nakken B, Varga T, Szatmari I, Szeles L, Gyongyosi A, Illarionov PA, Dezso B, Gogolak P, Rajnavolgyi E, Nagy L. Peroxisome proliferator-activated receptor gamma-regulated cathepsin D is required for lipid antigen presentation by dendritic cells. *J Immunol* 187: 240-7
311. Honey K, Rudensky AY. 2003. Lysosomal cysteine proteases regulate antigen presentation. *Nat Rev Immunol* 3: 472-82
312. Liaudet-Coopman E, Beaujouin M, Derocq D, Garcia M, Glondu-Lassis M, Laurent-Matha V, Prebois C, Rochefort H, Vignon F. 2006. Cathepsin D: newly discovered functions of a long-standing aspartic protease in cancer and apoptosis. *Cancer Lett* 237: 167-79
313. Yu KO, Im JS, Molano A, Dutronc Y, Illarionov PA, Forestier C, Fujiwara N, Arias I, Miyake S, Yamamura T, Chang YT, Besra GS, Porcelli SA. 2005. Modulation of CD1d-restricted NKT cell responses by using N-acyl variants of alpha-galactosylceramides. *Proc Natl Acad Sci U S A* 102: 3383-8
314. Mora JR, Iwata M, Eksteen B, Song SY, Junt T, Senman B, Otipoby KL, Yokota A, Takeuchi H, Ricciardi-Castagnoli P, Rajewsky K, Adams DH, von Andrian UH. 2006. Generation of gut-homing IgA-secreting B cells by intestinal dendritic cells. *Science* 314: 1157-60
315. McDonald KG, Leach MR, Brooke KW, Wang C, Wheeler LW, Hanly EK, Rowley CW, Levin MS, Wagner M, Li E, Newberry RD. 2012. Epithelial expression of the cytosolic retinoid chaperone cellular retinol binding protein II is essential for in vivo imprinting of local gut dendritic cells by lumenal retinoids. *Am J Pathol* 180: 984-97
316. Uematsu S, Fujimoto K, Jang MH, Yang BG, Jung YJ, Nishiyama M, Sato S, Tsujimura T, Yamamoto M, Yokota Y, Kiyono H, Miyasaka M, Ishii KJ, Akira S. 2008. Regulation of humoral and cellular gut immunity by lamina propria dendritic cells expressing Toll-like receptor 5. *Nat Immunol* 9: 769-76
317. Pantazi E, Marks E, Stolarczyk E, Lycke N, Noelle RJ, Elgueta R. 2015. Cutting Edge: Retinoic Acid Signaling in B Cells Is Essential for Oral Immunization and Microflora Composition. *J Immunol* 195: 1368-71
318. Wang C, Kang SG, HogenEsch H, Love PE, Kim CH. 2010. Retinoic acid determines the precise tissue tropism of inflammatory Th17 cells in the intestine. *J Immunol* 184: 5519-26
319. Cha HR, Chang SY, Chang JH, Kim JO, Yang JY, Kim CH, Kweon MN. 2010. Downregulation of Th17 cells in the small intestine by disruption of gut flora in the absence of retinoic acid. *J Immunol* 184: 6799-806
320. Collins CB, Aherne CM, Kominsky D, McNamee EN, Lebsack MD, Eltzschig H, Jedlicka P, Rivera-Nieves J. 2011. Retinoic acid attenuates ileitis by restoring the balance between T-helper 17 and T regulatory cells. *Gastroenterology* 141: 1821-31
321. Laffont S, Siddiqui KR, Powrie F. 2010. Intestinal inflammation abrogates the tolerogenic properties of MLN CD103+ dendritic cells. *Eur J Immunol* 40: 1877-83
322. DePaolo RW, Abadie V, Tang F, Fehlner-Peach H, Hall JA, Wang W, Marietta EV, Kasarda DD, Waldmann TA, Murray JA, Semrad C, Kupfer SS, Belkaid Y, Guandalini S, Jabri B. 2011. Co-adjuvant effects of retinoic acid and IL-15 induce inflammatory immunity to dietary antigens. *Nature* 471: 220-4
323. Zeng R, Oderup C, Yuan R, Lee M, Habtezion A, Hadeiba H, Butcher EC. 2013. Retinoic acid regulates the development of a gut-homing precursor for intestinal dendritic cells. *Mucosal Immunol* 6: 847-56

324. Zeng R, Bscheider M, Lahl K, Lee M, Butcher EC. 2016. Generation and transcriptional programming of intestinal dendritic cells: essential role of retinoic acid. *Mucosal Immunol* 9: 183-93
325. Bimczok D, Kao JY, Zhang M, Cochrun S, Mannon P, Peter S, Wilcox CM, Monkemuller KE, Harris PR, Grams JM, Stahl RD, Smith PD, Smythies LE. 2015. Human gastric epithelial cells contribute to gastric immune regulation by providing retinoic acid to dendritic cells. *Mucosal Immunol* 8: 533-44
326. Schulz O, Jaensson E, Persson EK, Liu X, Worbs T, Agace WW, Pabst O. 2009. Intestinal CD103+, but not CX3CR1+, antigen sampling cells migrate in lymph and serve classical dendritic cell functions. *J Exp Med* 206: 3101-14
327. Varol C, Zigmond E, Jung S. 2010. Securing the immune tightrope: mononuclear phagocytes in the intestinal lamina propria. *Nat Rev Immunol* 10: 415-26
328. Scott CL, Aumeunier AM, Mowat AM. 2011. Intestinal CD103+ dendritic cells: master regulators of tolerance? *Trends Immunol* 32: 412-9
329. Goverse G, Olivier BJ, Molenaar R, Knippenberg M, Greuter M, Konijn T, Cook EC, Beijer MR, Fedor DM, den Haan JM, Napoli JL, Bouma G, Mebius RE. 2015. Vitamin A metabolism and mucosal immune function are distinct between BALB/c and C57BL/6 mice. *Eur J Immunol* 45: 89-100
330. Sanders TJ, McCarthy NE, Giles EM, Davidson KL, Haltalli ML, Hazell S, Lindsay JO, Stagg AJ. 2014. Increased production of retinoic acid by intestinal macrophages contributes to their inflammatory phenotype in patients with Crohn's disease. *Gastroenterology* 146: 1278-88 e1-2
331. Tuna H, Avdiushko RG, Sindhava VJ, Wedlund L, Kaetzel CS, Kaplan AM, Bondada S, Cohen DA. 2014. Regulation of the mucosal phenotype in dendritic cells by PPARgamma: role of tissue microenvironment. *J Leukoc Biol* 95: 471-85
332. Bassaganya-Riera J, Reynolds K, Martino-Catt S, Cui Y, Hennighausen L, Gonzalez F, Rohrer J, Benninghoff AU, Hontecillas R. 2004. Activation of PPAR gamma and delta by conjugated linoleic acid mediates protection from experimental inflammatory bowel disease. *Gastroenterology* 127: 777-91
333. Desreumaux P, Dubuquoy L, Nutten S, Peuchmaur M, Englaro W, Schoonjans K, Derijard B, Desvergne B, Wahli W, Chambon P, Leibowitz MD, Colombel JF, Auwerx J. 2001. Attenuation of colon inflammation through activators of the retinoid X receptor (RXR)/peroxisome proliferator-activated receptor gamma (PPARgamma) heterodimer. A basis for new therapeutic strategies. *J Exp Med* 193: 827-38
334. Shah YM, Morimura K, Gonzalez FJ. 2007. Expression of peroxisome proliferator-activated receptor-gamma in macrophage suppresses experimentally induced colitis. *Am J Physiol Gastrointest Liver Physiol* 292: G657-66
335. Qualls JE, Tuna H, Kaplan AM, Cohen DA. 2009. Suppression of experimental colitis in mice by CD11c+ dendritic cells. *Inflamm Bowel Dis* 15: 236-47
336. Villablanca EJ, Raccosta L, Zhou D, Fontana R, Maggioni D, Negro A, Sanvito F, Ponzoni M, Valentinis B, Bregni M, Prinetti A, Steffensen KR, Sonnino S, Gustafsson JA, Doglioni C, Bordignon C, Traversari C, Russo V. 2010. Tumor-mediated liver X receptor-alpha activation inhibits CC chemokine receptor-7 expression on dendritic cells and dampens antitumor responses. *Nat Med* 16: 98-105
337. Toura I, Kawano T, Akutsu Y, Nakayama T, Ochiai T, Taniguchi M. 1999. Cutting edge: inhibition of experimental tumor metastasis by dendritic cells pulsed with alpha-galactosylceramide. *J Immunol* 163: 2387-91
338. Fujii S, Shimizu K, Kronenberg M, Steinman RM. 2002. Prolonged IFN-gamma-producing NKT response induced with alpha-galactosylceramide-loaded DCs. *Nat Immunol* 3: 867-74
339. Smyth MJ, Crowe NY, Pellicci DG, Kyparissoudis K, Kelly JM, Takeda K, Yagita H, Godfrey DI. 2002. Sequential production of interferon-gamma by NK1.1(+) T cells and natural killer

cells is essential for the antimetastatic effect of alpha-galactosylceramide. *Blood* 99: 1259-66

340. Dhodapkar MV, Geller MD, Chang DH, Shimizu K, Fujii S, Dhodapkar KM, Krasovsky J. 2003. A reversible defect in natural killer T cell function characterizes the progression of premalignant to malignant multiple myeloma. *J Exp Med* 197: 1667-76
341. Giaccone G, Punt CJ, Ando Y, Ruijter R, Nishi N, Peters M, von Blomberg BM, Scheper RJ, van der Vliet HJ, van den Eertwegh AJ, Roelvink M, Beijnen J, Zwierzina H, Pinedo HM. 2002. A phase I study of the natural killer T-cell ligand alpha-galactosylceramide (KRN7000) in patients with solid tumors. *Clin Cancer Res* 8: 3702-9
342. Tahir SM, Cheng O, Shaulov A, Koezuka Y, Bubley GJ, Wilson SB, Balk SP, Exley MA. 2001. Loss of IFN-gamma production by invariant NK T cells in advanced cancer. *J Immunol* 167: 4046-50
343. Parekh VV, Lalani S, Kim S, Halder R, Azuma M, Yagita H, Kumar V, Wu L, Kaer LV. 2009. PD-1/PD-L blockade prevents anergy induction and enhances the anti-tumor activities of glycolipid-activated invariant NKT cells. *J Immunol* 182: 2816-26
344. Parekh A, Long RA, Chancellor MB, Sacks MS. 2009. Assessing the effects of transforming growth factor-beta1 on bladder smooth muscle cell phenotype. II. Modulation of collagen organization. *J Urol* 182: 1216-21
345. Uldrich AP, Crowe NY, Kyparissoudis K, Pellicci DG, Zhan Y, Lew AM, Bouillet P, Strasser A, Smyth MJ, Godfrey DI. 2005. NKT cell stimulation with glycolipid antigen in vivo: costimulation-dependent expansion, Bim-dependent contraction, and hyporesponsiveness to further antigenic challenge. *J Immunol* 175: 3092-101
346. Chang DH, Osman K, Connolly J, Kukreja A, Krasovsky J, Pack M, Hutchinson A, Geller M, Liu N, Annable R, Shay J, Kirchhoff K, Nishi N, Ando Y, Hayashi K, Hassoun H, Steinman RM, Dhodapkar MV. 2005. Sustained expansion of NKT cells and antigen-specific T cells after injection of alpha-galactosyl-ceramide loaded mature dendritic cells in cancer patients. *J Exp Med* 201: 1503-17
347. Nicol AJ, Tazbirkova A, Nieda M. 2011. Comparison of clinical and immunological effects of intravenous and intradermal administration of alpha-galactosylceramide (KRN7000)-pulsed dendritic cells. *Clin Cancer Res* 17: 5140-51
348. Nieda M, Okai M, Tazbirkova A, Lin H, Yamaura A, Ide K, Abraham R, Juji T, Macfarlane DJ, Nicol AJ. 2004. Therapeutic activation of Valpha24+Vbeta11+ NKT cells in human subjects results in highly coordinated secondary activation of acquired and innate immunity. *Blood* 103: 383-9
349. Richter J, Neparidze N, Zhang L, Nair S, Monesmith T, Sundaram R, Miesowicz F, Dhodapkar KM, Dhodapkar MV. 2013. Clinical regressions and broad immune activation following combination therapy targeting human NKT cells in myeloma. *Blood* 121: 423-30
350. Motohashi S, Ishikawa A, Ishikawa E, Otsuji M, Iizasa T, Hanaoka H, Shimizu N, Horiguchi S, Okamoto Y, Fujii S, Taniguchi M, Fujisawa T, Nakayama T. 2006. A phase I study of in vitro expanded natural killer T cells in patients with advanced and recurrent non-small cell lung cancer. *Clin Cancer Res* 12: 6079-86
351. De Libero G, Mori L. 2012. Novel insights into lipid antigen presentation. *Trends Immunol* 33: 103-11
352. Bene K, Varga Z, Petrov VO, Boyko N, Rajnavolgyi E. 2017. Gut Microbiota Species Can Provoke both Inflammatory and Tolerogenic Immune Responses in Human Dendritic Cells Mediated by Retinoic Acid Receptor Alpha Ligation. *Front Immunol* 8: 427
353. Dubuquoy L, Rousseaux C, Thuru X, Peyrin-Biroulet L, Romano O, Chavatte P, Chamaillard M, Desreumaux P. 2006. PPARgamma as a new therapeutic target in inflammatory bowel diseases. *Gut* 55: 1341-9
354. Carlsson JA, Wold AE, Sandberg AS, Ostman SM. 2015. The Polyunsaturated Fatty Acids Arachidonic Acid and Docosahexaenoic Acid Induce Mouse Dendritic Cells Maturation but Reduce T-Cell Responses In Vitro. *PLoS One* 10: e0143741

355. Draper E, DeCourcey J, Higgins SC, Canavan M, McEvoy F, Lynch M, Keogh B, Reynolds C, Roche HM, Mills KH, Loscher CE. 2014. Conjugated linoleic acid suppresses dendritic cell activation and subsequent Th17 responses. ***J Nutr Biochem*** **25: 741-9**

13. PUBLICATIONS RELATED TO DISSERTATION

UNIVERSITY AND NATIONAL LIBRAY
UNIVERSITY OF DEBRECEN
H-4002 Egyetem tér 1, Debrecen
Phone: +3652/410-443, email: publikaciok@lib.unideb.hu

Registry number: DEENK/303/2018.PL
Subject: PhD Publikációs Lista

Candidate: Adrienn Gyöngyösi
Neptun ID: I83XOF
Doctoral School: Doctoral School of Molecular Cellular and Immune Biology
MTMT ID: 10038878

List of publications related to the dissertation

1. **Gyöngyösi, A.**, Szatmári, I., Pap, A., Dezső, B., Pos, Z., Széles, L., Varga, T., Nagy, L.: RDH10, RALDH2, and CRABP2 are required components of PPARγ-directed ATRA synthesis and signaling in human dendritic cells.
   J. Lipid Res. 54 (9), 2458-2474, 2013.
   DOI: http://dx.doi.org/10.1194/jlr.M038984
   IF: 4.73
2. Nakken, B., Varga, T., Szatmári, I., Széles, L., **Gyöngyösi, A.**, Illarionov, P. A., Dezső, B., Gogolák, P., Rajnavölgyi, É., Nagy, L.: Peroxisome proliferator-activated receptor [gamma]-regulated cathepsin D is required for lipid antigen presentation by dendritic cells.
   J. Immunol. 187 (1), 240-247, 2011.
   DOI: http://dx.doi.org/10.4049/jimmunol.1002421
   IF: 5.788
3. **Gyöngyösi, A.**, Nagy, L.: Potential Therapeutic Use of PPAR[gamma]-Programed HumanMonocyte-Derived Dendritic Cells in Cancer Vaccination Therapy.
   PPAR Research. 2008, [1-10], 2008.
   DOI: http://dx.doi.org/10.1155/2008/473804

DEBRECENI EGYETEM * Egyetemi és Nemzeti Könyvtár *

14. LIST OF OTHER PUBLICATIONS

UNIVERSITY of DEBRECEN

UNIVERSITY AND NATIONAL LIBRAY
UNIVERSITY OF DEBRECEN
H-4002 Egyetem tér 1, Debrecen
Phone: +3652/410-443, email: publikaciok@lib.unideb.hu

List of other publications

4. **Gyöngyösi, A.**, Dócs, O., Czimmerer, Z., Orosz, L., Horváth, A., Török, O., Méhes, G., Nagy, L., Bálint, B. L.: Measuring expression levels of small regulatory RNA molecules from body fluids and formalin-fixed, paraffin-embedded samples.
Methods Mol. Biol. 1182, 105-119, 2014.
DOI: http://dx.doi.org/10.1007/978-1-4939-1062-5_10

5. Tsakiris, I., Törőcsik, D., **Gyöngyösi, A.**, Dózsa, A., Szatmári, I., Szántó, A., Soós, G., Nemes, Z., Igali, L., Márton, I., Takáts, Z., Nagy, L., Dezső, B.: Carboxypeptidase-M is regulated by lipids and CSFs in macrophages and dendritic cells and expressed selectively in tissue granulomas and foam cells.
Lab. Invest. 92 (3), 345-361, 2012.
DOI: http://dx.doi.org/10.1038/labinvest.2011.168
IF: 3.961

Total IF of journals (all publications): 14,479
Total IF of journals (publications related to the dissertation): 10,518

The Candidate's publication data submitted to the iDEa Tudóstér have been validated by DEENK on the basis of Web of Science, Scopus and Journal Citation Report (Impact Factor) databases.

12 September, 2018

DEBRECENI EGYETEM Egyetemi és Nemzeti Könyvtár

15. SUPPLEMENT

1, Gyöngyösi, A., Szatmari, I., Pap, A., Dezső, B., Pos, Z., Széles, L., Varga, T., Nagy, L.: RDH10, RALDH2, and CRABP2 are required components of PPARγ-directed ATRA synthesis and signaling in human dendritic cells. J Lipid Res. 54(9):2458-2474, 2013 DOI: http//dx.doi.org/10.1194/jlr.M038984.

2, Nakken, B., Varga, T., Szatmári, I., Széles, L., **Gyöngyösi, A.**, Illarionov, PA., Dezső, B., Gogolák, P., Rajnavölgyi, É., Nagy, L.: Peroxisome proliferator-activated receptor γ-regulated cathepsin D is required for lipid antigen presentation by dendritic cells. J. Immunol. 187(1):240-207, 2011. DOI: http//dx.doi.org/10.4049/jimmunol.1002421.

3, Gyöngyösi, A., Nagy L.: Potential Therapeutic Use of PPARgamma-Programed Human Monocyte-Derived Dendritic Cells in Cancer Vaccination Therapy. PPAR Research 2008, 21-10, 2008. DOI: http//dx.doi.org/10.1155/2008/473804.